



<https://theses.gla.ac.uk/>

Theses Digitisation:

<https://www.gla.ac.uk/myglasgow/research/enlighten/theses/digitisation/>

This is a digitised version of the original print thesis.

Copyright and moral rights for this work are retained by the author

A copy can be downloaded for personal non-commercial research or study,
without prior permission or charge

This work cannot be reproduced or quoted extensively from without first
obtaining permission in writing from the author

The content must not be changed in any way or sold commercially in any
format or medium without the formal permission of the author

When referring to this work, full bibliographic details including the author,
title, awarding institution and date of the thesis must be given

Enlighten: Theses

<https://theses.gla.ac.uk/>
research-enlighten@glasgow.ac.uk

ProQuest Number: 10754017

All rights reserved

INFORMATION TO ALL USERS

The quality of this reproduction is dependent upon the quality of the copy submitted.

In the unlikely event that the author did not send a complete manuscript and there are missing pages, these will be noted. Also, if material had to be removed, a note will indicate the deletion.



ProQuest 10754017

Published by ProQuest LLC (2018). Copyright of the Dissertation is held by the Author.

All rights reserved.

This work is protected against unauthorized copying under Title 17, United States Code
Microform Edition © ProQuest LLC.

ProQuest LLC.
789 East Eisenhower Parkway
P.O. Box 1346
Ann Arbor, MI 48106 – 1346

**Characterisation of the *Out cold*
mutations of *Drosophila melanogaster***

by

Helen Anne Lindsay

A thesis submitted for the degree of Doctor of Philosophy

Division of Molecular Genetics

Institute of Biomedical and Life Sciences

University of Glasgow

December 2005

GLASGOW
UNIVERSITY
LIBRARY:

Table of contents

<i>Table of contents</i>	2
<i>List of figures</i>	6
<i>List of tables</i>	8
<i>List of accompanying material</i>	9
<i>Acknowledgements</i>	10
<i>Abstract</i>	11
<i>Declaration</i>	12
<i>List of abbreviations</i>	13
1 Introduction	17
1.1 <i>Drosophila</i> as a genetic model organism	18
1.2 Human mitochondrial disorders and fly models	20
1.3 Human seizure disorders and fly models	22
1.4 The <i>Out cold</i> mutations	25
1.4.1 Introduction	25
1.4.2 <i>Ocd</i> phenotype	25
1.4.3 Mapping <i>Ocd</i>	28
1.5 What causes cold-sensitivity?	31
1.6 Project Aims	35
2 Materials and methods	36
2.1 <i>Drosophila</i>	37
2.1.1 <i>Drosophila</i> stocks	37
2.1.2 <i>Drosophila</i> rearing conditions	38
2.1.3 Isogenisation of <i>Drosophila</i> chromosomes	39
2.1.4 Auditory behavioural assay	39
2.1.5 Cold-sensitive paralysis assay	40
2.1.6 Cold-sensitive male lethality assay	40

2.1.7	SNP mapping	41
2.1.8	<i>P</i> element mapping	41
2.1.9	Complementation tests	42
2.1.10	Rescue of male semi-lethality	42
2.1.11	Dichlorodiphenyltrichloroethane (DDT) contact assay	43
2.1.12	KCl and NaCl sensitivity assay	44
2.2	Molecular biology	44
2.2.1	Materials	44
2.2.2	DNA extraction from <i>Drosophila</i>	45
2.2.3	Quantification of DNA concentration	45
2.2.4	Polymerase Chain Reaction	46
2.2.5	Agarose gel electrophoresis	46
2.2.6	Extraction of DNA from agarose gels	46
2.2.7	Purification of PCR products	46
2.2.8	DNA sequencing	47
2.2.9	SNP genotyping	47
2.2.10	Determination of <i>P</i> element insertion position	48
2.3	Proteomics	50
2.3.1	Protein extraction from <i>Drosophila</i>	50
2.3.2	2D difference gel electrophoresis	50
2.3.3	Mass spectrometry (protein identification)	51
2.4	Electrophysiology	51
2.4.1	Staging and dissection for voltage clamp recordings	51
2.4.2	Patch clamping	52
2.4.3	Solutions	52
3	<i>Identification of the Ocd gene</i>	53
3.1	Introduction	54
3.2	Preliminary <i>Ocd</i> characterisation	54
3.3	Sequencing of mitochondrial candidates	56
3.4	SNP mapping	58
3.5	<i>P</i> element mapping	65
3.6	Complementation tests	70

3.6.1	Complementation tests between <i>Ocd</i> and <i>hang</i>	71
3.6.2	Complementation tests between <i>Ocd</i> and <i>para</i>	72
3.7	Sequencing of candidate genes	74
4	<i>Confirmation that Ocd and para are allelic</i>	75
4.1	Introduction to sodium channel biology	76
4.1.1	Voltage-gated sodium channels	76
4.1.2	<i>paralytic</i> , a <i>Drosophila</i> sodium channel gene	78
4.1.3	Human sodium channel disorders	81
4.1.4	Evolutionary aspects	86
4.2	Identification of missense mutations in <i>para</i>	88
4.3	Rescue of the <i>Out cold</i> phenotype by expression of a <i>para</i> transgene	92
4.3.1	The $P\{UAS:para\}$ transgene	92
4.3.2	Rescue of <i>Ocd</i> semi-lethality	94
5	<i>Characterisation of the Ocd phenotype</i>	98
5.1	Introduction	99
5.2	Proteomics	100
5.3	Electrophysiology	110
5.4	Auditory behavioural assay	117
5.5	Sensitivity to potassium and sodium	118
5.6	Pesticide resistance	121
6	<i>Discussion</i>	127
6.1	Project summary	128
6.2	<i>Ocd</i> as a model for human sodium channelopathies	129
6.3	Future directions	129
6.3.1	Creation of <i>Ocd</i> -like and other novel <i>para</i> mutations	130
6.3.2	Characterisation of pre-existing and novel <i>para</i> strains	132
6.3.2.1	Testing for sensitivity to cold, potassium, and rest after exercise	132
6.3.2.2	Chemical challenge	132
6.3.2.3	Investigation into the electrophysiological phenotype of <i>Ocd</i>	133
6.3.3	Identification of genes that suppress the <i>Ocd</i> phenotype	134

6.3.4 The role of mitochondria in the <i>Ocd</i> mutant phenotype	135
6.4 Conclusions	136
<i>List of references</i>	<i>137</i>
<i>Accompanying material</i>	<i>162</i>

List of figures

Figure 1.1 The GAL4/UAS system in <i>Drosophila</i>	20
Figure 1.2 2D gel electrophoresis of mitochondrial proteins in wild-type and <i>Ocd</i> flies	28
Figure 1.3 Deficiency mapping of <i>Ocd</i>	30
Figure 2.1 Chromosome substitution for the isogenisation of <i>Ocd</i> mutations	39
Figure 2.2 Schematic representations of the <i>P</i> elements used	42
Figure 2.3 Crossing scheme to generate a stock of <i>Ocd</i> flies carrying the $P\{UAS:para^+\}$ construct	43
Figure 3.1 Dominant cold-sensitivity assay in Glasgow <i>Ocd</i> and wild-type lines	55
Figure 3.2 Cold-sensitive male lethality assay in Glasgow <i>Ocd</i> lines	56
Figure 3.3 Mapping <i>Ocd</i> using SNPs	58
Figure 3.4 Relative positions of genes containing SNPs identified across the <i>Ocd</i> region and used in mapping	60
Figure 3.5 Crossing strategy to generate recombinant flies	60
Figure 3.6 Estimated relative positions of <i>Ocd</i> , <i>rudimentary (r)</i> , and <i>forked (f)</i>	62
Figure 3.7 GeneScan electrophoregrams	63
Figure 3.8 Genotypes of recombinant males	64
Figure 3.9 Crossing scheme to generate recombinant flies	66
Figure 3.10 The <i>Ocd</i> region showing relative positions of <i>P</i> element insertions	68
Figure 3.11 Topographical representation of the <i>Ocd</i> region after mapping	69
Figure 4.1 Schematic representation of sodium channel structure	77
Figure 4.2 Approximate locations of the alternative exons identified in <i>para</i>	80
Figure 4.3 Mutations identified in <i>SCN4A</i>	83
Figure 4.4 Multiple amino acid sequence alignment (ClustalW) of the III-IV cytoplasmic linker	87
Figure 4.5 <i>para</i> coding mutations identified through sequencing of exon 28.	88
Figure 4.6 Approximate positions of the <i>Ocd</i> mutations in the Para sodium channel	90
Figure 4.7 The <i>Ocd</i> mutations lie in highly conserved regions of Para	91
Figure 4.8 The $P\{UAS:para^+\}$ construct	93
Figure 4.9 Rescue of <i>Ocd</i> ^{<i>l-G</i>} semi-lethality by GAL4 driven expression of <i>para</i> ⁺ .	95
Figure 5.1 Representative example of an overlaid fluorescent cyanine dye image of wild-type and <i>Ocd</i> proteomes (2D DIGE)	102

Figure 5.2 Example of a standardised abundance graph generated by DeCyder Biological Variance Analysis (BVA) analysis	103
Figure 5.3 Comparison of one-way and nested ANOVA	104
Figure 5.4 Simplified diagram of the TCA (Krebs' cycle)	108
Figure 5.5 Voltage-gated sodium current in wild-type aCC/RP2 motoneurons	112
Figure 5.6 Transient current-voltage relationships in Canton-S, <i>Ocd^{5-S}</i> and <i>Ocd^{7-S}</i>	113
Figure 5.7 Mean peak transient sodium currents (I_{Na}) at -15mV in wild-type and <i>Ocd</i> flies	114
Figure 5.8 General Linear Model ANOVA for peak transient current data	115
Figure 5.9 Male-male courtship test for deafness in <i>Ocd^{5-G}</i> and wild-type flies	118
Figure 5.10 NaCl sensitivity assay in heterozygous <i>Ocd</i> females and wild-type females	119
Figure 5.11 KCl sensitivity assay in heterozygous <i>Ocd</i> females and wild-type females	120
Figure 5.12 Preliminary data from DDT contact assay	123
Figure 5.13 DDT lethality assay in wild-type and <i>Ocd</i>	124

List of tables

Table 1.1 Lethal deletions used to map <i>Ocd</i>	30
Table 2.1 <i>Drosophila</i> lines used	38
Table 2.2 Molecular biology kits and suppliers	44
Table 2.3 Standard thermal cycling conditions for PCR	46
Table 2.4 PCR primers used to amplify region around SNPs in SNP mapping	48
Table 2.5 Minisequencing primers for SNaPshot genotyping.	48
Table 2.6 Inverse PCR primers and reaction annealing temperatures	49
Table 2.7 Primer sequences for inverse PCR and sequencing of PCR products	49
Table 3.1 Mitochondrial candidate genes in and around the region 13F1-16A2	57
Table 3.2 SNPs identified across the <i>Ocd</i> region.	59
Table 3.3 The five <i>P</i> element lines used in mapping	67
Table 3.4 Number of parental and recombinant flies in <i>P</i> element mapping	67
Table 3.5 Genetic distances between pairs of markers used in the five crosses	68
Table 3.6 Data from complementation tests between <i>Ocd</i> and <i>para</i>	73
Table 4.1 Inherited sodium channel disorders	82
Table 4.2 <i>para</i> mutations identified in <i>Ocd</i> lines	89
Table 5.1 Mitochondrial proteins differentially expressed in wild-type and <i>Ocd</i> flies	105
Table 5.2 Non-mitochondrial proteins differentially expressed in wild-type and <i>Ocd</i> flies	106
Table 5.3 Sodium channel neurotoxins and corresponding receptor sites	122
Table 5.4 Resistance levels of wild-type and <i>Ocd</i> lines to DDT	124

List of accompanying material

Karp, N. A., Spencer, M., Lindsay, H., O'Dell, K. & Lilley, K. S. (2005) Impact of Replicate Types on Proteomic Expression Analysis. *J Proteome Res*, 4, 1867-1871.

Acknowledgements

Firstly I would like to thank my supervisor Kevin O'Dell for guidance, patience and support throughout the last three years, and also my 'unofficial supervisor' Howy Jacobs, for giving me the opportunity to work in Tampere, and for encouraging me to pursue this project. Thank you to Richard Wilson and Julian Dow, my assessors, for their comments and suggestions, and thanks to BBSRC for funding.

I thank everyone in Stephen Goodwin's group for use of equipment, advice and friendship, and Darren Monckton and everyone on Level 5 for letting me use the facilities there and 'borrow' reagents. Thank you Graham Hamilton for help in computer crises and Colin Moran and Richard Wilson for help with the necessary evil that is statistics. Thank you Jean-Christophe for proof-reading this thesis.

Thanks to Kathryn Lilley at Cambridge for assisting with the 2D DIGE experiment, Richard Baines and Ed Pym at Warwick for the electrophysiology data, and Sam Boundy and Richard ffrench-Constant at Bath for help with the DDT bioassay.

I would like to thank many friends for support and happy times. There are too many to mention but thank you to all in Molecular Genetics at Glasgow University, all in Howy Jacobs' and Hans Spelbrink's labs in Tampere, and of course the Gala birds.

I would like to thank my family, especially Mum and Dad for vast emotional (and financial) support. I count myself lucky to have such a wonderful family. And finally, thanks to Dave for always being there for me throughout the stress and tears. I love you all very much.

This thesis is dedicated to the memory of Sofia Patisso.

Abstract

Out cold (Ocd) is an X-linked *Drosophila* gene, mutations in which lead to dominant cold-sensitive paralysis. Previous studies have suggested that *Ocd* may have some involvement in mitochondrial energy metabolism. The primary objective of this work was to identify the *Ocd* gene and gene product, and determine how mutations in it result in this complex phenotype. Two strategies were employed to narrow down the *Ocd* critical region: SNP mapping and *P* element mapping. From an original area of 1.5Mb, the critical region was reduced to less than 100kb and only six candidate genes. Complementation tests between *Ocd* and *paralytic (para)*, a voltage-gated sodium channel gene, suggested the two are allelic. Subsequent sequencing of *Ocd* lines revealed mutations within highly conserved regions of *para*, both within transmembrane segment S6 of domain III (I1545M, T1551I), and in the linker between domains III and IV (G1571R), the putative location of the channel inactivation gate. Further evidence for allelism between *Ocd* and *para* was obtained from electrophysiology and pesticide resistance experiments. In addition, a proteomics study was conducted which supports the notion of mitochondrial defects arising as a consequence of the *Ocd* mutations. The G1571R mutation is of particular interest as mutations of the orthologous residue in the human skeletal muscle sodium channel gene *SCN4A*, G1306, have been associated with cases of periodic paralysis and myotonia, including the cold-sensitive disorder paramyotonia congenita. The mechanisms by which sodium channel mutations lead to such phenotypes are not well understood. In the absence of a suitable vertebrate model system, *Ocd* provides a system in which genetic, molecular, physiological and behavioural tools can be exploited to determine mechanisms underlying sodium channel periodic paralyses.

Declaration

The research reported in this thesis is my own original work, except where otherwise stated, and has not been submitted for any other degree.

Helen Lindsay

Helen Anne Lindsay

December 2005

List of abbreviations

μ	micro (10^{-6})
2D DIGE	two dimensional difference gel electrophoresis
A	adenine
A	Ampere
aa	amino acid
ANOVA	analysis of variance
ATP	adenosine triphosphate
b	base
BBSRC	Biotechnology and Biological Sciences Research Council
bp	base pair
BLAST	basic local alignment tool
BSA	bovine serum albumin
BVA	biological variance analysis
$^{\circ}\text{C}$	degrees Celsius
C	cytosine
cAMP	cyclic adenosine monophosphate
CO_2	carbon dioxide
CCP	Cambridge Centre for Proteomics
cM	centimorgans
CNS	central nervous system
CS	Canton-S
<i>da</i>	<i>daughterless</i>
Da	Dalton
dB	decibel
<i>Ddc</i>	<i>Dopa decarboxylase</i>
DDT	dichlorodiphenyltrichloroethane
<i>Df</i>	deficiency
DNA	deoxyribonucleic acid
DNaseI	deoxyribonuclease I
dNTP	deoxynucleotide triphosphate
<i>Dp</i>	duplication
<i>E. coli</i>	<i>Escherichia coli</i>

EDTA	ethylenediaminetetraacetic acid
EGTA	ethyleneglycoltetraacetic acid
<i>elav</i>	<i>embryonic lethal, abnormal vision</i>
EMS	ethylmethanesulphonate
EtBr	ethidium bromide
<i>ey</i>	<i>eyeless</i>
F	Faraday
<i>g</i>	centrifugal force equal to gravity acceleration
<i>g</i>	gram
G	guanine
GABA	gamma-aminobutyric acid
GEFS+	generalised epilepsy with febrile seizures plus
GFP	green fluorescent protein
GLM	general linear model
hr	hour
<i>hang</i>	<i>hangover</i>
HEPES	N-2-hydroxyethylpiperazine-N'-2-ethanesulfonic acid
<i>Hsp70</i>	<i>Heat-shock protein 70</i>
HOKPP	hypokalemic periodic paralysis
HYPP	hyperkalemic periodic paralysis
I	current
k	kilo (10^3)
kb	kilobase pairs
KCl	potassium chloride
l	litre
LD ₅₀	LD ₅₀
LQTS	long QT syndrome
m	milli (10^{-3})
M	molar
Mb	megabase pairs
<i>Mef2</i>	<i>Myocyte enhancing factor 2</i>
MELAS	mitochondrial encephalomyopathy, lactic acidosis and stroke-like episodes
MERRF	myoclonic epilepsy with ragged red fibres
mRNA	messenger RNA

ms	milliseconds
MS	mass spectrometry
mtDNA	mitochondrial DNA
MW	molecular weight
n	nano (10^{-9})
Na ⁺	sodium ions
NaCl	sodium chloride
NARP	neuropathy, ataxia, and retinitis pigmentosa
NCBI	National Centre for Biotechnology Information
nt	nucleotides
<i>Ocd</i>	<i>Out cold</i>
OD	optical density
ORR	Oregon-R
OXPPOS	oxidative phosphorylation
p	pico (10^{-12})
PAGE	polyacrylamide gel electrophoresis
PAM	potassium-aggravated myotonia
<i>para</i>	<i>paralytic</i>
PMC	paramyotonia congenita
PCR	polymerase chain reaction
pI	isoelectric point
pmol	picomoles
PNS	peripheral nervous system
RNA	ribonucleic acid
RNase A	ribonuclease A
rpm	revolutions per minute
RT	room temperature
s	seconds
<i>sbl</i>	<i>smellblind</i>
SDS	sodium dodecyl sulphate
<i>Sgs3</i>	<i>Salivary gland secretion 3</i>
SIDS	sudden infant death syndrome
SNP	single nucleotide polymorphism
T	thymine
TCA	tricarboxylic acid

TE	Tris-EDTA
Tris	tris(hydroxymethyl)aminomethane
U	unit
UAS	upstream activating sequence
UCP	uncoupling protein
UV	ultraviolet
V	volt
VNC	ventral nerve cord
v	volume
w	weight
w	<i>white</i>
wt	wild-type

1 Introduction

1.1 *Drosophila* as a genetic model organism

The fruit fly *Drosophila melanogaster* has for almost a century been widely appreciated as a tractable genetic model organism, thanks to features such as a short life cycle and high fecundity (O'Kane, 2003). Due to their small size, fruit flies are also inexpensive and relatively easy to maintain in the laboratory. Although mammalian models are, rightly so, regarded as the ideal model for studying human disorders, the completion of the human and fly genome projects has revealed the striking similarity of these two species at the genetic, molecular and cellular level (Kornberg and Krasnow, 2000).

The fruit fly is composed of many the major cell types found in mammals, and the cellular processes occurring throughout development are conserved. Although some systems are relatively simplified in flies, the functions remain the same. Because of this, *Drosophila* can be used as a model for dissecting genetic pathways and investigating how normal human cells function. One recent study estimated that approximately 77% of human disease genes have at least one *Drosophila* homologue (Reiter *et al.*, 2001). This remarkable degree of relatedness makes *Drosophila* an ideal organism in which to study the pathogenesis of human disorders, and further therapeutic developments. The fruit fly has been used successfully to model a multitude of diseases including cancer (Brumby and Richardson, 2005), neurodegenerative disease (Fortini and Bonini, 2000) and mitochondrial disorders (Jacobs *et al.*, 2004).

The wealth of tools available to *Drosophila* researchers has made the fruit fly an amazingly amenable model organism. Reverse genetics screens are routinely used to identify genes of specific functional relevance (reviewed by Adams and Sekelsky, 2002). The generation of mutant lines via ethylmethanesulphonate (EMS) or *P* element mutagenesis, or by reducing protein expression using RNA interference, can provide a vast amount of information about the wild-type gene function and, in most cases, this information will prove relevant to human disease genes. Mutation mapping techniques are well developed in *Drosophila*, commonly making use of *P* element insertions or single nucleotide polymorphisms (SNPs) (Hoskins *et al.*, 2001, Zhai *et al.*, 2003). However, sequencing of *P* element flanking regions means identification of disrupted genes is even simpler, and mapping is not required. Recent advances in *Drosophila* endogenous gene-targeting via homologous

recombination have made introducing defined mutations and gene knock-outs possible (Gong and Rong, 2003, Rong and Golic, 2000). This means mutations equivalent to those associated with human disease can be created in the fly, so that mechanisms of pathogenesis can be examined, and treatments developed.

An elegant expression system allowing targeted gene expression is now well established in *Drosophila*. The GAL4/UAS system (Brand and Perrimon, 1993) allows temporal or spatial specific expression of any gene of interest, and is widely used for the investigation of medically important genes and cellular processes (reviewed by Duffy, 2002). This system was developed to allow targeted gene expression in *Drosophila*, making the fruit fly one of the most tractable genetic model organisms. The *Saccharomyces cerevisiae* GAL4 protein regulates yeast genes by binding to upstream activating sequences (UAS). In *Drosophila*, GAL4 can be used to drive expression of UAS reporter genes. To do this, flies containing two separate constructs must be generated; one construct carrying a GAL4 driver and one carrying a UAS responder. Targeted gene expression of the gene of interest (the responder) is achieved through GAL4 directed expression in a particular spatial or temporal pattern (Figure 1.1).

Another advantage of using *Drosophila* is that modifier screens are simple to conduct. These screens can be used to identify alleles that suppress or enhance mutant phenotypes (reviewed by St Johnston, 2002). This is commonly achieved using a mutagenesis approach, but alternative methods can prove highly rewarding. For example, in any given mutant, selecting for a less severe (and therefore more wild-type) phenotype over many generations will inevitably lead to the accumulation of suppressors. One way to identify these might be to examine global gene expression patterns via microarrays, which are now commonly used in *Drosophila* research (reviewed by Gupta and Oliver, 2003). Characterising such modifier genes can help to identify pathways involved in pathogenesis. Most identified genes will have human homologues, which may be candidate genes for human disease, and may identify routes via which such diseases may be treated.

This project focuses on the characterisation of a set of unmapped *Drosophila* mutations, and the development of them as a model for human disease. Based on the mutant phenotype, which will be described in detail later, it is feasible that the mutants may provide a model for either mitochondrial or neurological (seizure) diseases, or both.

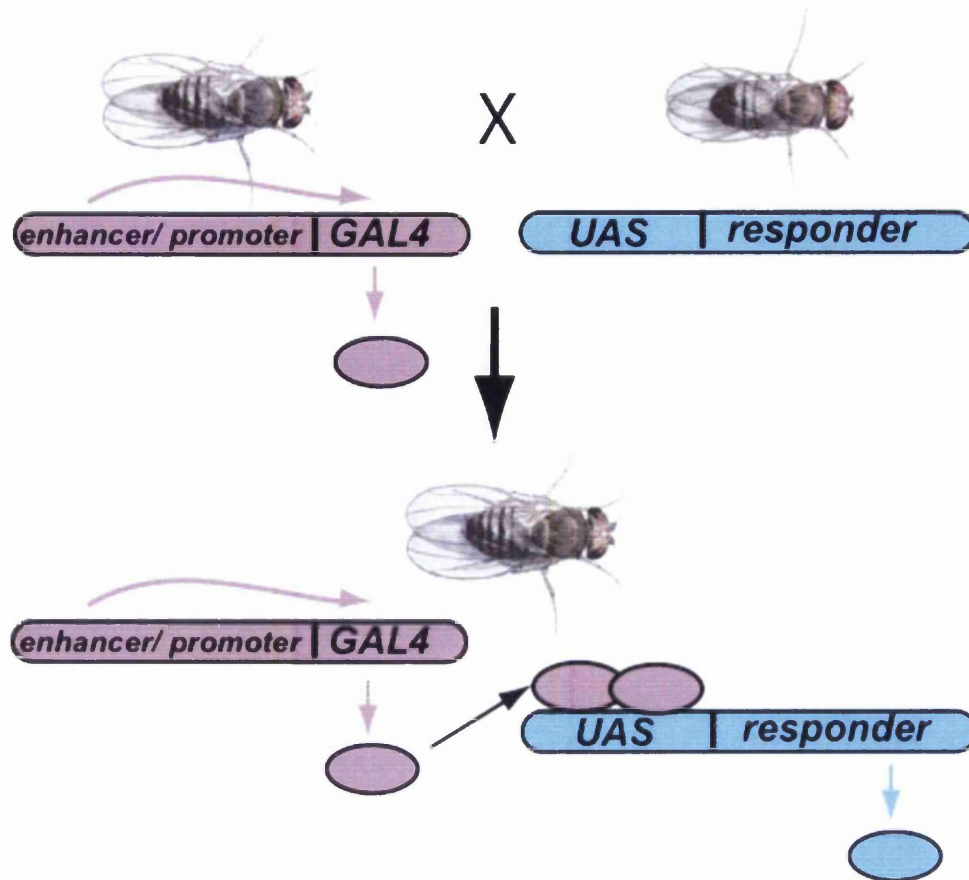


Figure 1.1 The GAL4/UAS system in *Drosophila*

A simplified overview of the GAL4/UAS system exploited in fruit flies. In the cross shown, a female fly expressing GAL4 in a defined spatial or temporal pattern under the control of an enhancer or promoter element is mated to a male carrying an upstream activating sequence (UAS) responder construct. In the absence of GAL4, the gene of interest, or responder, is not transcribed. Progeny from this cross however will contain both GAL4 and UAS elements. This means that the GAL4 protein is able to bind to the UAS element and drive expression of the responder gene. GAL4 will only be expressed in certain tissues and/or developmental stages so in this way, targeted gene expression is achieved.

1.2 Human mitochondrial disorders and fly models

In humans, mitochondria provide all cells of the body with energy in the form of adenosine triphosphate (ATP), generated through the process of oxidative phosphorylation (OXPHOS). It is not surprising then that mitochondrial dysfunction can affect a broad range of tissues and functions. They also play a central role in programmed cell death and the process of ageing (reviewed by Chomyn and Attardi, 2003). Human mitochondrial DNA (mtDNA) is a double-stranded circular DNA molecule, 16.5kb in length (Anderson *et al.*, 1981). This DNA encodes 13 polypeptides involved in the electron transport chain,

two ribosomal RNAs and 22 transfer RNAs. mtDNA is highly polymorphic as mutations accumulate relatively quickly due to a poor repair system compared to that of nuclear DNA, and also because errors are more likely to be tolerated as there are many copies of the mitochondrial genome in each cell. mtDNA is maternally inherited, although exceptions to this rule have been reported (for example, Schwartz and Vissing, 2002).

Human mitochondrial defects may arise not only from mutations in mtDNA, but from nuclear DNA defects or from environmental toxins. Nuclear genes encode several subunits of the OXPHOS complexes located in the mitochondrial inner membrane, and regulate the transport and the modification of such polypeptides. They also have a role in the maintenance of mtDNA and in the translation of mtDNA-encoded polypeptides (Singh, 1998). Therefore a nuclear mutation can have a direct or indirect mitochondrial effect. This results in a mitochondrial disease being inherited in an autosomal recessive or dominant manner, and not maternally. Such mutations have even been shown to predispose to mtDNA deletions (reviewed by Simon and Johns, 1999).

Mutations in mtDNA give rise to a broad range of phenotypes in humans, but generally tissues with high energy consumption, such as brain and muscle, are most affected (reviewed by Taylor and Turnbull, 2005). A single mutation may produce different symptoms in two different patients (clinical heterogeneity), and a single clinical phenotype may be associated with several mutations (genetic heterogeneity), making correct diagnosis and treatment problematic. There are various symptoms typical of mitochondrial dysfunction, including neurological anomalies (strokes, ataxia, seizures, deafness etc.), cardiomyopathy, and endocrine abnormalities. Mitochondrial disease is often not easily diagnosed. However, aside from identifying underlying mutations, abnormal mitochondrial proliferation in cells, particularly muscle cells, may be detected using staining techniques, and histochemical analysis may reveal cytochrome c oxidase (COX) deficiency in patient muscle (reviewed by Wallace, 1999, and Simon and Johns, 1999).

Some classic mitochondrial disorders which lead to a seizure phenotype in humans are mitochondrial encephalomyopathy, lactic-acidosis, and stroke-like episodes (MELAS) (Goto *et al.*, 1990), myoclonic epilepsy with ragged red fibres (MERRF) (Shoffner *et al.*, 1990), neuropathy, ataxia, and retinitis pigmentosa (NARP) (Holt *et al.*, 1990), and maternally inherited Leigh syndrome (de Vries *et al.*, 1993). The genetic bases of these conditions are largely understood - primarily missense mutations in mitochondrial tRNAs,

NADH dehydrogenase subunits, or ATPase genes - but they remain essentially untreatable. Developments of treatment at the gene level have been held back through the lack of appropriate model systems (Taylor and Turnbull, 2005). It is anticipated that research into mitochondrial dysfunction may aid in developing suitable animal models that may eventually yield improved therapeutic options.

The fruit fly is now widely recognised as a valid model of human mitochondrial function and dysfunction. A database exists listing *Drosophila* proteins targeted to the mitochondrion (Sardiello *et al.*, 2003). *Drosophila* and human mitochondrial genomes are remarkably similar, encoding exactly the same proteins, rRNAs and tRNAs (Clary and Wolstenholme, 1985). The role of mitochondria in oxidative phosphorylation, intermediary metabolism and programmed cell death is conserved from fly to man. *Drosophila* can be successfully used as a model of human mtDNA replication (Garesse and Kaguni, 2005), ageing (Ballard, 2005) and apoptosis (Twomey and McCarthy, 2005). In addition, it had been shown that it is possible to model specific mitochondrial diseases, such as mitochondrial deafness in *Drosophila*. Remarkably, mutations in the *Drosophila* ribosomal mitochondrial subunit S12 lead to phenotypes very similar to those observed in humans suffering from mitochondrial dysfunction, including deafness, seizures and antibiotic sensitivity (Toivonen *et al.*, 2001). Identifying genes or chemicals that mitigate the fly mutant phenotype via second-site modifier screens may identify routes by which the human disorder can be treated.

1.3 Human seizure disorders and fly models

Human seizure disorders are a heterogeneous group of relatively common nervous system conditions, including the epilepsies, which affect approximately 1% of the population (McNamara, 1994). Many of these disorders involve a genetic predisposition, although any person can be at risk from developing a seizure disorder following severe insult to the brain (Noebels, 1996). The term epilepsy is normally used to describe recurrent spontaneous attacks, resulting in altered motor activity, consciousness or behaviour, caused by abnormal electrical activity in cerebral neurons. Seizures - usually convulsions or fits - can also arise as isolated occurrences, as part of another disorder or following head trauma. Exogenous stimuli such as anticonvulsant drugs, sound, light, and hypoxia can induce seizure episodes (Guerrini *et al.*, 1998, Verrotti *et al.*, 2004, Jensen and Baram, 2000).

Despite the prevalence of these disorders, the genetic and molecular basis of most is as yet unclear. More than a dozen genes involved in human epilepsies have been identified (Upton and Stratton, 2003), and there are likely to be many more yet to be discovered.

As mentioned previously, mitochondrial mutations can cause the syndromic seizure disorders such as MERFF and MELAS, which are largely untreatable. Indeed, it is thought that oxidative stress, as well as being a consequence of seizures, plays a significant role in epileptogenesis (Patel, 2004).

Another common cause of seizures, are mutations in ion channel genes (Lerche *et al.*, 2005, Lerche *et al.*, 2001, Gutierrez-Delicado and Serratos, 2004). Ion channel mutations may induce seizures through prolonged depolarisation, or through repetitive firing of neurons. For example, molecular lesions in the voltage-gated sodium channel alpha subunits have been associated with the disorders generalised epilepsy with febrile seizures plus (GEFS+) and severe myoclonic epilepsy of infancy (Claes *et al.*, 2001, Escayg *et al.*, 2000). Additionally, mutations in two voltage-gated potassium genes, *KCNQ2* and *KCNQ3* have been found in families with benign familial neonatal convulsions (Biervert and Steinlein, 1999, Hirose *et al.*, 2000). Mutations in the voltage-gated chloride channel gene *CLCN2* have also been uncovered in cases of idiopathic generalised epilepsy (Haug *et al.*, 2003).

Mutations in subunits of both the gamma-aminobutyric acid (GABA) receptor and the nicotinic acetylcholine receptor have been implicated in the seizure disorders generalised epilepsy with febrile seizures plus and autosomal dominant nocturnal frontal lobe epilepsy, respectively (Baulac *et al.*, 2004, McLellan *et al.*, 2003). These classes of mutation alter neurotransmitter release or alter postsynaptic sensitivity at central synapses, leading to the onset of seizures.

Without a complete understanding of seizure pathogenesis, most seizure disorders remain largely untreatable, and are rather controlled through the administration of anticonvulsant drugs. Often, an underlying causative disorder will require treatment, for example brain lesions or endocrine abnormalities. Animal models provide an invaluable tool for dissecting such conditions at the molecular and cellular level, and thus paving the way for the development of novel, more effective treatments. Using an animal model can also

prove fruitful in identifying why certain mutations lead to specific types of seizure disorders, and also in exploring the effects of exogenous factors.

A plethora of mouse models for epilepsy exist, comprising both spontaneous mutations as well as targeted transgenic mutants and gene knockouts (reviewed by Upton and Stratton, 2003). These are of great value to seizure research, and many human epilepsy phenotypes have been successfully recapitulated in the mouse. For example, transgenic mice carrying a targeted gain-of-function mutation within the mammalian neural voltage-gated sodium channel gene *Scn2a* undergo a progressive seizure disorder (Kearney *et al.*, 2001). Human *SCN2A* mutations have been associated with the disorder GEFS+ (Sugawara *et al.*, 2001). Also, knockout of the GABA_{B1} receptor subunit in mice leads to spontaneous generalised seizures (Prosser *et al.*, 2001). Such models will be invaluable in developing effective anti-epileptic therapies. In addition, other tractable genetic models such as *Drosophila* can also provide insights into the genetics and neurobiology of seizure disorders.

One very rewarding approach is to search for modifier genes of seizure phenotypes in *Drosophila* (Kuebler and Tanouye, 2000). Several *Drosophila* mutants have been identified as putative models for seizure disorders, on the basis of their bang-sensitive paralytic phenotype. Bang-sensitivity refers to seizure susceptibility following mechanical stress, such as vortexing, or electrical shock (Ganetzky and Wu, 1982, Pavlidis and Tanouye, 1995). Studying bang-sensitive mutants and the interaction between these and other behavioural mutants has been successfully used to identify mutants which can suppress seizure susceptibility (Kuebler *et al.*, 2001). These suppressors include mutations in the sodium channel gene *paralytic*, the potassium channel gene *Shaker*, the gap junction connexin gene *shaking B* (Song and Tanouye, 2005), and the meiotic gene *mei-P26* (Glasscock *et al.*, 2005). A similar approach has also been applied to *Scn2a* seizure-susceptible mice. Here, dominant modifier alleles were mapped via comparisons of the genetic backgrounds of mutants. Although two modifier loci were identified, the genes themselves have not been cloned (Bergren *et al.*, 2005).

1.4 The *Out cold* mutations

1.4.1 Introduction

As part of a collaborative project with the University of Tampere, Finland, we are interested in the development of fly models of human mitochondrial disorders. This will hopefully allow the mechanisms underlying such disorders to be studied in depth, and will ultimately provide a platform for therapeutic studies. The *Drosophila melanogaster* *Out cold* (*Ocd*) dominant cold-sensitive paralytic mutations are of interest as they were originally believed to have a mitochondrial role (Søndergaard *et al*, 1975, Søndergaard, 1976, Søndergaard, 1979a, Søndergaard, 1979b, Søndergaard, 1986). It is hoped that they may provide a model for human seizure disorders, particularly those associated with mitochondrial defects.

1.4.2 *Ocd* phenotype

Søndergaard (1975, 1979a) originally isolated seven EMS generated mutant alleles of *Ocd*, *Ocd*¹ - *Ocd*⁷, each of which was identified in a screen for dominant cold-sensitive paralysis. *Ocd*¹ was originally isolated in a student laboratory course at the University of Copenhagen where flies were mutagenised using 20mM EMS and mutant phenotypes scored, in this case lethality in males. Following the discovery of *Ocd*¹, 400,000 mutagenised wild-type Oregon-R (ORR) flies were screened for cold-sensitivity. Of these, only 25 independent mutants were isolated, six of which were X-linked and subsequently found through recombination studies to be allelic (Søndergaard, 1979a). This finding suggests that there may be only one gene on the X chromosome that can be mutated to result in dominant cold-sensitive paralysis.

Eleven mutations mapped to the third chromosome, and nine to the second. The third chromosome mutants were found to be allelic and termed *Third Cold Paralytic* (*TCP*). These remain largely uncharacterised although were shown to have defects in mitochondrial energy metabolism (Søndergaard, 1980). The second chromosome mutants have not been studied further.

In the original experiments, cold-sensitivity was quantified in a custom-made cold chamber in which time taken for flies to display paralysis-associated behaviours or to recover from

paralysis was measured. The cold-sensitivity can also be assayed by placing flies at 4°C and measuring the time it takes for them to exhibit paralysis, which is preceded by uncoordinated behaviour such as leg twitching and wing flutter. Although wild-type flies will also eventually become paralysed at 4°C, this will take much longer than for *Ocd* flies, usually more than five minutes.

Hemizygous *Ocd/Y* males display a more severe phenotype than heterozygous *Ocd/FM7* females (Søndergaard, 1975, Søndergaard, 1979a). They generally only eclose when stocks are maintained at 25°C, and when they do eclose are very unfit and often drown in the food medium. These males are unable to fly, unable to mate and walk in a reeling manner, although the mutant phenotype varies greatly between individual flies. At 25°C heterozygous females appear wild-type, with the exception of *Ocd²/+* and *Ocd³/+* females, which are unsteady, and some have droopy wings. Viable homozygous or trans-heterozygous *Ocd* females are weak, have reduced activity, walk in a reeling manner and frequently fall over. The lines vary greatly in terms of male lethality: *Ocd²* males eclose the most frequently, and *Ocd⁴* is almost completely lethal in males. With respect to cold-sensitive paralysis - associated phenotypes such as leg shaking and wing flutter, *Ocd⁴* flies are also the most severely affected, and *Ocd³* the least.

Initial investigations into the molecular basis of the *Ocd* cold-sensitive paralysis involved the study of the reaction kinetics of mitochondrial enzyme. The activity of succinate cytochrome c reductase is a measure of enzyme activity in both complex II and complex III of the respiratory chain. This enzyme complex catalyzes electron transfer from succinate to cytochrome c and is involved in ATP production. Activity was measured at varying temperatures in mitochondrial isolates using a spectrophotometer. Abrupt changes in the activation energy of this mitochondrial enzyme were observed upon temperature decrease in all *Ocd* flies (Søndergaard, 1975, Søndergaard, 1976, Søndergaard, 1979a). This correlates with the restrictive temperature for paralysis. None of the lines differed significantly in this respect from *Ocd¹*, where the change occurred at 18°C, except *Ocd⁷*, in which the change occurs at 16°C. However, these flies also undergo paralysis at 16°C rather than 18°C and therefore display the mildest *Ocd* phenotype.

This change in activation energy is also observed in wild-type flies, but occurs at a much lower temperature, 8°C, a temperature below which wild-type flies would also eventually be paralysed (Søndergaard, 1975). The change in *Ocd¹* flies may be due to a change in the

properties and composition of mitochondrial membrane-bound phospholipids. If membrane fluidity is affected by temperature, it follows that properties of membrane-bound proteins will also be altered. Indeed, using thin-layer chromatographic analysis, *Ocd*^l flies were shown to have low levels of the mitochondrial phospholipid sphingomyelin compared to wild-type (Søndergaard, 1979a). Other classes of lipids were not significantly different. It might be that phospholipid composition might have some effect on succinate cytochrome c reductase activity. However, experiments where phospholipid extract from either *Ocd* or wild-type mitochondria were rebound to *Ocd* or wild-type lipid-deficient mitochondria revealed that the change in succinate cytochrome c reductase activity observed in *Ocd* flies was independent of the source of phospholipids used (Søndergaard, 1979b). It must therefore be the membrane proteins themselves that elicit this effect.

The connection between cold-induced changes in mitochondrial enzyme kinetics and paralysis is not clear. Mitochondrial dysfunction and oxidative stress, as well as being the cause of some epileptic disorders, is also a recognised consequence of seizures (reviewed by Patel, 2004). Seizures can result in oxidative damage to lipids, DNA and mitochondrial proteins, particularly iron-sulphur enzymes such as aconitase (Melov *et al.*, 1999). Therefore, it may be that the *Ocd* mutations confer cold-sensitive paralysis, which in turn affects mitochondrial function, rather than the mitochondrial effect observed being a direct result of the mutations.

Interestingly, an additional mitochondrial effect has been reported in *Ocd* flies. An abnormal pattern of mitochondrial polypeptides was identified upon 2D gel electrophoresis (Søndergaard, 1986). An unidentified extra protein was revealed in *Ocd* mutant males and females carrying the *Dp(1;4)r⁺f⁺* duplication (Figure 1.2). *Dp(1;4)r⁺f⁺* is a duplication of part of the X chromosome (14A1-16A2) onto the fourth chromosome which can partially rescue the *Ocd* phenotype (see next section). However, these flies display a mutant phenotype even at 25°C so a protein change is likely to occur at even at the permissive temperature. It is not clear whether a change in molecular weight or in isoelectric point elicited the creation of an aberrant protein. The protein change could be the result of a change in primary structure of a mitochondrial redox enzyme such that at 18°C the protein's conformation is altered. This might explain the observation of altered activation energy profile of succinate cytochrome c reductase in *Ocd* mutants. This particular theory has yet to be investigated further.

The 2D gel analysis points towards the involvement of *Ocd* in the mitochondrion. Søndergaard (1986) speculates that *Ocd* may have a role in phospholipid synthesis, mitochondrial structure, the modification of nuclear encoded mitochondrial proteins, or processing of mitochondrial gene products. As noted previously, the mitochondrial effect observed may be a secondary consequence of the *Ocd* mutation, possibly induced by the seizures which affect *Ocd* flies.

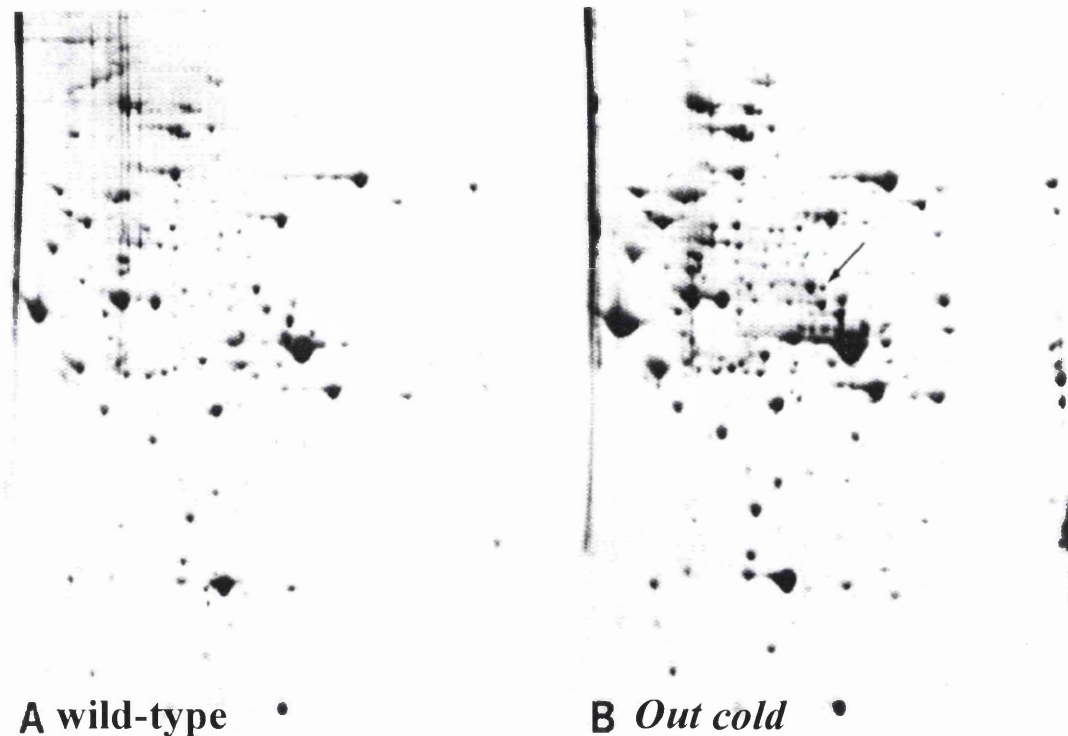


Figure 1.2 2D gel electrophoresis of mitochondrial proteins in wild-type and *Ocd* flies

The figure shows 2D electrophoretic separations of mitochondrial polypeptides isolated from males and females from A. wild-type (ORR) and B. *Ocd*¹; *Dp(1;4)r⁺f^{*}*. The aberrant polypeptide detected in *Ocd* flies by Søndergaard (1986) is indicated by an arrow. Taken from Søndergaard (1986).

1.4.3 Mapping *Ocd*

The *Out cold* gene has yet to be cloned. However, *Ocd* has already been partially mapped to a region of the X chromosome. A duplication of part of the X chromosome located on the fourth chromosome, *Dp(1;4)r⁺f^{*}*, can partially rescue the *Ocd* male phenotype in terms of coordination and ability to fly and mate, but there is pronounced variation between

individual flies (Søndergaard, 1975, Søndergaard, 1979a). The duplicated region is stated as either between 13F1 and 16A2 (Flybase: <http://flybase.org>) or 14A1 and 16A2 (Søndergaard, 1975). This places *Ocd* in a broad 1.5Mb region encompassing several hundred genes.

Recombination mapping placed *Ocd*^l 0.5cM±0.2 to the left of *rudimentary* (*r*), and the distance between *Ocd* and *forked* (*f*) was calculated as 1.7cM±0.2. This placed *Ocd* at X-55.2cM±0.2 (Søndergaard, 1975). Each of the other mutant *Ocd* alleles were subsequently shown to be about 1.7 cM to the left of *f*, based on analysis of at least 1000 F₂ flies for each mutation (Søndergaard, 1979a). This, and the fact that no recombination occurred between any of the mutations in approximately 10,000 offspring, implies that they are all allelic. This was further supported by complementation tests performed between each of the *Ocd* alleles. Trans-heterozygotes of each combination of alleles were created. In order to do this males carrying *Dp(1;4)r⁺f^{*}* were used. These males are able to mate successfully due to the rescuing effect of the duplication. Complementation was assayed by measuring duration of cold-sensitive paralysis-associated behaviours at 18°C: abnormal leg movements and leg stretching. Between each of the *Ocd* combinations, there was no significant difference in this duration. Although these observations would suggest that all of the *Ocd* mutations are allelic, only *Ocd*^l, *Ocd*^s and *Ocd*⁶ were shown through complementation to be truly allelic, on the basis that trans-heterozygotes of each combination of these alleles behaved like the respective homozygous females (Søndergaard, 1979a).

The original mapping data was generated using three cytologically defined deletions (*l*^D), and the duplication *Dp(1;4)r⁺f^{*}* (Søndergaard, 1975). Heterozygous *Ocd*^l females were crossed to deficiency (*l*^D) males which also carried *Dp(1;4)r⁺f^{*}*. Each of the deletions were stated as covering a region from at least 14D1 to 15A5-6. If any of the deletions covered the *Ocd* gene, *Ocd*/*l*^D females would be expected to behave like homozygous *Ocd* females or *Ocd* males. Because, in the case of each deletion, resulting *Ocd*^l/*l*^D females had a phenotype no more severe than heterozygous *Ocd* females, it was concluded that *Ocd* lies outside the deleted regions, and therefore was mapped to 14A1-14C8. Notably, the temperature at which these crosses were carried out and at which the phenotypes were scored was not stated.

However, in light of more recent mapping data generated on these deletions, the critical region is likely to be slightly larger (Table 1.1 and Figure 1.3).

Deficiency name (Flybase)	Annotation in Søndergaard, 1975	Breakpoints	Reference
<i>Df(1)D7</i>	l^{D7}	14C7-14F1	Loughney <i>et al.</i> , 1989
<i>Df(1)r-D17</i>	l^{d17}	14F6-15A6	Stern <i>et al.</i> , 1990
<i>Df(1)D34</i>	l^{d34}	14C6-14D1	Broadie and Bate, 1993

Table 1.1 Lethal deletions used to map *Ocd*

These are the lethal deficiencies described in Søndergaard (1975). The annotation has changed since, so both Søndergaard's and Flybase annotation is noted. In his paper, Søndergaard states that each of the deletions extend from and including the bands 15A5-6 and including at least band 14D1. However, approximations of the exact breakpoints of each deficiency have since changed, and the current estimated breakpoints are listed in the table. The breakpoints define the maximum possible length of the deletion based on estimates. *Df(1)D34* is in fact a small deletion within the voltage-gated sodium channel gene *paralytic* which results in a null mutation, abolishing sodium current (Baines and Bate, 1998).

The current estimated breakpoints of each deletion used in the deficiency mapping are shown in Table 1.1. The deletions are smaller than was originally stated (Søndergaard, 1975), and between them extend from 14C6 to 15A6, but there are gaps across the region which are not included, within which *Ocd* could conceivably lie. From this data, the critical region of *Ocd* is indeed approximately 14A1-14C8, but the gene could also lie somewhere between 14F1 and 14F6, or between 15A6 and 16A2, the right hand breakpoint of the duplication which rescues *Ocd* (Figure 1.3).

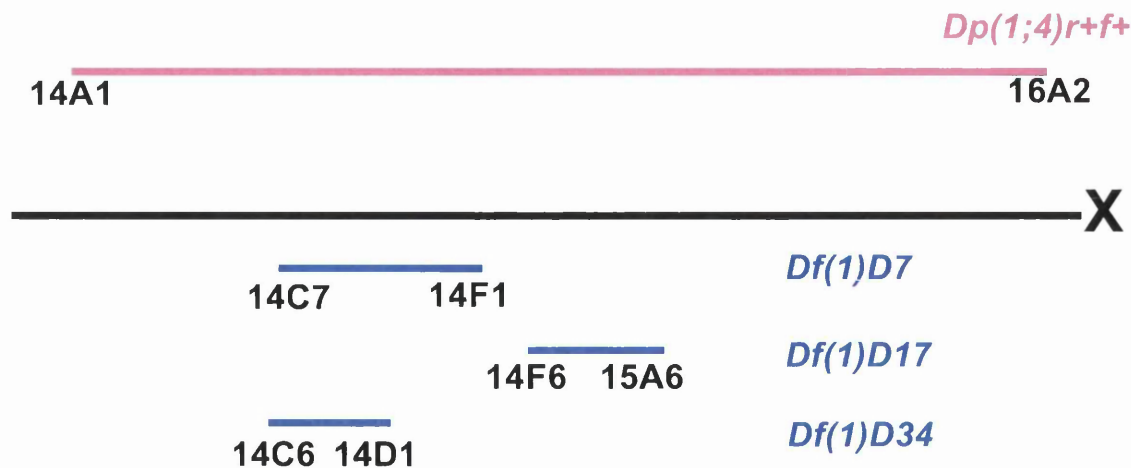


Figure 1.3 Deficiency mapping of *Ocd*

A duplication (magenta) and three deletions (blue) within the *Ocd* regions are shown, with estimated breakpoints displayed. The duplication *Dp(1;4)r⁺f⁺* is located on the fourth chromosome, and rescues the *Ocd* phenotype so *Ocd* must lie between 14A1 to 16A2 (Søndergaard, 1975). *Ocd*/*P* females do not behave like homozygous *Ocd* females or *Ocd* males, so it is unlikely that *Ocd* lies within any of the deleted regions. Estimates of the breakpoints of the deletions have changed since the Søndergaard's publication.

Several X-linked mutants were crossed to *Ocd*^l to test for any interaction and behavioural effect which might indicate complementation (Søndergaard, 1975). *paralytic*^{ts1} (*para*^{ts1}) and *shibire*^{ts} (*shi*^{ts}), two recessive temperature-sensitive paralytic mutants, were crossed to *Ocd*^l and the heterozygous phenotype examined. For each, cold-sensitive paralytic behaviour akin to heterozygous *Ocd* females was observed, but no heat-sensitive paralysis was observed upon temperature shift from 25°C to 30°C. It was thus concluded that *Ocd* is neither allelic with *para* nor *shi*. *Ocd*^l was also crossed to *Hyperkinetic* (*Hk*) mutants. *Hk* flies shake their legs under etherisation, and this phenotype was also observed in *Ocd*^l mutants. + *Ocd*^l/*Hk* + trans-heterozygotes displayed great variation in the degree of leg shaking between individuals, therefore no conclusions were reached regarding any interaction between the two mutations.

1.5 What causes cold-sensitivity?

Conditional mutants, such as those that are temperature-sensitive, provide a useful tool for studying mutant phenotypes such as behaviour in *Drosophila*. Because mutant behaviours can be switched on or off in one animal, the pathogenic mechanisms which lead to particular mutant phenotypes can be studied in depth. Conditional mutations can also be highly informative in mosaic animals, where tissue specificity of the mutations can be determined (Suzuki *et al.*, 1971). Many mutant genes are first isolated on the basis of their temperature-sensitivity, and there is a wealth of temperature-sensitive mutant lines available to researchers. In *Drosophila*, screening for temperature-sensitive mutants has proved invaluable in identifying genes involved in different processes, for example ribosome assembly (Falke and Wright, 1975a) and neurodegeneration (Palladino *et al.*, 2002). Indeed, temperature-sensitive mutations have been identified in genes as diverse as *nervous wreck*, which regulates synaptic growth at neuromuscular junctions (Coyle *et al.*, 2004); *pale*, a tyrosine hydroxylase involved in locomotory behaviour (Neckameyer and White, 1993); *bicoid interacting protein 1*, a regulator of transcription (Singh *et al.*, 2005); and *alpha actinin*, a structural constituent of the cytoskeleton (Fyrberg *et al.*, 1990).

Temperature-sensitive phenotypes often arise due to missense mutations, which alter folding properties and confer conformational changes to proteins at restrictive temperatures. Most temperature-sensitive *Drosophila* mutants isolated tend to be heat-sensitive rather than cold-sensitive. This might be simply due to the selection processes adopted by particular researchers, but it is reasonable to expect that mutations are more

likely to be heat-sensitive due to protein instability; most proteins are more stable at lower temperatures, although there are exceptions (Marshall, 1997). Mutations in some genes, for example *Acetylcholine esterase (Ace)*, can be either cold or heat-sensitive, but both classes affect protein secretion by affecting folding (Mutero *et al.*, 1994). Missense mutations are not necessarily the basis of temperature-sensitivity however.

The *Ocd* mutations lie somewhere in the region 14A1-16A2, an area which encompasses hundreds of genes. Aside from mitochondrial evidence, the analysis of cold-sensitivity or tolerance, even across species, may provide some clues as to what the *Ocd* gene might do, or a pathway which *Ocd* might be involved in. One important point to note with the issue of cold-sensitivity is that insects are poikilothermic; they lack a body temperature regulation system like that of mammals. This means they are subjected to a direct effect of temperature, which in turn can directly affect their genetic and biochemical machinery. Therefore, unlike mammals, there is a need to make internal compensations for changes in temperature in *Drosophila*.

Although there may be only one X-linked gene that mutates to result in dominant cold-sensitive paralysis (Søndergaard, 1979a), mutations in *comatose (comt)*, which encodes a N-ethylmaleimide-sensitive fusion protein and is important for neurotransmitter secretion (Dellinger *et al.*, 2000), can result in recessive cold-sensitive paralysis (Siddiqi and Benzer, 1976). However, *comatose* maps genetically to X-40, too far a distance from *Ocd* for the two to be allelic. A second X-linked gene is known to mutate to cause recessive cold-sensitive paralysis. The *hypoactive D (hypoD)* mutation is an allele of *slow receptor potential (slrp)*. Mutants are paralysed at 15°C (Homyk and Pye, 1989). *slrp* has not yet been cloned, but maps to 13F1-14B2, so is a possible candidate gene for *Ocd*.

In *Drosophila*, several temperature-sensitive paralytic mutants have been isolated with malfunctions in ion pump or channels. For example, the voltage-gated calcium channel *cacophony (cac)* mutants (Kawasaki *et al.*, 2000) and the voltage-gated sodium channel *paralytic (para)* mutants (Loughney *et al.*, 1989). A *P* element insertion in the sodium pump alpha subunit gene has also been shown to result in cold-sensitive recessive lethality (Feng *et al.*, 1997). *paralytic (para)* encodes the major functional voltage-gated sodium channel in *Drosophila* (Loughney *et al.*, 1989). Two *para* olfactory mutants, *para^{smellblind1}* and *para^{smellblind2}*, are associated with recessive cold-sensitive lethality (Lilly *et al.*, 1994b). The *para* gene lies within the *Ocd* critical region, and several previously characterised

mutations have been heat-sensitive paralytic (Suzuki *et al.*, 1971, Loughney *et al.*, 1989). In the *para* mutants *para^{smellblind1}* and *para^{smellblind2}*, flies actually survive to adulthood but then die prematurely at the restrictive temperature. An important point to note is that, unlike *Ocd*, mutants of these particular alleles of *para* have not been reported to undergo any paralytic behaviour. The process of action potential conduction is known to be temperature-sensitive; more sodium channel activity is required to maintain conduction at higher temperatures. A cold-sensitive human disorder associated with mutations of a sodium channel gene does exist, which manifests as the muscle disease paramyotonia congenita (Ptacek *et al.*, 1992).

In *Drosophila*, many recessive X-linked cold-sensitive mutants have been identified, but display an phenotype other than paralysis, for example lethality or sterility (Mayoh and Suzuki, 1973, Wright, 1973). Understanding the underlying processes leading to the cold-sensitivity in these mutants is also useful for speculating on the nature of the gene product *Ocd* encodes.

Studies in *Aspergillus* (Waldron and Roberts, 1974), *Neurospora* (Schlitt and Russell, 1974), and *Saccharomyces* (Bayliss and Ingrahm, 1974) have shown that eukaryotic cold-sensitive lethal mutants are often defective in ribosome assembly. This had previously been shown to be the case in prokaryotes, for example *Escherichia coli* (Guthrie *et al.*, 1969). One study in *Drosophila* involved the analysis of 13 cold-sensitive mutant lines and found eight to have deficiencies in ribosome assembly (Falke and Wright, 1975b). This was deduced from sucrose density gradient analysis of ribosome synthesis on a mitochondria-free extract. Evidence for a ribosomal defect was further strengthened by the fact that many strains were also female sterile, and also possessed some phenotypical characteristics similar to the *bobbed* mutant, which is known to have low ribosomal DNA levels. This finding would suggest that selecting for cold-sensitive mutants provides a route by which ribosome assembly defective lines can be identified.

Low temperatures can result in increased RNA secondary structures, which subsequently affects translation. Chilled bacteria express cold shock proteins that act as RNA chaperones to reduce RNA secondary structure and rescue translation (Jiang *et al.*, 1997). The closest *Drosophila* homologue of the major cold-shock protein in *E. coli*, *CspA*, is *CG9705* (de Bono *et al.*, 2005), which maps to 73C4.

Heat shock factor (HSF) regulates heat shock proteins that are important in the development of heat stress resistance. In *Drosophila*, the role of heat shock factor in resistance to cold stress has been investigated, but was found not to be of great importance (Muhlig Nielsen *et al.*, 2005). The gene *Frost*, which maps to 85E2, is implicated in the response and recovery to cold shock (Goto, 2001). *Frost* is up-regulated during recovery to cold shock (0°C) specifically - no difference in gene expression was detected following heat shock.

In contrast to vertebrates, both plants and insects can store amino acids. Cold tolerance in plants has been correlated with significant increases in proline levels (reviewed by Hare and Cress, 1997). This has also been demonstrated in flies (Misener *et al.*, 2001) and beetles (Bonnot *et al.*, 1998). Indeed, plants are known to undergo transcriptional changes in proline biosynthesis genes in response to many different stressors. Proline pool differences between cold tolerant and sensitive species have been demonstrated in *Drosophila* (Misener *et al.*, 2001). *Pyrroline 5-carboxylate reductase (P5cR)*, which maps to 91E4, is a housekeeping gene involved in proline biosynthesis and is continually present in higher levels than is ever required. As a consequence, *Drosophila* proline is always kept at elevated levels, which could theoretically help flies cope with stress. A large proline pool is important for *Drosophila* metabolism and survival during cold stress. It is therefore plausible that mutations in proline metabolism genes might lead to a cold-sensitive phenotype. However, Misener *et al.* (2001) detected no changes in transcript abundance in two genes encoding enzymes important for proline metabolism in response to low temperature. It is possible though that post-translational events may regulate proline pool changes.

In insects, membrane phospholipid composition is important in developing cold- or heat-tolerance. For species in certain parts of the world, it is important to be both cold- and heat-tolerant. To do this, a particular membrane composition must be adopted such that membrane fluidity is maintained at both hot and cold temperatures (Ohtsu *et al.*, 1998). Rapid cold hardening in insects is known to induce changes in the composition of membrane phospholipid fatty acids (Overgaard *et al.*, 2005). In theory genes regulating phospholipid synthesis, if mutated, could lead to cold- (or heat-) sensitive phenotypes. The *easily shocked (eas)* gene, which is involved in the biosynthesis of phosphatidylethanolamine, a dominant membrane phospholipid, is located within the

critical region for *Ocd*, at 14B7. This is of particular interest as it has already been shown that *Ocd*^l mutants have an altered phospholipid composition (Søndergaard, 1979b).

Mitochondrial uncoupling proteins (UCPs) are known to play a role in the regulation of body weight and in adaptive thermogenic processes. Murine mutations in UCP genes can lead to cold-sensitive phenotypes (Enerback *et al.*, 1997). Four UCPs have been identified in *Drosophila*, one of which, *Ucp4a*, lies close to the *Ocd* region, at 16E1 (Hanak and Jezek, 2001). However, UCP function in flies has not yet been fully characterised, and at present no mutant alleles have been described.

Ocd might be a novel or uncharacterised gene and analysis of the mutant lines are likely to shed some light on the mechanisms of cold-sensitivity and/or paralysis and seizure susceptibility.

1.6 Project Aims

The primary aim of this project was to identify the *Out cold* gene and gene product, and determine how mutations in it result in the complex phenotype of cold-induced paralytic seizures. Mapping the gene will make use of the wealth of SNP and *P* element markers available to the *Drosophila* researcher. This will confine the *Ocd* critical region to a manageable size for sequencing. Following the identification of *Ocd*, further characterisation of the mutant phenotype will further the development of *Ocd* as a model for human disease.

In the longer term, it is anticipated that the *Ocd* mutations will shed some light on human seizure disorders and/or mitochondrial disease, and provide a tractable model in which the questions of pathogenic mechanism and therapy can be addressed. Although the discovery of an *Ocd* human homologue is not guaranteed, understanding the nature of the *Ocd* gene should reveal a pathway that is likely to be involved in human seizure disorders and/or mitochondrial dysfunction, even if the orthologous gene in humans product is not.

2 Materials and methods

2.1 Drosophila

2.1.1 Drosophila stocks

<i>Drosophila</i> line	Description	Abbreviation	Reference(s)
wild-type Oregon-R Canton-S <i>white</i> ¹¹¹⁸ Oregon-R (S) FM7 CyO	wild-type wild-type ORR with the <i>w</i> ¹¹¹⁸ mutation wild-type (<i>Ocd</i> progenitor) X chromosome balancer Second chromosome balancer	ORR CS <i>w</i> ¹¹¹⁸ ORR-S FM7 CyO	
<i>Ocd</i> alleles (Glasgow)* <i>Out cold</i> ^{1-G} <i>Out cold</i> ^{3-G} <i>Out cold</i> ^{4-G} <i>Out cold</i> ^{5-G} <i>Out cold</i> ^{7-G} <i>white</i> ¹¹¹⁸ , <i>Out cold</i> ^{1-G}	dominant cold-sensitive paralytic mutants with mitochondrial defects <i>Ocd</i> ^{1-G} with the <i>w</i> ¹¹¹⁸ mutation	<i>Ocd</i> ^{1-G} <i>Ocd</i> ^{3-G} <i>Ocd</i> ^{4-G} <i>Ocd</i> ^{5-G} <i>Ocd</i> ^{7-G} <i>w</i> , <i>Ocd</i> ^{1-G}	Søndergaard, 1975 Søndergaard, 1979a
<i>Ocd</i> alleles (Søndergaard)* <i>Out cold</i> ^{1-S} <i>Out cold</i> ^{2-S} <i>Out cold</i> ^{3-S} <i>Out cold</i> ^{4-S} <i>Out cold</i> ^{5-S} <i>Out cold</i> ^{6-S} <i>Out cold</i> ^{7-S}	dominant cold-sensitive paralytic mutants with mitochondrial defects	<i>Ocd</i> ^{1-S} <i>Ocd</i> ^{2-S} <i>Ocd</i> ^{3-S} <i>Ocd</i> ^{4-S} <i>Ocd</i> ^{5-S} <i>Ocd</i> ^{6-S} <i>Ocd</i> ^{7-S}	Søndergaard, 1975 Søndergaard, 1979a
<i>P</i> element lines <i>y</i> ¹ , <i>w</i> , <i>P</i> { <i>SUPor-P</i> } <i>kat80</i> ^{KG02315} <i>y</i> ¹ , <i>w</i> ^{67c23} , <i>P</i> { <i>EPgy2</i> } <i>EY04615</i> <i>y</i> ¹ , <i>w</i> ^{67c23} , <i>P</i> { <i>EPgy2</i> } <i>EY3459</i> <i>y</i> ¹ , <i>w</i> ^{67c23} , <i>P</i> { <i>EPgy2</i> } <i>CG4239</i> ^{EY01983} <i>w</i> , <i>P</i> { <i>GT1</i> } <i>BG00710</i>	<i>CG3415</i> disrupted <i>small wing</i> disrupted <i>Furin 2</i> disrupted <i>CG4239</i> disrupted <i>hangover</i> disrupted	KG02315 EY04615 EY03459 EY01983 BG00710	Bellen <i>et al.</i> , 2004
GAL4 driver lines <i>w</i> ; <i>P</i> { <i>GAL4-Heat-shock protein 70.PB</i> } <i>w</i> ; <i>P</i> { <i>GAL4-daughterless.G32</i> } <i>w</i> ; <i>P</i> { <i>GAL4-1407</i> } <i>w</i> ; <i>P</i> { <i>GAL4-Myocyte enhancing factor 2.R</i> } <i>w</i> ; <i>P</i> { <i>GAL4-eyeless</i> }	GAL4 expressed upon heat-shock GAL4 ubiquitously expressed GAL4 expressed in neuroblasts and throughout development in neurons of the CNS and PNS GAL4 expressed in muscle GAL4 expressed in eye discs	<i>hs</i> :GAL4 <i>da</i> :GAL4 <i>1407</i> :GAL4 <i>dme</i> <i>f2</i> :GAL4 <i>ey</i> :GAL4	Jarman <i>et al.</i> , 1993 Wodarz <i>et al.</i> , 1995 Sweeney <i>et al.</i> , 1995 Ranganayakulu <i>et al.</i> , 1996 Bonini <i>et al.</i> , 1997

GAL4 driver lines (continued)			
<i>W: P{GALA-Dopa decarboxylase}</i>	GAL4 expressed in serotonergic and dopaminergic neurons	<i>Ddc:GAL4</i>	Li <i>et al.</i> , 2000
UAS responder lines			
<i>w; P{UAS-para13.5}</i>	<i>para</i> splice variant 13.5 expressed under GAL4 regulation. Insertion on second chromosome	<i>P{UAS:para⁺}</i> (II)	Warmke <i>et al.</i> , 1997
Other mutant lines			
<i>hangover^{AE10NT}</i>	<i>P</i> element insertion in <i>hangover</i>	<i>hang^{AE10}</i>	Scholz <i>et al.</i> , 2005
<i>Df(1)D34</i>	internal deletion of <i>para</i>	<i>para^{Df(1)D34}</i>	Broadie and Bate, 1993
<i>slow receptor potential^f</i>	cold-sensitive paralytic mutant	<i>slrp^f</i>	Homyk and Pye, 1989

Table 2.1 *Drosophila* lines used

**Out cold* lines are split into two groups - the Glasgow lines and Søndergaard's lines. There are slight variations in phenotypes between the two groups, likely to be due to the accumulation of modifiers. The Glasgow lines were obtained from Leif Søndergaard's laboratory at the University of Copenhagen in 1997. Most of the work in this project was conducted on them. Following the identification of the *Ocd* gene in 2004, the *Ocd* lines were obtained from Søndergaard and these were characterised further. Other lines were obtained from the Bloomington *Drosophila* stock centre, the Bellen lab (Baylor College of Medicine), Kevin O'Dell, Tony Dornan, (University of Glasgow), Richard Baines (University of Warwick), and Henrike Scholz (University of Würzburg).

2.1.2 *Drosophila* rearing conditions

Fly stocks were maintained in plastic vials or bottles (for large-scale amplification) containing food medium (1% (w/v) bacto-agar, 1.5% (w/v) sucrose, 3% (w/v) glucose, 3.5% (w/v) active dried yeast, 1.5% (w/v) maize meal, 1% (w/v) wheat germ, 1% (w/v) soya flour, 3% (w/v) treacle, 0.5% (v/v) propionic acid, 0.1% (w/v) nipagin M in H₂O). Stocks were reared at 18°C, room temperature (RT) or 25°C, with ambient humidity on a 12/12 hour light/dark cycle. Basic technique for the laboratory culture of *Drosophila* was as described by Ashburner (1989). All behavioural assays were conducted at 25°C unless otherwise stated.

In fly crosses, six females were crossed with six males of the required genotype in each vial. This gives the optimum amount of offspring, with no overcrowding. The parent flies were removed prior to the next generation hatching.

2.1.3 Isogenisation of *Drosophila* chromosomes

The *Out cold* mutations are X-linked. To isogenise the mutations, the method of chromosome substitution was used (Figure 2.1). This means that the X chromosome, and therefore roughly 20% of the genome remains from the original *Ocd* strain, but the other chromosomes are from a wild-type Canton-S line. This was necessary as at the time, the molecular nature of *Ocd* was unknown. Simply selecting for an *Ocd*-like (cold-sensitive) phenotype would prove problematic as it would result in the accumulation of modifiers. Once the underlying mutation is known, it is possible to isogenise the X chromosome as well, as flies can be confirmed as carrying the *Ocd* mutation via molecular techniques.

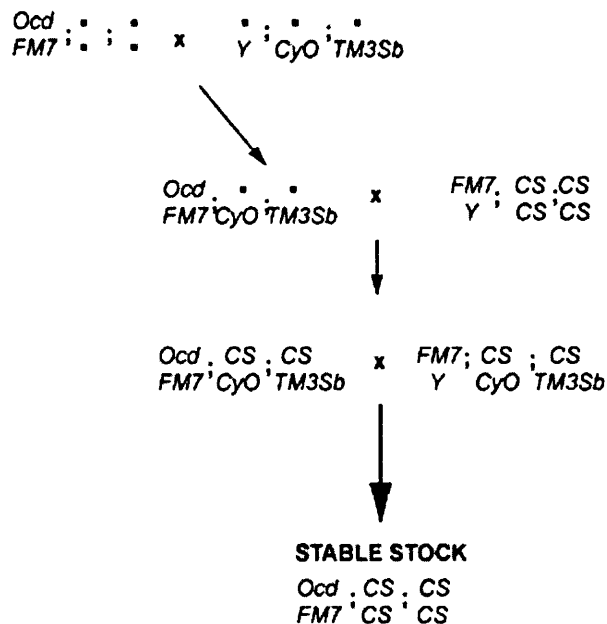


Figure 2.1 Chromosome substitution for the isogenisation of *Ocd* mutations
 In this isogenisation of *Ocd*, the X chromosome remains the same, but the other chromosomes are derived from wild-type Canton-S. In the crossing scheme the dots represent any chromosome; they are crossed out so their origin is not important.

2.1.4 Auditory behavioural assay

Deafness was measured using a modified version of the induced male-male courtship assay of Eberl *et al.* (1997). Six mute wingless males, aged between six and nine days, were transferred to mating chambers and subjected to five minutes of silence followed by 10 minutes of species-specific courtship song (*D. melanogaster*), provided by Mike Ritchie (University of St. Andrews). The courtship song was artificially generated, with a mean

interpulse interval of 35ms, which oscillated rhythmically. The basic pulse was 10ms with bursts of 72ms every six seconds. The song was played at 60, 80 or 100dB. The rate of courtship was measured 20 seconds before the song was played, and after 9 minutes, 30 seconds of the song's duration. Courtship was quantified by scoring the number of males involved in courtship behaviour such as following or orientation. To simplify the scoring, passive recipients were included in the system. The effect of song was calculated as the mean number of flies courting after song minus the number before song. $n=10$ for each mean value. $2 \times 2 \chi^2$ analysis was performed on the raw data to test for significant deviation from wild-type.

2.1.5 Cold-sensitive paralysis assay

Female flies were placed in batches of 10 in empty vials in a 4°C refrigerator for three minutes and the number of flies upright after each 30 second interval were scored. Flies on their backs with little or no leg movement were scored as having undergone paralysis. Standard error of the proportion was calculated as the square root of PQ/n , where P is the percentage of flies upright, Q is the percentage paralysed, and n is the sample size.

SNP and *P* element mapping: to determine which flies carried the *Ocd* mutation, male flies were placed in empty vials in a 4°C refrigerator for one minute, after which those flies that had undergone paralysis were scored as cold-sensitive. This is a stringent test for male flies, where the cold-sensitive paralysis is more severe than that of females.

2.1.6 Cold-sensitive male lethality assay

Replicate vials containing six females and three males were placed at either 18°C or 25°C. The numbers of males flies eclosing of each genotype were counted. The percentage of *Ocd* males out of the total number of males eclosing was determined and standard error of the proportion was calculated from the square root of PQ/n , where P is the percentage of *Ocd* males eclosing, Q is the percentage of FM7 males eclosing, and n is the sample size. $2 \times 2 \chi^2$ analysis was performed on the raw data to test for significant deviation between observations at 25°C and 18°C.

2.1.7 SNP mapping

Eight SNPs between *Ocd*^{*l-G*} and Oregon-R were identified through sequencing. Flies carrying a recombinant *Ocd*/ORR chromosome were generated, and the eight SNPs were genotyped using the ABI Prism SNaPshot™ Primer Extension Kit (section 2.2.9). The genotypes and phenotypes of recombinant flies allow an estimation of the relative position of *Ocd*, and the right hand limit of the *Ocd* region was defined. This is described in more detail in Chapter 3.

2.1.8 P element mapping

Ocd was mapped using five molecularly defined *P* element insertions, obtained from the BDGP Gene Disruption Project (Bellen *et al.*, 2004). The *P* elements were of three types (Figure 2.2). Insertion sites were confirmed using inverse PCR (section 2.2.10). The *Ocd*^{*l-G*} mutation was crossed into a *white* (*w*¹¹⁸) background. Flies recombinant between *Ocd* and each *P* element insertion were generated. Presence of each *P* element was scored by the presence of red eyes. Presence of the *Ocd*^{*l-G*} mutation was scored by tests for cold-sensitivity (section 2.1.5). Genetic distances between *Ocd* and each *P* element were calculated from the proportions of recombinant flies observed. Genetic distance, in centimorgans (cM) = number of recombinants divided by the total number of flies. Standard errors were calculated as the square root of PQ/n, where P is the percentage of recombinant genotypes, Q is the percentage of parental genotypes, and n is the sample size. This is described in more detail in Chapter 3.

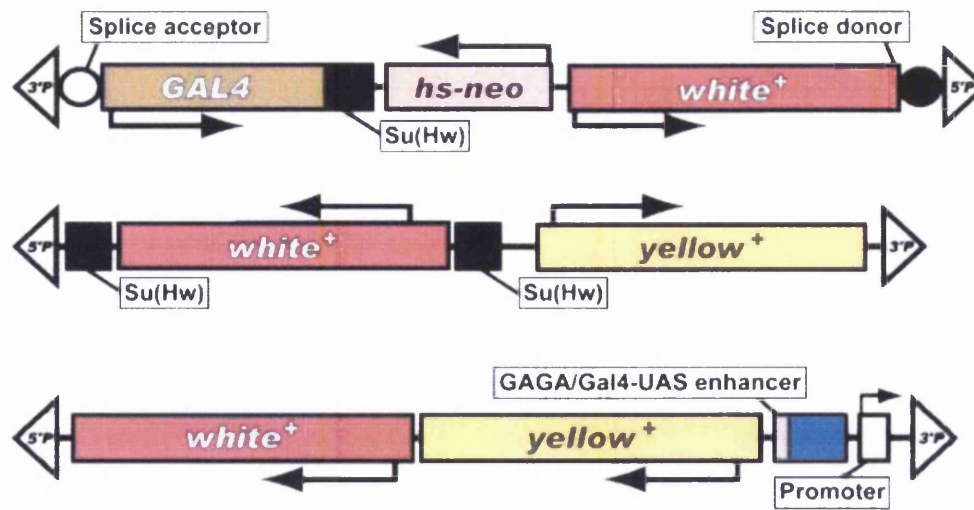


Figure 2.2 Schematic representations of the *P* elements used

Three different types of transposon insertion lines were used in mapping: Baylor genetrap (BG) lines (Lukacsovich *et al.*, 2001), Karpén genome (KG) lines (Roseman *et al.*, 1995) and EP yellow (EY) lines (Bellen *et al.*, 2004). BG elements are *P{GTI}* dual-tagging gene trap elements which drive expression of *white*⁺ when inserted into a gene, and also fuse a GAL4-containing exon with the target gene. EY elements are *P{EPgy2}* elements containing intronless *yellow*⁺ and mini-*white*⁺ gene markers. A GAGA/GAL4-UAS enhancer allows regulated misexpression of the adjacent downstream gene from the *P* element promoter under the control of GAL4. KG elements are *P{SUPor-P}* transposons which contain *suppressor of hairy-wing* (*Su(Hw)*) binding regions that act as chromatin insulators. This reduces positional effects on *white*⁺ expression, and can also alter gene expression by blocking interactions between enhancer/silencer elements and their promoter. Modified from Bellen *et al.*, 2004.

2.1.9 Complementation tests

Where possible, replicates of six heterozygous *Ocd*/FM7 females were crossed to three male flies mutant in one of the candidate genes. In the case of the *para* deficiency *Df(1)D34*, where males are lethal, replicates of six heterozygous *Df(1)D34*/FM7 females were crossed to three viable *Ocd* males. Only males from certain *Ocd* lines were viable and able to mate, for example Søndergaard's *Ocd*^{1-S}, *Ocd*^{5-S} and *Ocd*^{7-S} strains. Crosses were carried out at 25°C or 18°C. Trans-heterozygote female flies, recognised by absence of the markers carried on the FM7 balancer chromosome, were examined for mutant phenotypes, such as cold-sensitivity, uncoordinated behaviour and wing aberrations.

2.1.10 Rescue of male semi-lethality

Flies carrying the construct *P{UAS:para*⁺*}* on the second chromosome were crossed to *Ocd*^{1-G} flies using various balancer chromosomes in a series of crosses to give rise to *Ocd*^{1-G}/FM7 ; *P{UAS:para*⁺*}* females (Figure 2.3). In the rescue crosses, these females were

crossed to male flies. The male flies were either wild-type (Canton-S or Oregon-R) as a negative control, or carried a GAL4 construct to direct wild-type *para* expression in a specific fashion. The numbers of *Ocd*^{l-G} and FM7 males eclosing over four days from the first eclosion were counted, and the percentage of *Ocd*^{l-G} males eclosing out of the total males was calculated. Similarly, as a further control, *Ocd*^{l-G}/FM7 heterozygous females (without the *P{UAS:para}*⁺ construct) were crossed to males flies carrying each GAL4 construct and the number of *Ocd*^{l-G} and FM7 males eclosing counted. Standard error of the proportion for each value was calculated as the square root of PQ/n, where P is the percentage of *Ocd*^{l-G} eclosing, Q is the percentage of FM7 males eclosing, and n is the sample size. 2x2 χ^2 analysis was performed on the raw data to test for significant deviation from the results obtained in each negative control (absence of the *P{UAS:para}*⁺ construct and absence of the GAL4 driver).

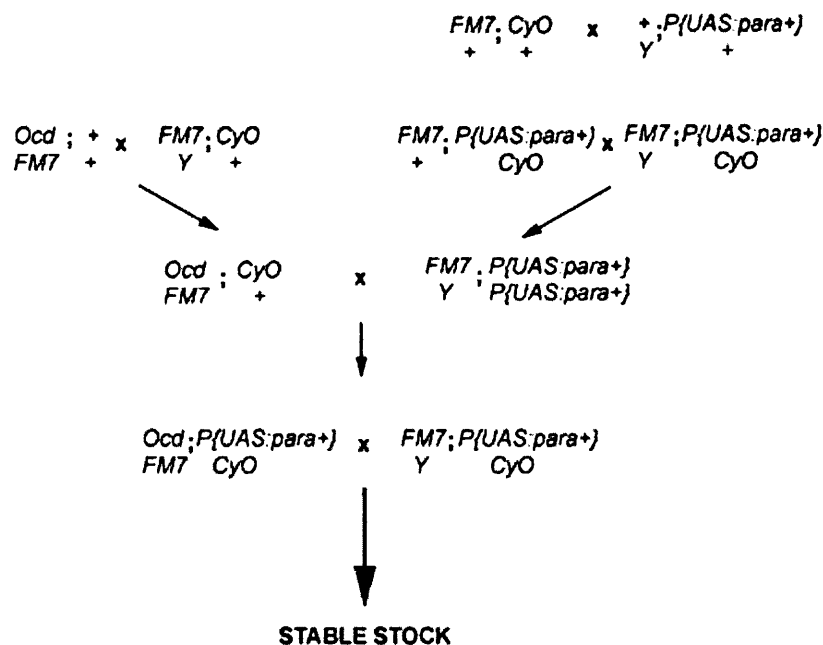


Figure 2.3 Crossing scheme to generate a stock of *Ocd* flies carrying the *P{UAS:para}*⁺ construct

The scheme shown is to generate an *Ocd* stock carrying *P{UAS:para}*⁺ on the second chromosome, using *CyO*, a balancer for the second chromosome.

2.1.11 *Dichlorodiphenyltrichloroethane (DDT) contact assay*

The DDT bioassays were performed by Sam Boundy in Professor Richard ffrench-Constant's laboratory, Department of Biology and Biochemistry, University of Bath. For DDT bioassays, 20 adult flies less than 72h post-eclosion were placed in glass vials with

interior surfaces evenly coated with varying concentrations of DDT (Sigma) dissolved in 200 μ l acetone and allowed to air dry. The vials were sealed with cotton wool soaked in 5% sucrose solution. Mortality was scored after 24h with flies being unable to move being scored as dead. Dose-response curves were estimated from six different concentrations of DDT with three replicates per dose. Probit analysis was performed using the computer programme POLO (Robertson *et al.*, 1980).

2.1.12 KCl and NaCl sensitivity assay

Sensitivity to KCl and NaCl was tested using the protocol described in Huang *et al.*, (2002). Briefly, adult flies, aged between one and four days, were grouped in batches of 10 in vials containing food with the appropriate concentrations (0, 0.2, 0.4, 0.6, or 0.8M) of KCl or NaCl added in place of water. After four days at 25°C, the survival of flies was scored with those unable to move being classed as dead. The percentage of flies surviving at each concentration was calculated, and standard error of the proportion was calculated as the square root of PQ/n, where P is the percentage of surviving flies, Q is the percentage of dead flies, and n is the sample size.

2.2 Molecular biology

2.2.1 Materials

All kits and reagents were used as per manufacturer's instructions unless stated otherwise. The kits used are shown in Table 2.2.

Kit	Supplier
ABI PRISM® SNaPshot Multiplex Kit	Applied Biosystems
BigDye® Terminator Cycle Sequencing Kit	Applied Biosystems
QIAquick® Gel Extraction Kit	Qiagen
QIAquick® PCR Cleanup Kit	Qiagen

Table 2.2 Molecular biology kits and suppliers

Molecular biology and analytical grade chemicals were obtained from Merck Ltd (BDH), Sigma, or Fisher Scientific.

Restriction endonucleases, DNA polymerases and other DNA modification enzymes, e.g. T4 DNA ligase, were supplied by New England Biolabs, Invitrogen, Finnzymes or Promega.

2.2.2 DNA extraction from *Drosophila*

20 adult flies were homogenised in 500 μ l lysis buffer (100mM Tris-HCl pH 8.5, 50mM EDTA, 80mM NaCl, 5% sucrose, 0.5% SDS in H₂O). The sample was incubated at 70°C, followed by the addition of 40 μ l 8M KAc and 30 minutes on ice. Debris was removed by centrifugation at 10400rpm at 4°C for 10 minutes. The supernatant was extracted once with an equal volume of phenol/chloroform and once with an equal volume of chloroform (centrifugations 10400rpm). The DNA was precipitated with 0.75 volumes of isopropanol for 20 minutes at room temperature, followed by centrifugation for 30 minutes at 10400rpm. The pellet was washed with 1ml 70% ethanol, briefly air dried and resuspended in 100 μ l H₂O containing 30 μ l/ml RNase A. The sample was then incubated for 1 hour at 37°C.

For single fly DNA extractions, one fly was homogenised using a pipette tip containing 50 μ l grinding buffer 2 (10mM Tris-Hcl pH 8.5, 1mM EDTA, 25mM NaCl in H₂O). The buffer was expelled once the fly was completely ground. 50 μ l lysis buffer was added and the sample was incubated for 10 minutes at 70°C, followed by the addition of 40 μ l 3M KAc and 10 minutes on ice. Debris was removed by centrifugation at 10400rpm for 10 minutes. The DNA was precipitated with 200 μ l 95% ethanol at room temperature for five minutes, followed by centrifugation for five minutes at 10400rpm. The pellet was washed with 200 μ l 70% ethanol and resuspended in 20 μ l H₂O.

2.2.3 Quantification of DNA concentration

Concentration and purity of DNA were determined by spectrophotometry. Genomic DNA samples were diluted in H₂O. An absorbance value of 1.0 at 260nm corresponds to 50 μ g/ml double stranded DNA. DNA concentration was calculated by $A_{260} \times \text{dilution factor} \times 50$.

2.2.4 Polymerase Chain Reaction

Because much of the reactions performed were for use in sequencing reactions, high fidelity enzymes were chosen. Primers were manufactured by TAG Copenhagen or Sigma Genosys. 25 μ l or 50 μ l reactions contained 1x polymerase buffer, 0.2mM dNTPs, 0.8pmol/ μ l of each primer, *Pfu* polymerase (Promega) or DyNAzyme EXT™ (Finnzymes), and an appropriate amount of genomic DNA template in H₂O. The thermal cycle reactions all followed the essentially similar sequence shown in Table 2.3.

Step	
1	Long denaturation: 95°C for 4 minutes
2	Annealing: 55-65°C for 30 seconds (°C dependent on primer melting temperature)
3	Elongation: 72°C (time dependent on length of DNA fragment)
4	Short denaturation: 95°C for 45 seconds
5	Repeat steps 2-4 for 25-34 additional cycles
6	Final extended elongation: 72°C for 10 minutes

Table 2.3 Standard thermal cycling conditions for PCR

2.2.5 Agarose gel electrophoresis

DNA was resolved by electrophoresis on agarose gels ranging from 0.8 - 2%, depending on the expected size of the DNA fragment(s), with 150ng/ml ethidium bromide in 1xTBE (40mM Tris-borate, 1mM EDTA in H₂O). DNA was visualised under UV irradiation.

2.2.6 Extraction of DNA from agarose gels

DNA bands of interest were excised under UV illumination using a scalpel and extracted using Qiagen's QiaQuick Gel Extraction Kit, according to the protocol provided.

2.2.7 Purification of PCR products

PCR products were purified using Qiagen's QIAquick PCR Purification kit, according to the protocol provided. Where more than one DNA fragment was amplified using PCR, the fragment of interest was gel extracted and purified using Qiagen's QIAquick Gel Extraction Kit.

2.2.8 DNA sequencing

(a) Glasgow: DNA sequencing reactions on purified PCR products were carried out by the Molecular Biology Support Unit at the University of Glasgow. Sequences were analysed using ABI Prism EditView or 4peaks software.

(b) Tampere: Sequencing was performed using the BigDye® Terminator Cycle Sequencing Kit on an ABI 310 genetic analyzer (Applied Biosystems), according to the protocol provided. Sequencing reactions were prepared containing 50ng template, 5pmol primer and dye terminator ready reaction mix (BigDye), to a final volume of 10 μ l. The thermal extension reaction was run using the following basic cycle for 25 cycles: denaturation for 30 seconds at 96°C; annealing for 15 seconds at 57°C; extension for four minutes at 60°C. Extension products were then precipitated with ethanol to remove unincorporated ddNTPs for 10 minutes at room temperature and centrifuged for 20 minutes. The DNA pellet was washed with 70% ethanol, dried and resuspended in 12.5 μ l Template Suppression Reagent, vortexed for 10 seconds, and denatured for two minutes at 95°C. Samples were then loaded onto an ABI 310 automated sequence analyser. Sequences were analysed using ABI Prism software.

2.2.9 SNP genotyping

Genotyping was performed on purified PCR products amplified from DNA derived from single recombinant males using the ABI Prism SNaPshot™ Primer Extension Kit, according to the protocol provided. The primers used for both PCR and primer extension are listed in Tables 2.4 and 2.5. The annealing temperature for all PCR reactions was 62°C. Genotyping primers for each SNP were designed to have melting temperatures of between 60°C and 65°C, and to terminate at the base directly before the base of interest. The annealing temperature in primer extension was 59°C. Samples were then loaded onto an ABI 310 automated sequence analyser. Data was analysed using ABI Prism GeneScan® analysis software, using the GS POP4 (1ml) E module.

Name	Sequence 5'-3'	Target	Size of PCR product
9240-7	GACCCAATAAATGGCCTATGTTTTCG	CG9240	440bp
9240-9B	CAGCAGCATCACAACCTGCGCAT		
8288-1	GTTTTGACAGCTCTTTTGGTTATTCTGC	CG8288	281bp
8288-6	GTCACATACTGTAATTTCTTGCGCA		
8931-8	AGCATGCTCCGAACGTGGGTT	CG8931	299bp
8931-10	CGAAAAGGTAAGGGAATCTAAACGAAG		
9219-4	GCAGCAGCTGTATTGCCAGCACT	disco-r	380bp
9219-5B	CTCAATTTGAATAACAACAAGAGCGGC		
eas-11	TAATTCAAGGGGCAAGGAACTGT	eas	360bp
eas-4	GTATATATCCCACGTTCCGCACACC		
3560-3	CTGGGCAGATGGGCCTACAATC	CG3560	342bp
3560-4	TTCCCAGTCCTCACGCTCCTC		
para-3	CTGCATCCTGATGATAATGCCGAC	para	418bp
para-5	CAAGTTTGACCTAAATACACATCTGCATAAA		
r-7	TTAATGGCCCCCAAATATATATGCC	r	407bp
r-8	TGCACTCAGTTATAAGTACTTTGCACTCC		

Table 2.4 PCR primers used to amplify region around SNPs in SNP mapping
Primers were designed to amplify fragments of approximately 300-400bp containing each SNP of interest.

Name	Sequence 5'-3'	Target SNP	Direction	Ocd/ORR
9240-ms1	CAGCCTTTTACAAAAGCTTTTCTTTTGATA	CG9240	reverse	G/C
8288-ms1	GGAGACCCAGTAATTGATTAATAACGCT	CG8288	reverse	A/C
8931-ms1	TGTCCTTTCCACCACGAAAGCAG	CG8931	forward	A/C
9219-ms1	AGTCCGCTTCTGTTTGCCGGA	disco-r	forward	T/C
eas-ms1	ACAACACACTATACAATGCAAAAAAACGAA	eas	forward	A/T
3560-ms1	CTGTATGAGAACGAGGATGTGAAGGA	CG3560	forward	A/G
para-ms2	CAAATCAAGTGTCTTTGGGACTTGGG	para	reverse	C/G
r-ms1	AAGAGTTCTGTTTTTCAGGGGTATTAACGA	r	forward	C/T

Table 2.5 Minisequencing primers for SNaPshot genotyping.

These primers were used with ABI Prism SNaPshot™ Primer Extension Kit to genotype each recombinant flies in SNP mapping. The base read depends on the direction of the primer (forward or reverse). The bases shown here as Ocd¹ or ORR are the bases shown on a GeneScan electrophoregram, in the appropriate colour.

2.2.10 Determination of P element insertion position

Inverse PCR was performed according to the BDGP protocol. Briefly, 10 μ l genomic DNA was digested with 10U *Hpa*II or *Hin*P1I and 8 μ g/ml RNase A in a 25 μ l reaction with appropriate buffer. This was followed by heat inactivation at 65°C. The digestion reaction was checked on a 0.8% agarose gel. 10 μ l of the digestion reaction was then used in a

400 μ l ligation reaction containing 0.25U T4 ligase, 1x ligase buffer, and ddH₂O. This reaction was incubated overnight at 4°C, followed by precipitation of the DNA using ethanol and sodium acetate. The DNA was resuspended in TE for at least 1 hour at room temperature. 25 μ l inverse PCR reactions were comprised of 5 μ l ligation reaction, 1 μ l 2.5mM dNTPs, 0.5 μ l of each primer (Tables 2.6 and 2.7), 1x Taq buffer, 1U Taq polymerase, and ddH₂O. Thermal cycling was performed using the following conditions: 95°C for 5 minutes, 35 cycles of 95°C for 30 seconds, annealing temperature for 1 minute (Table 2.6), and 68°C for 2 minutes, followed by 72°C for 10 minutes. PCR products were then purified and sequenced using the appropriate primers (Tables 2.6 and 2.7). Sequences were then used to search the NCBI BLAST programme for identical *Drosophila* sequences, to check exactly where in the genome *P* elements were inserted.

<i>P</i> element type	5' or 3' flanking sequence	iPCR primer 1 sequence 5'-3'	iPCR primer 2 sequence 5'-3'	Annealing temperature	Sequencing primer
KG lines: P{SUPorP}	5'	Plac1	Pwht1	60°C	5.SUP.seq1
	3'	3.rev.hpa2	Pry4	55°C	3.SUP.seq1
EY lines: P{EPgy2}	5'	Plac1	Pwht1	60°C	5.SUP.seq1
	3'	Pry1	Pry4	55°C	3.SUP.seq1
BG lines: P{GT1}	5'	pGT1.5a	pGT1.5d	55°C	Sp1
	3'	Pry1	Pry4	55°C	Spep1

Table 2.6 Inverse PCR primers and reaction annealing temperatures

Three different types of line were used in *P* element mapping (Figure 2.2). The primers used are shown, depending on whether the 5' or 3' flanking region was amplified. For primer sequences, see Table 2.7.

Primer	Sequence 5'-3'
Plac1	CACCCAAGGCTCTGCTCCCACAAT
Pwht1	GTAACGCTAATCACTCCGAACAGGTCACA
3.rev.hpa2	TTGCCACTTGCTCATAACGTC
Pry4	CAATCATATCGCTGTCTCACTCA
Pry1	CCTTAGCATGTCCGTGGGGTTTGAAT
pGT1.5a	CCGCACGTAAGGGTTAATG
pGT1.5d	GAAGTTAAGCGTCTCCAGG
5.SUP.seq1	TCCAGTCACAGCTTTGCAGC
3.SUP.seq1	TATCGCTGTCTCACTCAG
Sp1	ACACAACCTTTCCTCTCAACAA
Spep1	GAACTCAGAATACTATTC

Table 2.7 Primer sequences for inverse PCR and sequencing of PCR products

2.3 Proteomics

2.3.1 Protein extraction from *Drosophila*

Protein was extracted from *Drosophila* according to the Cambridge Centre for Proteomics (CCP) protocol. Briefly, 12 adult male flies aged between one and two days were frozen in liquid nitrogen then homogenised in 100 μ l lysis buffer (10mM Tris-HCl pH 8, 5mM magnesium acetate, 8M urea, 4% (w/v) 3-((3-Cholamidopropyl)dimethyl-ammonio)-1-propanesulfonate in H₂O). The pestle was washed with 50 μ l lysis buffer. When all flies were completely ground, the homogenate was left on ice for one hour. The sample was centrifuged for 10 minutes at 4°C at 13000rpm and the supernatant transferred to a chilled tube and stored at -20°C. Three biological replicates were generated for each group (mutant or wild-type). In addition, each biological replicate was used in 2D DIGE three times. Protein concentration was determined at the CCP using the BioRad DC protein assay (BioRad, UK)

2.3.2 2D difference gel electrophoresis

2D DIGE was performed at the CCP according to their protocol (see Swatton *et al*, 2004). Individual protein samples were minimally labelled with the CyDyes Cy3 or Cy5 (GE Healthcare, Sweden). A pooled protein sample was minimally labelled with Cy2 and acted as an internal standard. Proteins labelled with Cy2, Cy3 and Cy5 were mixed and separated firstly by isoelectric focussing using immobilised pH gradient (IPG) DryStrips, pH3-10 (GE Healthcare, Sweden), and secondly according to molecular weight using 12% SDS-polyacrylamide gels. Protein gels were scanned for Cy2, Cy3 and Cy5 fluorescence using the Typhoon 9400 imager (GE Healthcare, Sweden), and image analysis was performed using DeCyder V4.0 automated software (GE Healthcare, Sweden). The DeCyder Biological Variation Analysis (BVA) software module was used to identify spots with increased or decreased expression between samples, based upon calculated standardised abundances. Standardised abundance was calculated by dividing spot volumes by the Cy2 internal standard for each spot. Statistical analysis was applied using standard analysis of variance (ANOVA). Spots with $p < 0.05$ for random occurrence were considered to differ significantly between samples. CyDye and DeCyder are trademarks of Amersham Biosciences Limited.

2.3.3 Mass spectrometry (protein identification)

Protein gels were fixed and stained using Colloidal Coomassie Brilliant Blue and spots of interest excised manually within a laminar flow cabinet. Mass spectrometry to identify proteins from 2D DIGE experiments was performed at the CCP. Proteins spots within the gel were first reduced, carboxyamidomethylated, and then digested to peptides using trypsin on a MassPrepStation (Micromass, Manchester, UK). The resulting peptides were applied to either matrix-assisted laser desorption ionization time of flight MS (TofSpec2E; Micromass), for peptide mass fingerprinting, or LC-MS/MS. For LC-MS/MS, the reverse phase liquid chromatographic separation of peptides was achieved with a PepMap C18 reverse phase, 75 μm i.d., 15-cm column (LC Packings, Amsterdam) on a capillary LC system (Waters) attached to QToF2 (Micromass) mass spectrometer or the same column attached to a Dionex Dual Gradient LC system attached to a QSTAR XL (Applied Biosystems, Framingham, MA, USA). The MS/MS fragmentation data achieved was used to search the National Center for Biotechnology Information database using the MASCOT search engine (<http://www.matrixscience.com>). Probability-based MASCOT scores were used to evaluate identifications. Only matches with $P < 0.05$ for random occurrence were considered significant (further explanation of MASCOT scores can be found at <http://www.matrixscience.com>).

2.4 Electrophysiology

All electrophysiology experiments were performed by Dr Richard Baines, Department of Biological Sciences, University of Warwick, using the protocols described in Baines and Bate (1998) and Mee *et al.*, (2004).

2.4.1 Staging and dissection for voltage clamp recordings

First instar larvae were fixed at anterior and posterior ends to a Sylgard (Dow-Corning) coated coverslip using cyanoacrylate glue under dissection saline. Larvae were opened dorsally, following the line of the trachea, using sharp tungsten needles then glued flat to the Sylgard coverslip. Gut and fat body were removed using sharp tungsten needles to expose the ventral nerve cord (VNC). The larvae were viewed using a 63x water immersion lens combined with Nomarski optics. A section of the neurilemma surrounding the nerve cord between abdominal segments A1-A4 was ruptured using protease in

external saline solution. A large diameter (10-20 μ m) patch pipette containing protease saline was used to degrade the neurilemma on the dorsal surface of the nerve cord using gentle suction and expulsion. This results in the underlying aCC and RP2 neurons being exposed. These neurons are identified on the basis of their size and position in the VNC.

2.4.2 Patch clamping

Standard patch electrodes (thick walled borosilicate glass), fire-polished to resistances between 15 and 20M Ω were used to generate whole-cell recordings. Amplification and voltage control were achieved using an Axoclamp-1D patch clamp amplifier and pCLAMP6 software running on an IBM-compatible computer (Axon Instruments, Foster City, CA). Leak subtraction within pCLAMP6 was used to resolve sodium currents. Current recordings were taken at voltages held at between -60 and 45mV, and were made at three temperatures: 16°C, 22°C and 28°C. Data was analysed using GLM-ANOVA on Minitab software.

2.4.3 Solutions

- External saline: 135mM NaCl, 5mM KCl, 2mM MgCl₂, 0.5mM CaCl₂, 5mM *N*-Tris, 36mM sucrose in H₂O
- Internal saline: 140mM CsCl₂, 2mM MgCl₂, 11mM EGTA, 10mM HEPES in H₂O, pH 7.4.
- Sodium conductance saline: 100mM NaCl, 50mM TEA, 10mM 4-aminopyridine, 10mM MgCl₂, 10mM HEPES, 10mM glucose in H₂O, pH 7.4

3 Identification of the *Ocd* gene

3.1 Introduction

To characterise the *Ocd* mutations, the underlying gene first had to be identified. Understanding the nature of the gene product and the mutations within it is crucial in determining the mechanisms by which these mutations generate the *Ocd* phenotype.

The critical region for *Ocd* is defined as between 13F1 and 16A2 (Søndergaard, 1975), determined by the ability of a molecularly defined duplication to rescue *Ocd*. This duplication is approximately 1.5Mb, and encompasses more than 200 genes (Flybase: <http://flybase.org>). Much of the previous *Ocd* literature suggests a mitochondrial role for the gene (Søndergaard, 1975, Søndergaard, 1976, Søndergaard, 1979a, Søndergaard, 1979b, Søndergaard, 1986). Therefore, genes in or around the *Ocd* region known to be expressed in the mitochondrion were sequenced to check for any *Ocd*-specific mutation(s).

In parallel, a major objective was to reduce and redefine the *Ocd* region, to a more manageable size and number of genes that could subsequently be sequenced. To this end, two separate mapping strategies were employed: SNP mapping and *P* element mapping. Using these combined approaches, new left and right hand flanking markers were defined, reducing the critical region from 204 to only six genes.

3.2 Preliminary *Ocd* characterisation

To confirm and clarify Søndergaard's original observations, the Glasgow *Ocd* lines were tested for dominant cold-sensitive paralysis (Figure 3.1). This was necessary for the development of a stringent test for the *Ocd* phenotype, which would be required in the mapping experiments described later. Most heterozygous females are paralysed within two to three minutes, in contrast to wildtype controls, although there is lots of variation between individual flies. Viable *Ocd* males display a more severe cold-sensitive phenotype; almost all are paralysed at 4°C in under one minute (data not shown).

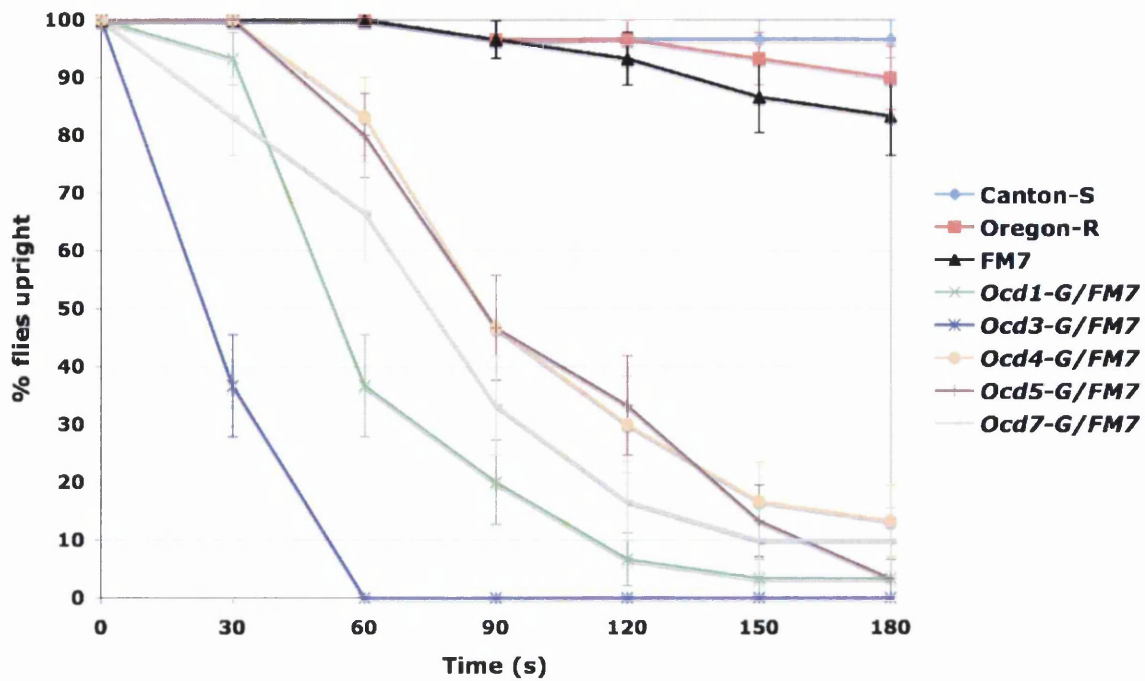


Figure 3.1 Dominant cold-sensitivity assay in Glasgow *Ocd* and wild-type lines

This experiment assayed cold-sensitive paralysis in heterozygous *Ocd* females, wild-type (Canton-S and Oregon-R), and balancer FM7 females as controls. Cold-sensitivity was assayed by placing 30 flies at 4°C and measuring how many flies remained upright after each 30 second time interval. Error bars represent standard errors of the proportion.

An analysis of any temperature-sensitivity of the *Ocd* male semi-lethality was undertaken. Crosses of heterozygous *Ocd* females with wild-type (Canton-S) males were performed at both 18°C and 25°C. The proportion of *Ocd* males out of the total number of males eclosing from each cross was calculated (Figure 3.2). It was found that each of the *Ocd* mutations, with the exception of *Ocd^{4-G}* which is almost completely lethal at either temperature, were associated with cold-sensitive male lethality. The most severe effect was observed in *Ocd^{7-G}* flies, with 36.9% of the total males being *Ocd^{7-G}* at 25°C, and no *Ocd^{7-G}* males eclosing at 18°C. In fact, at 18°C, the *Ocd^{7-G}* mutation appears to induce lethality similar to that observed in *Ocd^{4-G}* flies; *Ocd^{7-G}* homozygous females, though viable at 25°C, do not eclose at 18°C.

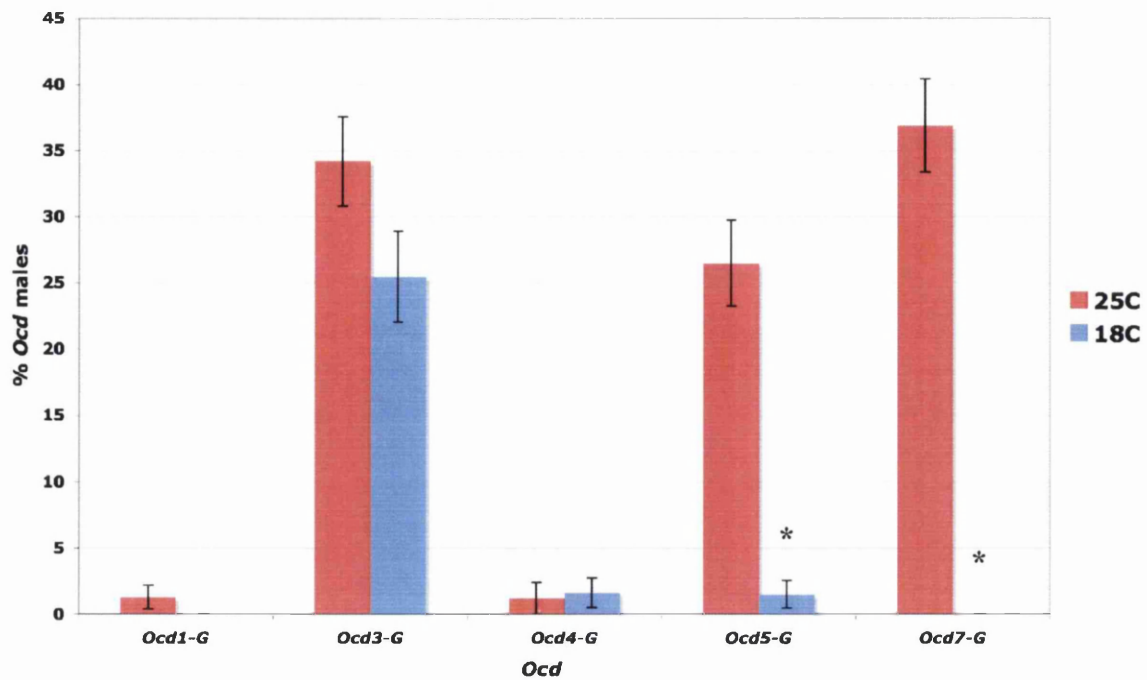


Figure 3.2 Cold-sensitive male lethality assay in Glasgow *Ocd* lines

Heterozygous *Ocd*/*FM7* females from selected *Ocd* lines were crossed to wild-type males at 18°C and 25°C and the proportion of cold-sensitive males calculated. Standard errors of the proportion are shown. All lines were observed to be cold-sensitive with regards to male lethality, with the most pronounced effect of temperature being observed in *Ocd*^{7-G} flies. Standard errors of the proportion are shown. Asterisks indicate significant deviation from observations at 25°C (*Ocd*^{5-G} and *Ocd*^{7-G}), as calculated from χ^2 analysis ($p < 0.05$).

3.3 Sequencing of mitochondrial candidates

Based on the evidence for a mitochondrial role of *Ocd* (section 1.4.2), candidate genes involved directly or indirectly in mitochondrial energy metabolism within the critical region were analysed.

Five nuclear encoded mitochondrial candidates in this region were identified and selected for sequencing throughout the coding region (Table 3.1). Although *easily shocked* (*eas*) is not exclusively mitochondrial, it encodes an ethanolamine kinase, involved in the pathway to synthesise phosphatidylethanolamine, a major membrane phospholipid which is abundant in mitochondria (Pavlidis *et al.*, 1994). The *eas* gene is also a good candidate due to the seizure susceptibility observed in *eas* mutants. The *Ocd*^{1-G} line and a wild-type control were used in sequence analysis.

Gene name	Cytogenetic map position	Gene product/ function
CG9240	13E8	mitochondrial peptidase/ mitochondrial protein processing
CG8288/ <i>mitochondrial ribosomal protein L3 (mRpL3)</i>	13E14	large subunit of mitochondrial ribosome/ protein biosynthesis
CG8931	14A5	mitochondrial substrate carrier/ energy transfer
CG3525/ <i>easily shocked (eas)</i>	14B7	ethanolamine kinase/ phospholipid biosynthesis
CG3560	14B8	ubiquinol-cytochrome-c reductase/ mitochondrial electron transport

Table 3.1 Mitochondrial candidate genes in and around the region 13F1-16A2

The genes CG8288 and CG3560 are both listed on the MitoDrome database which identifies nuclear *Drosophila* genes encoding mitochondrial proteins (D'Elia *et al.*, 2004, Sardiello *et al.*, 2003). CG9240 and CG8931 are largely uncharacterised, but bioinformatics analysis suggests CG9240 is localised to the mitochondrial membrane, and encodes a mitochondrial peptidase, and that CG8931 contains a mitochondrial substrate carrier protein domain (Flybase: <http://flybase.org>). NB. *eas* is not exclusively mitochondrial (see main body of text). Cytogenetic map positions are from Flybase (<http://flybase.org>). Coding regions of the genes were sequenced. No mutations unique to the *Ocd* lines were discovered.

Although many single nucleotide polymorphisms (SNPs) were found between *Ocd*^{*l-G*} and wild-type (ORR) DNA, no mutations unique to the mutant strain were uncovered within the coding regions of these genes. Non-coding regions were not sequenced, but we would expect mutations resulting in temperature-sensitive paralysis to be missense mutations, rather than mutations affecting transcription levels. Temperature-sensitive mutations commonly affect protein folding. A change in the primary structure, by as little as one amino acid, can be sufficient to cause conformational changes, often causing the protein to be unstable so that it dissociates at elevated temperatures. This is not always the case, however, and several of the temperature-sensitive alleles of *para*, a *Drosophila* voltage-gated sodium channel gene, are caused by insertions, even in intronic regions (Gamo *et al.*, 1998, Loughney *et al.*, 1989). These insertions are likely to result in reduced sodium channel expression. The temperature-sensitivity may reflect an increased need for sodium channel function at higher temperatures, or may be the result of temperature-dependent instability in sodium channels (Stern *et al.*, 1990).

Instead of further sequencing of other genes in the region, and of non-coding DNA and regulatory sequences of the mitochondrial candidates, an alternative approach to finding the *Ocd* gene was undertaken. Because SNPs between *Ocd*^{*l-G*} and wild-type (Oregon-R) were uncovered during sequencing, an attempt to map *Ocd* using SNPs was carried out.

This would narrow down the critical region further, to a manageable size for sequence analysis.

3.4 SNP mapping

Traditionally, geneticists have tended to use visible marker mutations in classical recombination mapping, for example bristle and wing variations. However, the use of single nucleotide polymorphisms (SNPs) in mapping offers several advantages. SNPs are highly abundant (occurring on average every 200-300bp), exist in only two codominant variants, and are usually phenotypically neutral (Berger *et al.*, 2001). The completion of the *Drosophila* genome project, and the availability of different wild-type strains carrying a wealth of SNP markers, make it feasible to use molecular techniques to identify the *Ocd* gene. Indeed, it should be possible to map mutations to the subgenic level.

SNP mapping is based on the phenomenon of recombination during meiosis. In a heterozygous gamete, crossovers may occur between two chromosomes (in this case, mutant and wild-type). The resulting progeny can be genotyped for each SNP variant. If the chromosome is recombinant and has a mixture of mutant and wild-type SNPs, this can yield clues to the position of the mutated gene (Figure 3.3).

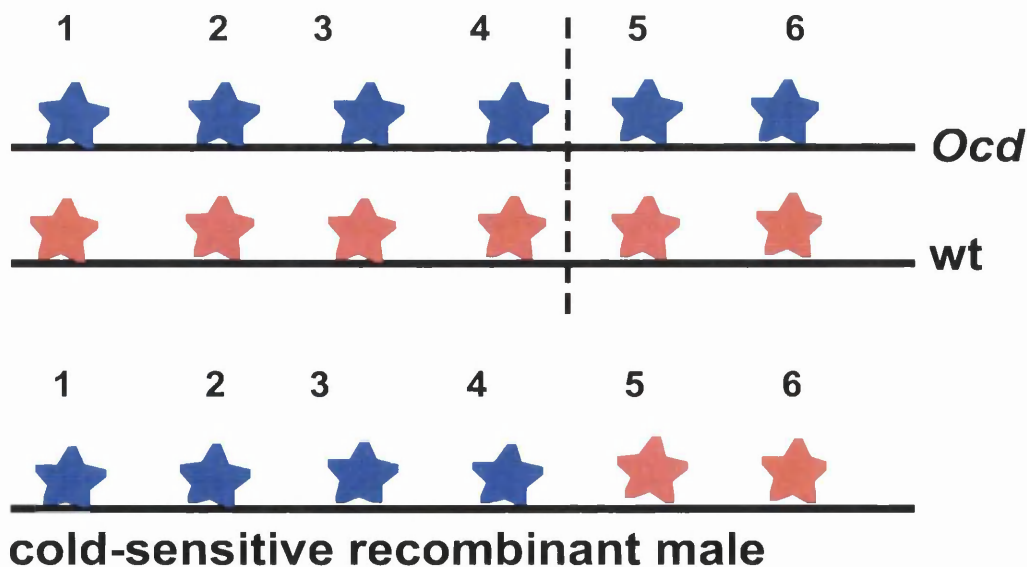


Figure 3.3 Mapping *Ocd* using SNPs

A theoretical example of mapping the *Ocd* mutation using SNP markers. SNPs (1-6) are characterised that differ between *Ocd* and wild-type (wt). Heterozygous females with one wt and one *Ocd* X chromosome are generated and backcrossed to wt males to produce potential recombinants. In this example, the recombinant male is cold-sensitive so must carry the *Ocd* mutation. The position of crossover is indicated by a dotted line. The *Ocd* gene must lie within the *Ocd*-derived segment of the chromosome, i.e. to the left hand side of SNP 5.

A *Drosophila* SNP database does exist (Hoskins *et al.*, 2001), but at the start of this project no markers located across the *Ocd* region had been reported. Therefore SNPs spanning the critical interval were identified through sequencing non-coding *Ocd^{l-G}* and Oregon-R DNA. Although the *Ocd* mutations were originally reported to be isolated in an Oregon-R background (Søndergaard, 1975, Søndergaard, 1979a), we found that the *Ocd* lines were far more similar to our Canton-S line than our Oregon-R line, with respect to the SNPs sequenced. Eight SNPs were chosen for the experiment, which differ between *Ocd^{l-G}* and our Oregon-R line (Table 3.2). The eight SNPs are spread across and just beyond the *Ocd* region, as defined on Flybase as 13F1-16A2.

Gene	Map location & gene orientation (forward or reverse strand)	SNP location	Position of SNP in gene	Flanking sequence	<i>Ocd^l</i>	ORR
<i>CG9240</i>	13E8 reverse	AE003499.5 nt:5748	110bp 3' of gene	AAATG-TATCA	C	G
<i>mitochondrial ribosomal protein L3 (mRpL3)</i>	13E14 forward	AE003500.4 nt:55600	intron 1	ATGCG-AGCGT	T	G
<i>CG8931</i>	14A5 forward	AE003500.4 nt: 277193	838bp 5' of gene	AGCAG-CGAAC	A	C
<i>disco-related (disco-r)</i>	14B1 reverse	AE003501.4 nt:213518	exon 2	CCGGA-TGCCG	T	C
<i>easily shocked (eas)</i>	14B7 forward	AE003501.4 nt: 272377	intron 2	ACGAA-CCATC	A	T
<i>CG3560</i>	14B8 forward	AE003501.4 nt: 277695	exon 3	AAGGA-GCCGT	A	G
<i>paralytic (para)</i>	14D1-14E1 reverse	AE003502.4 nt: 123890	intron 6	GTAAC-CCTAA	G	C
<i>rudimentary (r)</i>	14F5-15A1 forward	AE003503.4 nt: 28093	intron 5	AACGA-TTAAT	C	T

Table 3.2 SNPs identified across the *Ocd* region.

The genes in or around which SNPs were identified are shown, together with their cytogenetic map position (Flybase: <http://flybase.bio.indiana.edu>), orientation on the X chromosome (forward or reverse strand), and the nucleotide (nt) position of each SNP in the corresponding NCBI GenBank *Drosophila melanogaster* genomic scaffold (AE#), and the position of the SNP relative to the associated gene. Where the gene is read on the reverse strand, the nucleotide position refers to that of the reverse complemented strand. The flanking sequence of each SNP is also shown, along with the base present in either *Ocd^{l-G}* (blue) or wild-type Oregon-R (red) DNA.

Figure 3.4 shows the relative positions of the eight SNPs across the critical region used in the mapping experiment. Also shown in the map is the *forked (f)* locus, which maps to the right of the critical region (15F4-15F7). *Ocd^{l-G}* carries the recessive *forked* mutation so all *Ocd^l* males have a forked bristle phenotype. This facilitates mapping as male flies in the output from the final cross can be identified that are cold-sensitive but have normal

bristles, or males which are not cold-sensitive but have forked bristles, thus confining the SNP analysis to recombinant chromosomes that have undergone at least one recombination event between the *Ocd* and *f* loci. This should identify which of the chosen markers flanks *Ocd* on the right hand side, and should also generate an accurate location of the gene.

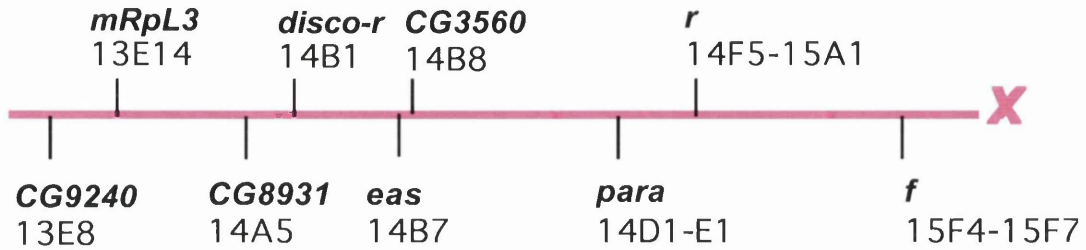


Figure 3.4 Relative positions of genes containing SNPs identified across the *Ocd* region and used in mapping

This diagram is not to scale and shows only the relative positions of the SNPs on the X chromosome. The *Ocd* region is defined on Flybase as 13F1-16A2. The *forked* locus is also shown to the right of the eight SNPs, at 15F4-15F7. The *Ocd*^{1-G} line is marked with *forked*, which facilitates mapping of the *Ocd* gene.

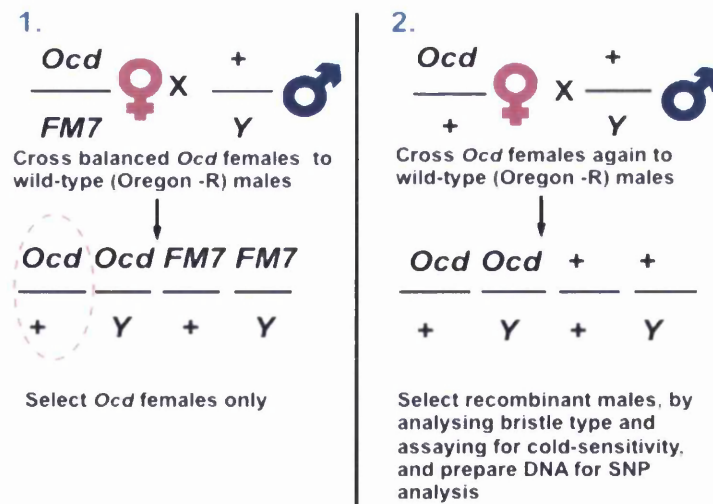


Figure 3.5 Crossing strategy to generate recombinant flies

Ocd⁺ females were generated and backcrossed to wild-type males. Progeny of this cross should include recombinants. To simplify the analysis, male flies only were assayed for cold-sensitivity and bristle type, to check whether they carried mutant or wild-type copies of the *Out cold* and *forked* genes. If recombinant, DNA was extracted from single flies and SNPs were genotyped.

Figure 3.5 shows the crossing strategy used to generate recombinant flies. *Ocd^{l-G}* flies are maintained over the balancer chromosome FM7. *Ocd^{l-G}/+* females were generated and backcrossed to ORR males. Progeny from this cross will include some recombinants. Male flies were analysed, firstly because the cold-sensitive phenotype is more striking in males than in heterozygous females, and secondly, because subsequent analysis of SNPs is simpler in males as they only have one X chromosome. Choosing to analyse males did prove problematic however, as *Ocd^{l-G}* males eclose at a relatively low frequency, and even when they survive to eclosion they are usually very sick and susceptible to getting stuck in the food medium, making testing for cold-sensitivity difficult.

SNP genotyping was carried out using a 'minisequencing' or primer extension reaction, using the ABI Prism SNaPshot™ kit. This method is similar to the Sanger method of sequencing, but only one base is added during primer extension. This is because only ddNTPs are added to the reaction, and not a mixture of dNTPs and ddNTPs. PCR primers were designed to amplify a 300-400bp fragment surrounding each SNP. Initially these fragments were designed to be of easily separable sizes so that the SNP genotyping reactions could be carried out in multiplex. However, despite several attempts at optimisation, this was not possible. Most flies were initially genotyped only at the SNPs at the far ends of the region (at *CG9240* and *rudimentary*). This meant that recombinants could be identified immediately prior to genotyping the SNPs inbetween. It should be noted however that this strategy would fail to identify any double recombinant chromosomes. Minisequencing primers were designed to anneal to the appropriate PCR product template DNA up to the base preceding the SNP of interest. Upon thermal cycling a fluorescently labelled ddNTP is incorporated, depending on the SNP variant present on the template. Electrophoresis of minisequencing products and analysis was carried out on an ABI Prism Genetic Analyser using GeneScan software.

The initial analysis, which involved genotyping only at the *CG9240* and *rudimentary* (*r*) markers in most cases, included 35 non cold-sensitive males (*Ocd⁺*) with forked bristles (*f*). Because *Ocd^{l-G}* flies carry the *f* marker, these males must be recombinant, between *Ocd* and *f*. Of these males, 27 had wild-type (Oregon-R) variants of all eight SNPs, indicating that there must have been a crossover event between *r* and *f*. However, eight flies carried the *Ocd* SNP variant at *r*, implying crossover to the left of *r*. Recombination frequencies then clearly place *Ocd* on the *para* side of *r*, closer to *r* than *f* is. Crudely, the mapping implies that *Ocd* lies 8/27 from *r* of the distance (*r-f*), on the *para* side (Figure 3.6). This

would place the *Ocd* mutations within *para*, although confidence limits place it within 100kb or so of *para*, on either side of it. However, the sample size here is too small to make more accurate measurements.

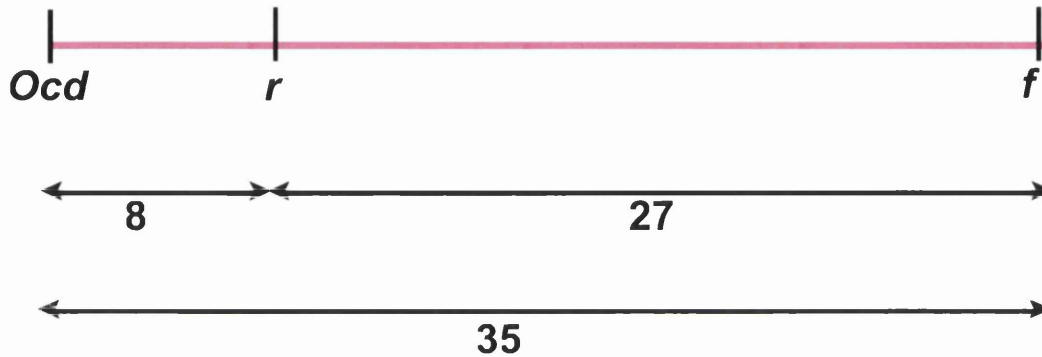


Figure 3.6 Estimated relative positions of *Ocd*, rudimentary (*r*), and forked (*f*)

Positions were calculated from recombination rates observed during SNP mapping. The numbers represent the number of recombination events observed between each pair of markers. From these numbers, the distance from *Ocd* and *r* can be calculated as $8/27$ of the distance between *r* and *f*. The distance between the genes *r* and *f* is approximately 597kb. $8/27$ of this distance is 177kb. This places *Ocd* approximately 177kb to the left of *r*, within the gene *paralytic*. However, the numbers used are too small to give a very accurate location so further mapping is required.

In order to determine which side of *para* *Ocd* lies, the SNP at *para* was genotyped in the eight males recombinant between *Ocd* and *r*. After minisequencing, it was found that six of these flies had the wild-type variant of the *para* SNP and one had the *Ocd*^{*l-G*} variant (Figure 3.7). These flies were also genotyped for the remaining SNP markers, and all of them were wild-type. Unfortunately, the result for one fly was undeterminable, even after several repetitions of the minisequencing reaction. This may have been due to the PCR product being degraded or contaminated.

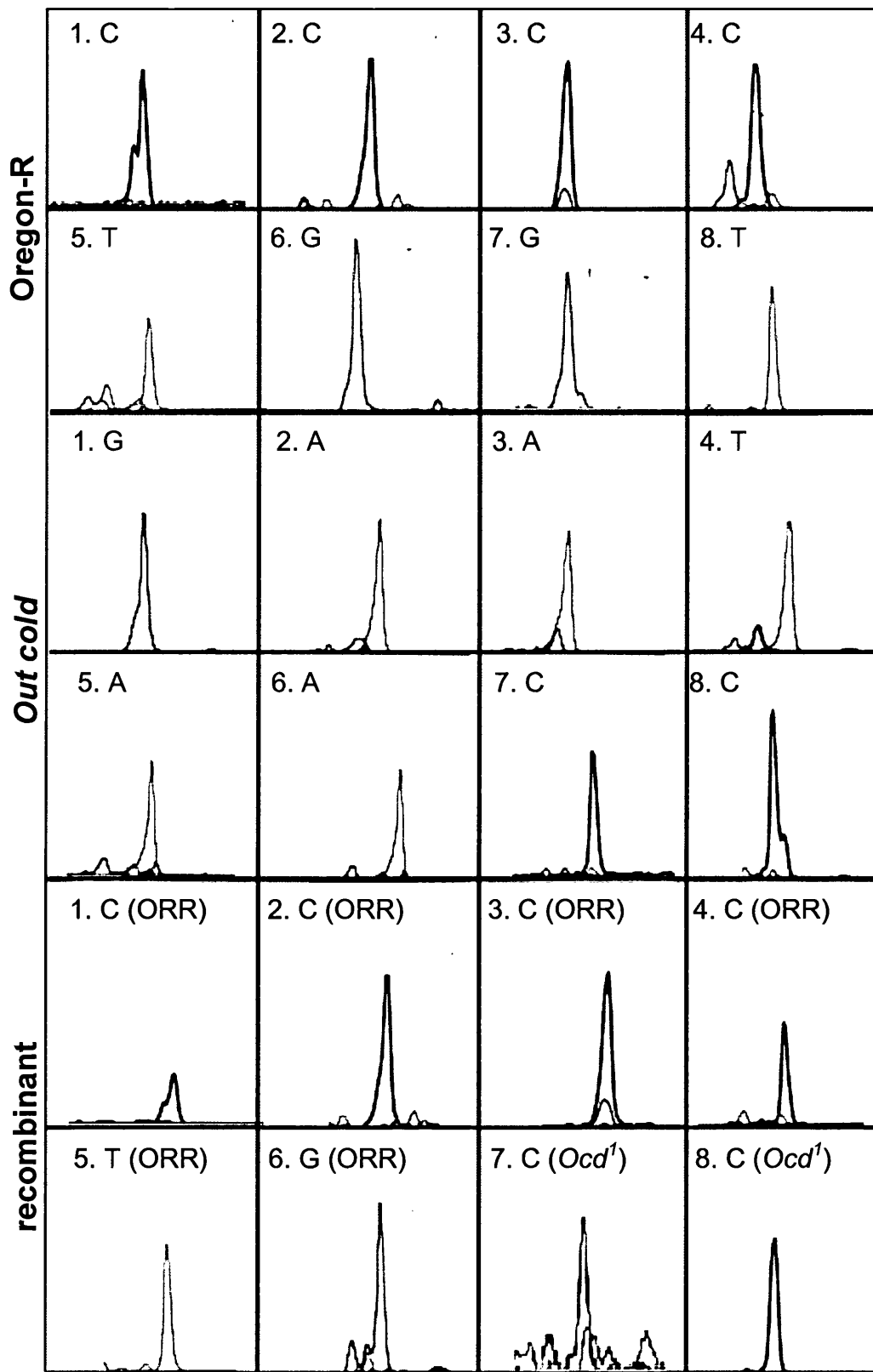


Figure 3.7 GeneScan electrophoregrams

The electrophoregrams represent the genotypes for Oregon-R, *Out cold*, and one informative recombinant at all eight SNPs. The recombinant did not carry the *Ocd*^{1-G} mutation, but carried the *forked* marker. SNP analysis revealed the Oregon-R (ORR) variants at SNPs 1-6, and the *Ocd*^{1-G} variants at SNPs 7 and 8. Therefore the *Ocd*^{1-G} mutation lies upstream of marker 7 (*para*). See section 2.2.9 for details of SNP genotyping.

The fact that one fly harbours the *Ocd*^{1-G} variant of the *para* SNP, and so is recombinant between *eas* and *para*, is highly informative. This fly has an Oregon-R derived chromosome between *CG9240* and *eas*, and an *Ocd*-derived chromosome at both *para* and *r* SNPs. Because this fly is not cold-sensitive we know that *Ocd* must lie to the left of, and close to, the SNP in *para*.

The genotypes for each of the recombinants are summarised in Figure 3.8. From this mapping experiment, *r* could be excluded as a candidate gene for *Ocd*. However, *para* could not yet be. The SNP in *para* used for mapping is in an intronic region between exons 6 and 7. Because *para* mRNA is transcribed on the reverse complemented strand, this leaves a large region encompassing exons 7-31 (~50kb) which would still need to be sequenced in order to eliminate the possibility of *Ocd* and *para* being allelic. Since this is such a large region to sequence, particularly if non-coding DNA was included, an alternative mapping strategy using more closely linked markers was employed to narrow down the region even further. Also, although the *para* SNP flanks *Ocd* closely on the right hand side, the left hand side of the region is relatively ill defined.

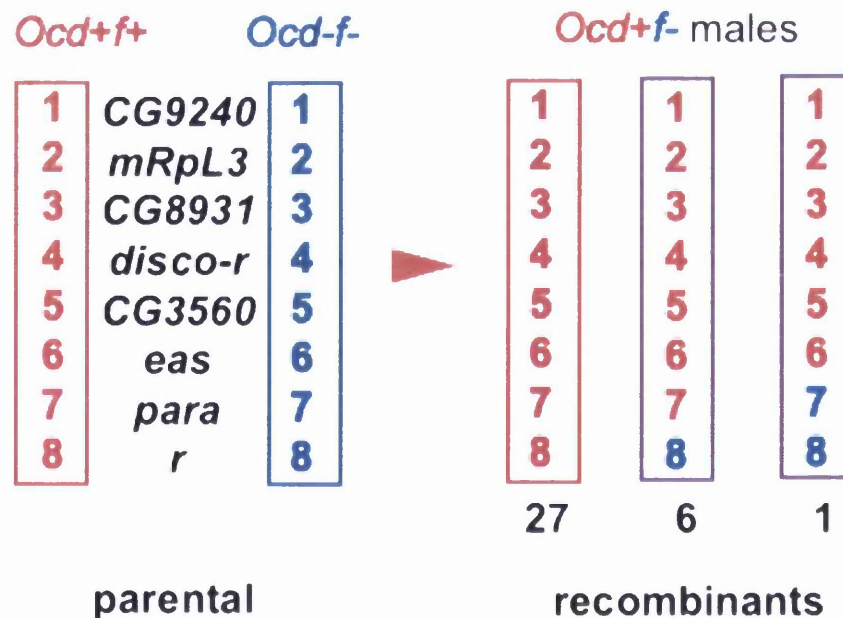


Figure 3.8 Genotypes of recombinant males

SNPs are labelled 1-8 corresponding to *CG9240* through to *r*. The two parental chromosomes were crossed to result in a total of 35 recombinant males, which were not cold-sensitive, but carried the *forked* marker. Of these, 27 carried wild-type markers for all eight SNPs, and therefore recombinant between *r* and *f*, and six were recombinant between *para* and *r*. One fly was recombinant between *eas* and *para*, so we know that the *Ocd*^{1-G} mutation must lie upstream of the SNP in *para*. NB one fly was not successfully genotyped for all markers, so this data is omitted.

3.5 *P* element mapping

Mapping using molecularly defined *P* element insertions offers several advantages over SNP mapping (Zhai *et al.*, 2003). In SNP mapping, polymorphisms must first be identified through sequencing. In analysing recombinants, SNPs need to be detected via molecular means, namely sequencing or restriction enzyme digestion.

Over 7000 *P* element insertion lines, which together disrupt more than 40% of all annotated *Drosophila* genes, are now publicly available from the BDGP Gene Disruption Project (Bellen *et al.*, 2004). On average the insertions occur every 20-30kb. These *P* elements have commonly been manipulated to contain a visible marker such as the *white* eye colour gene, so it is simple to score for their presence, provided the lines used in mapping are in a *white* background. This also makes *P* element mapping a relatively low cost strategy, as no molecular reagents are required for scoring.

P element mapping, like SNP mapping, is based on meiotic recombination. Using as many insertions as possible across the *Ocd* region, recombinants between *Ocd* and molecularly defined *P* elements were generated using the crossing scheme outlined in Figure 3.9. To identify recombinants, progeny were simply scored for eye colour and cold-sensitivity. Because the *Ocd*^{1-G} line is marked with the *forked* mutation, the distance between *Ocd* and *f* can also be calculated to act as an internal control. This value should remain constant irrespective of which *P* element insertion is crossed in. From previous mapping experiments, it is estimated that the distance from *Ocd* to *forked* is approximately 1.7cM (Søndergaard, 1979a). The crosses carried out are effectively three point test crosses and the distances between each of the three markers can be calculated by counting different classes of progeny; parental and recombinant. Genetic distance, in centimorgans (cM), is equal to the number of recombinants divided by the total number of progeny and multiplied by 100, i.e. the percentage recombination between two markers.

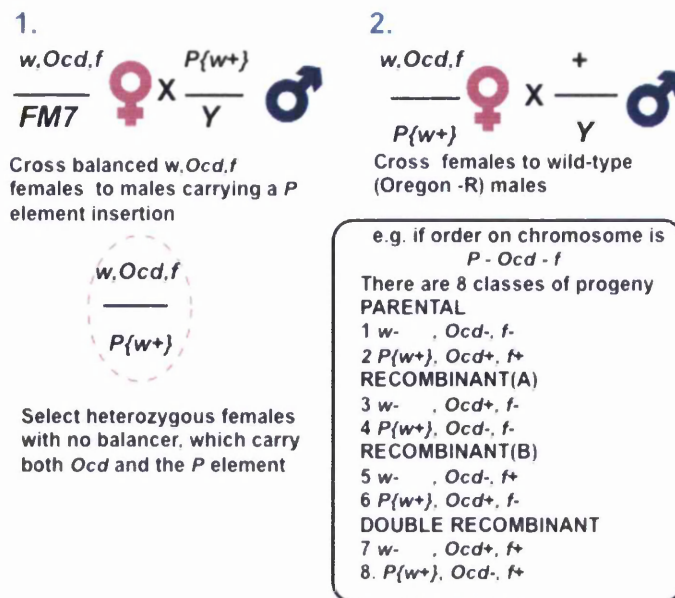


Figure 3.9 Crossing scheme to generate recombinant flies

Ocd^{1-G} flies were first crossed into a $white^-$ background. Heterozygous Ocd^1 females were then crossed to males containing the P element insertion ($P\{w^+\}$) of interest. Females from this cross were crossed to wild-type males and the male progeny of the cross were analysed for the presence of the P element, as well as the Ocd and *forked* mutations. This placed each fly into one of eight possible categories as shown.

By searching the BDGP Gene Disruption Project database, it was possible to identify insertions in many of the genes contained in the *Ocd* region. These fly lines were obtained and analysed for male viability. Initial crosses were carried out to determine whether or not using each insertion would be informative. Some crosses gave uninterpretable results, which may have been due to the presence of more than one P element or contamination. The strategy employed would only be successful if each P element line was a single insertion and in a $white^-$ background. Five insertions gave clear results, with the distance between *Ocd* and *f* remaining fairly constant (Table 3.3). Each point of insertion, as cited on the BDGP database, was checked by inverse PCR, using the protocol described on the BDGP Gene Disruption Project database. The flanking sequences were used to search the NCBI BLAST programme for identical *Drosophila* sequences, and points of insertion were found to correlate with the BDGP database.

<i>P</i> element line	Associated gene	Map position according to BDGP	Map position according to Flybase	Point of insertion
KG02315	<i>CG3415</i>	14B11	14B7	5' of 5' UTR
EY04615	<i>small wing (sl)</i>	14B18	14B15-17	5' of 5' UTR
EY03459	<i>Furin 2 (Fur2)</i>	14C1	14C1-2	5' of 5'UTR
EY01983	<i>CG4239</i>	14C3	14C2	5' UTR
BG00710	<i>hangover (hang)</i>	14C6	14C4-6	5' of 5' UTR

Table 3.3 The five *P* element lines used in mapping

Each *P* element is inserted in or around one gene, the cytogenetic location of which is cited on the BDGP database. The Flybase database also lists cytogenetic map positions of each of these genes. Because there are some discrepancies between these two positions, both are listed.

Each of the five lines were crossed into *Ocd*^{*l-G*} using the crossing scheme shown in Figure 3.9. Numbers of parental and recombinant flies with respect to each pair of markers (*Ocd*-*P* element, *Ocd*-*f* and *P* element-*f*) were calculated and genetic map distances between each were calculated (Tables 3.4 and 3.5).

Genotype	KG02315	EY04615	EY03459	EY01983	BG00710
<i>Ocd f</i> (parental)	70	203	135	106	83
<i>P</i> { <i>w</i> ⁺ } <i>Ocd</i> ⁺ <i>f</i> ⁺ (parental)	1767	1657	1232	1316	1647
<i>Ocd</i> ⁺ <i>f</i> ⁺	6	14	5	6	2
<i>P</i> { <i>w</i> ⁺ } <i>Ocd</i> ⁺ <i>f</i>	49	1	1	0	0
<i>Ocd</i> ⁺ <i>f</i>	4	7	9	6	1
<i>P</i> { <i>w</i> ⁺ } <i>Ocd</i> ⁺ <i>f</i>	38	36	31	31	37
<i>Ocd</i> ⁺ <i>f</i>	0	0	0	0	0
<i>P</i> { <i>w</i> ⁺ } <i>Ocd</i> ⁺ <i>f</i> ⁺	3	0	2	2	1
<i>P</i> { <i>w</i> ⁺ }- <i>Ocd</i> recombinants	58	15	8	8	3
<i>Ocd</i> - <i>f</i> recombinants	45	43	42	39	39
<i>P</i> { <i>w</i> ⁺ }- <i>f</i> recombinants	97	58	46	43	40
Total	1937	1918	1415	1467	1771

Table 3.4 Number of parental and recombinant flies in *P* element mapping

The table shows the numbers of flies counted of each possible genotype. In each case there are two parental and six recombinant genotypes. All lines are in a *white*⁻ background. The number of recombinants between each pair of markers which was used to calculate genetic distance is listed. The total number of flies counted is also shown. *P*{*w*⁺} indicates the presence of a *P* element, scored by red eye colour.

Line	Map (BDGP)	Genetic distance between markers (cM)					
		$P\{w^+\}$ - <i>Ocd</i>	SE	<i>Ocd</i> - <i>f</i>	SE	$P\{w^+\}$ - <i>f</i>	SE
KG02315	14B11	2.99	0.39	2.32	0.34	5.01	0.50
EY04615	14B18	0.78	0.20	2.24	0.34	3.02	0.39
EY03459	14C1	0.57	0.20	2.97	0.45	3.25	0.47
EY01983	14C3	0.55	0.19	2.66	0.42	2.93	0.44
BG00710	14C6	0.17	0.10	2.20	0.35	2.26	0.35

Table 3.5 Genetic distances between pairs of markers used in the five crosses

Genetic distances and standard errors (SE) are shown. $P\{w^+\}$ refers to the *P* element. In each case, the order of the three markers (deduced from the genetic distances) is $P\{w^+\}$ -*Ocd*-*f*, meaning that each of these *P* element insertions lie to the left hand side of *Ocd*. The genetic distances between each insertion and *Ocd* clearly correlate with their cytogenetic locations. The distance between *Ocd* and *f*, which is included as a control, remains fairly constant, at between 2.2 and 3cM. Genetic distance (cM) is the percentage recombination between two given markers.

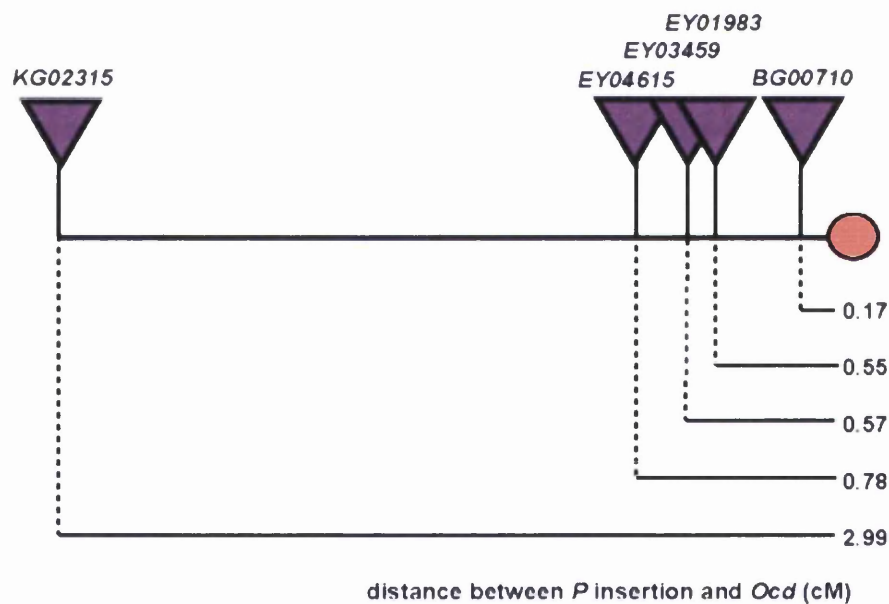


Figure 3.10 The *Ocd* region showing relative positions of *P* element insertions

P elements are represented by triangles, and the *Ocd* gene is represented by a red circle. The map shows relative positions and the calculated genetic distances (cM) between each *P* element insertion and *Ocd*.

The *P* element mapping data determined the closest right hand flanking marker for *Ocd*: BG00710 (Figure 3.10). This insertion is located at 14C6 at approximately 50bp 5' of the 5'UTR of *hangover* (*hang*). As described earlier, SNP mapping reveals that the right hand flanking marker is a SNP within *paralytic*. Therefore, the *Ocd* critical region was reduced to an area encompassing only six genes (Figure 3.11).

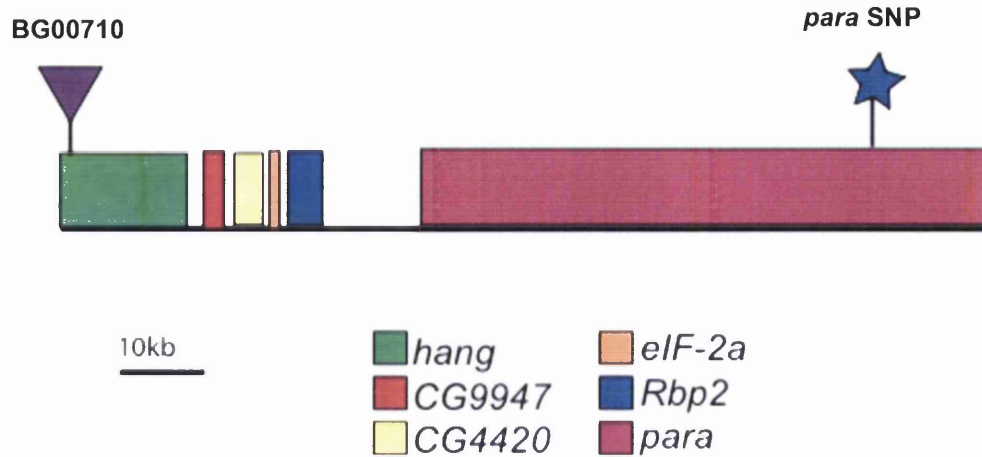


Figure 3.11 Topographical representation of the *Ocd* region after mapping

The region encompasses six genes over a 100kb region, and between cytogenetic bands 14C6 and 14E1. *para* makes up 64kb of the region. The *P* element defining the left hand limit is represented by a triangle, and the SNP defining the right hand limit is indicated by a star.

Four of the genes in the newly defined *Ocd* region have already been characterised, while two are genes defined only by the genome project, the putative functions of which have been assigned via bioinformatic analysis (Flybase: <http://flybase.org>). The *Ocd* mutations could potentially reside in any one of these genes.

The 14.6kb gene *hangover* (*hang*) has only recently been characterised (Scholz *et al.*, 2005). *hang* encodes a large nuclear zinc finger protein, so may have a role in DNA binding. One transposon-induced mutant allele is defective in responses to several environmental stressors such as heat, ethanol and paraquat, a free-radical generating agent. It is feasible that because *hang* mutants are broadly stress-sensitive, mutations elsewhere in the gene could also result in cold-sensitivity. However, although *hang* mutants do not thrive well when grown at 18°C, they are not reported to be cold-sensitive paralytic (H. Scholz, *personal communication*).

CG9947 is uncharacterised, although is putatively thought to have a role in cell cycle control (Flybase). This was determined through bioinformatic analysis however, and no mutant alleles have been described. Similarly, *CG4420* is as yet uncharacterised. It is cited on Flybase as encoding an endopeptidase. This is of particular interest as the aminopeptidase mutant *slamdance* (*sda*) has a seizure (bang-sensitive) phenotype. It is unclear how such a mutation might result in a neural disorders, although it has been

speculated that the peptidase may be involved in neuropeptide processing and degradation (Zhang *et al.*, 2002).

eIF-2 α encodes a translation initiation factor (Qu and Cavener, 1994). This particular initiation factor is known to regulate translation under a variety of stress conditions, for example heat shock, when regular protein synthesis is inhibited (Duncan *et al.*, 1995). It seems unlikely that mutations in such a gene product would result in such a specific phenotype. However, mutant subunits of a human translation initiation factor (eIF2B) have been implicated in the primarily neural disorder vanishing white matter (VWM) (Leegwater *et al.*, 2001). Although eIF2B, and other translation initiation factors are involved in regulating translation in both cold and heat shock conditions, no temperature-sensitive *eIF2B* disorder has yet been identified in humans.

RNA-binding protein 2 (Rbp2) contains an RNA recognition motif and is thought to have role in translation initiation (Kim and Baker, 1993). This is of particular interest as cold is known to affect translation by increasing RNA secondary structures (Gracey *et al.*, 2004). This is likely to be modulated by RNA binding proteins. *Rbp2* is largely uncharacterised however, and the only mutant allele reported is a *P* element intronic insertion derived from the BDGP Gene Disruption Project (Bellen *et al.*, 2004). No discernible phenotype has been reported for this mutant allele, so it could be that the *P* element insertion has little or no effect. These flies are not cold-sensitive paralytic (data not shown).

paralytic (para) encodes the major *Drosophila* voltage-gated sodium channel (Loughney *et al.*, 1989). The first mutant allele described was a temperature-sensitive paralytic mutant (Suzuki *et al.*, 1971). A cold-sensitive human disorder associated with mutations in a sodium channel gene has also been described (McClatchey *et al.*, 1992b). The *smellblind* alleles of *para* are cold-sensitive developmental lethal (Lilly *et al.*, 1994b). However, there is no published data on cold-sensitive paralytic *paralytic* mutant alleles.

3.6 Complementation tests

To determine whether candidate genes were allelic to *Ocd*, complementation tests were performed. Of the six genes within the defined critical region, we were able to obtain mutant alleles of only two: *hangover* and *paralytic*. In parallel with the sequencing of candidate genes, these mutants were used to test for complementation with *Ocd*. The

crosses were carried out at two temperatures, 25°C and 18°C, to address the cold-sensitivity of aspects of the *Ocd* phenotype.

Complementation can only be achieved when combining two recessive mutations. The *Ocd* mutations cause dominantly inherited cold-sensitivity. However, in addition, the mutations lead to recessive lethality, as well as recessive traits such as lack of coordination, general weakness and droopy wings, so it should be possible to acquire valuable information from complementation crosses.

This strategy was used to determine whether each of the *Ocd* mutations were allelic to each other (Søndergaard, 1979a). *Ocd* trans-heterozygotes were generated by crossing heterozygous *Ocd* females with *Ocd* males carrying the *Dp(1;4)r⁺f^{*}* duplication. Here, the time before wing flutter commenced at 18°C was measured. There was no significant difference in the time taken between flies of each of the different trans-heterozygous allelic combinations. Furthermore, analysis of the general behaviour of homozygous and trans-heterozygous *Ocd* females revealed that homozygous *Ocd* females behave like the respective *Ocd* males, and that this is also the case with certain trans-heterozygous females carrying combinations of the alleles *Ocd^l*, *Ocd^f* and *Ocd⁷*, confirming that they are truly allelic (Søndergaard, 1979).

In addition, complementation tests were previously carried out between *Ocd* and mutants of *paralytic*, *Hyperkinetic* and *shibire*, where no evidence for allelism was found (Søndergaard, 1975). The temperature at which these crosses were carried out was not specified.

The gene *slow receptor potential (slrp)* has not been cloned but maps to 13F1-14B2, so is a candidate for *Ocd*. Mutants are cold-sensitive paralytic (at 15°C) (Homyk and Pye, 1989). Complementation tests at 25°C and 18°C between *slrp⁴* and *Ocd* revealed no evidence for allelism; although cold-sensitive, *slrp⁴/Ocd* trans-heterozygotes behave no differently to either of the respective heterozygous mutants (data not shown).

3.6.1 Complementation tests between *Ocd* and *hang*

The *hang^{AE10}* allele is a *P* element insertion within the coding region of the first exon of *hang*. Mutants are viable but defective in responses to several environmental stressors

(Scholz et al., 2005). We also obtained an imprecise excision mutant derived from *hang*^{AE10}. Although *hang*^{AE10} mutants have been described as cold-sensitive (H. Scholz, *personal communication*), this is because they do not thrive at 18°C, and not because they display cold-induced paralysis.

Complementation tests were performed at 18° and 25°C between each of the Glasgow *Ocd* alleles and each of the *hang* mutants. 50 trans-heterozygotes of each combination were examined. In each case, *Ocd/hang* trans-heterozygous females were viable, and displayed cold-sensitivity due to the dominant *Ocd* mutation. This cold-sensitivity was no more pronounced than for age-matched *Ocd* heterozygous females. No other phenotype was observed. Therefore no evidence was found from these crosses for *Ocd* and *hang* being allelic.

3.6.2 Complementation tests between *Ocd* and *para*

We obtained several mutant lines of *para*, including *Df(1)D34*, a lethal deletion specific to the gene (Ganetzky, 1984), which was used for complementation on the basis of its lethal phenotype. Complementation data had previously been compiled for *Ocd* and *para*^{ts1}, a heat-sensitive paralytic mutant (Søndergaard, 1975), where it was concluded that there is no interaction between the two and that they are non-allelic.

Some of Søndergaard's *Ocd* lines have acquired modifiers that seem to improve their viability. Some stocks (*Ocd*^{l-S}, *Ocd*^{5-S}, *Ocd*^{6-S} and *Ocd*^{7-S}) can be maintained as homozygous stocks, and *Ocd* males are healthy enough to mate. To test for complementation between *Ocd* and *para*, *Ocd*^{l-S}, *Ocd*^{5-S} and *Ocd*^{7-S} males were crossed to *para*^{Df(1)D34} (*Df(1)D34*) females, at 18°C and 25°C. The results are shown in Table 3.6.

In each cross, resulting *Ocd/para*^{Df(1)D34} females were viable but displayed a phenotype distinct from that of either balanced mutation. This was more pronounced at 18°C than at 25°C. Although the cold-sensitivity again was no more severe than in *Ocd* heterozygotes, the double mutants are uncoordinated, many hold their wings out or down in a drooped position (with the exception of *Ocd*^{l-S/para}^{Df(1)D34}), and most are generally unfit. This droopy wing phenotype has been described previously in *Ocd*² and *Ocd*³ males (Søndergaard, 1979a). The phenotype observed is specific to *Ocd/para*^{Df(1)D34} flies; neither

heterozygous *para*^{Df(1)D34} females nor heterozygous *Ocd* flies show these additional phenotypes, nor do *Ocd/hang*^{AE10} flies.

Cross	Temperature (°C)	<i>Ocd</i> /FM7	<i>Ocd/para</i> ^{Df(1)D34*}	Wing phenotype
<i>para</i> ^{Df(1)D34} /FM7 x <i>Ocd</i> ^{1-S} /Y	25	70	54	0
	18	100	67	0
<i>para</i> ^{Df(1)D34} /FM7 x <i>Ocd</i> ^{5-S} /Y	25	55	45	15 (33.3%)
	18	75	22	14 (63.6%)
<i>para</i> ^{Df(1)D34} /FM7 x <i>Ocd</i> ^{7-S} /Y	25	55	24	24 (100%)
	18	53	12	12 (100%)

Table 3.6 Data from complementation tests between *Ocd* and *para*

Heterozygous *para*^{Df(1)D34}/FM7 females were crossed to viable *Ocd* males from Søndergaard's lines at 18°C and 25°C. The numbers of heterozygous *Ocd*/FM7 and trans-heterozygote *Ocd/para*^{Df(1)D34} flies eclosing were counted. Numbers of trans-heterozygote females with a wing phenotype were also counted, for example, droopy wings or wings held out. *All trans-heterozygote flies were observed to be uncoordinated and generally unfit.

From the table, *Ocd*^{7-S} is the strongest allele, and all trans-heterozygotes have a pronounced wing phenotype, at both temperatures. In crosses with both *Ocd*^{5-S} and *Ocd*^{7-S}, far fewer trans-heterozygote females eclosed compared to *Ocd*/FM7 females at 18°C, suggesting there is cold-sensitive lethality in these flies. In contrast, *Ocd*^{1-S} appears to be the weakest allele, as no wing phenotype was observed in trans-heterozygotes, at either temperature. There also does not seem to be any temperature-sensitive lethality in this line.

These observations strongly imply that *Ocd* and *para* are allelic. If there were no interaction between the two, we would not expect to see any phenotype in the double mutants other than cold-sensitivity. However, a previous report presented evidence to the contrary. Søndergaard (1975) reported that *Ocd*¹/*para*^{ts1} flies, though cold-sensitive paralytic, were not heat-sensitive. Flies were generated carrying the *Ocd*¹ mutations and two copies of the *para*^{ts1} mutation. These females behaved like *para* homozygous females when given a heat shock, and like *Ocd*¹ heterozygous females when given a cold shock. Generating these flies would require a recombination event to occur between the two mutations. The numbers of recombinant and parental flies were not disclosed. Assuming *Ocd* and *para* are allelic, it is possible that this was an intragenic recombination event. Given that *para* is such a large gene (~60kb), this is entirely plausible. Indeed, if *Ocd* and *para* are allelic, an instance of intragenic recombination has already been observed in the SNP mapping experiment described earlier.

If *Ocd* and *para* are allelic, the *Ocd/ para^{Df(1)D34}* flies have only one copy of *para*, and it is the mutant *para* form. In terms of gene dosage this is equivalent to *Ocd* hemizygous males, but the phenotypes are distinct. This is most likely due to hypertranscription of the X-linked *para* through dosage compensation mechanisms in males.

3.7 Sequencing of candidate genes

The six candidate genes were sequenced across the coding regions and checked for any missense mutations unique to any of the Glasgow *Ocd* lines. Although several SNPs were uncovered, no mutations were found in the coding regions of *hang*, *CG9947*, *CG4420*, *eIF-2a*, or *Rbp2*.

Analysis of sequence data for *para* in the Glasgow *Ocd* lines however uncovered three separate missense mutations in exon 28, occurring as a double mutant in one *Ocd* line and as a single mutant in another. Exon 28 of the *Ocd* lines and several wild-type controls were sequenced. The original *Ocd* lines *Ocd^{1-S}* to *Ocd^{7-S}*, as well as their progenitor wild-type strain (Søndergaard, 1975, Søndergaard, 1979a) were also sequenced to check for presence of the mutations.

None of the control lines harboured mutations in exon 28, whereas each of the *Ocd* lines did, with the sole exception of *Ocd⁴*. This sequencing data is described in full in Chapter 4. The data, taken together with the complementation test results and mapping data strongly implies that the *Ocd* mutations are mutations in the voltage-gated sodium channel *paralytic*.

4 Confirmation that *Ocd* and *para* are allelic

4.1 Introduction to sodium channel biology

4.1.1 Voltage-gated sodium channels

Voltage-gated sodium channels play a vital role in the initiation and propagation of action potentials in electrically excitable tissues and are involved in a wide range of cellular functions, including muscle contraction, neuron signalling and exocytosis (reviewed by Yu and Catterall, 2003). Excitable cell membranes depolarise through the influx of Na^+ into the cell, and this forms the basis of the action potential. Membrane hyperpolarisation subsequently occurs, induced by the action of potassium and calcium channels. Although other forms of sodium channel exist which are not voltage-gated and are structurally dissimilar, for example amiloride sensitive epithelial sodium channels (Alvarez de la Rosa *et al.*, 2000), this thesis will focus solely on voltage-gated channels.

Unlike the potassium channel (Doyle *et al.*, 1998), the complete structure of the sodium channel has not yet been resolved. However, some individual parts have been, yielding clues to functionally important domains. In general, sodium channels consist of a large 240-280kDa glycoprotein α subunit that is responsible for ion selectivity and voltage-gating. The exact size of this subunit is dependent on the species and splice variant - alternative splicing is common for sodium channels. Nine such genes are known to exist in the human genome, as well as four β accessory subunit genes. The smaller β subunits are thought to stabilise the α subunit, although some channels, for example the eel electric organ sodium channel, can function as normal without it (Miller *et al.*, 1983).

The voltage-gated sodium channels consist of four homologous domains I-IV containing multiple α -helical transmembrane sections S1-S6, connected by hydrophilic intervening segments (Figure 4.1). Section S4, the most highly conserved segment, is highly positively charged, containing basic lysine or arginine residues at every third residue, with hydrophobic bases inbetween. S4 is thought to function as a voltage sensor and regulates gating. The channel 'gate' can open or close under the control of these voltage sensors that respond to the level of the membrane potential, thus dictating whether or not Na^+ can flow through into the cell. Between sections S5 and S6 there is a hairpin-like-P-loop, the pore

loop, which controls ion selectivity and permeation. Intermembrane short segments SS1 and SS2 make up the pore region.

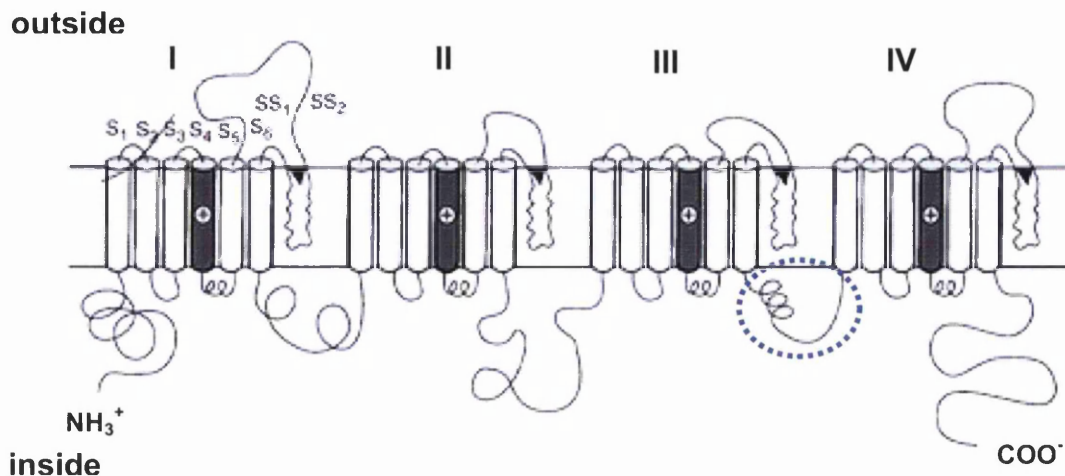


Figure 4.1 Schematic representation of sodium channel structure

The transmembrane arrangement consists of four homologous domains I, II, III and IV each comprised of six transmembrane segments S1-S6. S4 is thought to act as a voltage sensor. Intermembrane short segments SS1 and SS2 make up the pore region: black triangles represent entrance to the pore. The linker between domains III and IV contains the putative inactivation gate (circled). Modified from Zlotkin, 1999.

In the resting state, sodium channels adopt a closed conformation, meaning that they are impermeable to Na^+ . Cell membranes depolarise through the opening (activation) of the sodium channel. Here, the S4 segments (voltage sensors) of each domain change conformation, and in turn alter the positions of adjacent segments resulting in the formation of an open pore that Na^+ can pass through. Na^+ influx causes rapid membrane depolarisation and action potential initiation. Channel activation is transient and is followed by the inactivation phase, when the membrane becomes repolarised. For this to occur, channels become impermeable to sodium ions. This inactivation is accompanied by the opening of potassium channels and makes the cell refractory to firing, thus preventing both the breakdown of ionic gradients and cell death.

This type of channel inactivation (fast inactivation) is described as working according to a 'ball and chain' or 'hinged lid' mechanism (reviewed by Goldin, 2003). Slow inactivation is a distinct process which occurs if the membrane is depolarised for longer, and is probably a consequence of a structural rearrangement of the channel pore (Goldin, 2003, Vilin and Ruben, 2001). During fast inactivation, a cytoplasmic region occludes the pore by binding to a region nearby: the docking site. This cytoplasmic region, or 'inactivation gate', is widely believed to be the linker between domains III and IV (Vassilev *et al.*, 1988,

Stuhmer *et al.*, 1989), which includes the hydrophobic four amino acid stretch IFMT thought to be crucial for this function (West *et al.*, 1992). In *Drosophila*, the corresponding motif is MFMT. The phenylalanine and threonine residues are positioned to directly interact with the docking site (Rohl *et al.*, 1999). The docking site is comprised of multiple regions, including the cytoplasmic linkers between S4 and S5 in domains III and IV, and the cytoplasmic end of S6 in IV (Smith and Goldin, 1997) (McPhee *et al.*, 1998). Understanding the precise mechanisms underlying inactivation has important therapeutic implications, since, as will be discussed, many human sodium channel disorders are associated with inactivation defects.

There are at least nine distinct groups of neurotoxins that specifically target sodium channels, and they are characterised by the site to which they bind (Wang and Wang, 2003). Some toxins block channels, whilst others modify gating. Channel toxicology can provide further information about gating properties and ion transport. Future studies combining structural analysis, site-directed mutagenesis and toxicology experiments will more clearly define the specific molecular interactions involved in the process of inactivation.

Nine voltage-gated sodium channel major subunit genes have been found in the human genome (reviewed by George, 2005). These fall into three categories defined by expression mainly restricted to cardiac muscle, the nervous system, or skeletal muscle. In *Drosophila*, only two putative genes have been identified, one of which, *paralytic*, encodes the major functional channel.

4.1.2 *paralytic*, a *Drosophila* sodium channel gene

In genetic model organisms, ion channel genes are commonly identified either through their sequence homology to known channel genes, or by examination of mutant phenotypes. In *Drosophila*, mutations affecting sodium channel function commonly manifest as temperature-sensitive paralytic, and/or toxin resistant or sensitive mutants. The *Drosophila* gene *paralytic* (*para*) has been identified as encoding a sodium channel gene (Loughney *et al.*, 1989). Prior to this, the first allele to be described was *para^{ts1}*, an X-linked recessive mutation associated with heat-sensitive paralysis (Suzuki *et al.*, 1971). Since then, *para* mutations have been associated with a number of other phenotypes, including olfactory malfunction in the *para^{smellblind}* mutants (Lilly and Carlson, 1990, Lilly

et al., 1994a), and DDT and pyrethroid insecticide resistance amongst several different *para* mutants (Pittendrigh *et al.*, 1997, Martin *et al.*, 2000).

Another putative *Drosophila* sodium channel, *DSCI* (Ramaswami and Tanouye, 1989), located on the second chromosome, has also been identified based on sequence homology to other sodium channels. However, most evidence points towards *para* being the structural gene and the major functional component; the homologue of the mammalian α subunit (Loughney *et al.*, 1989, Hong and Ganetzky, 1994). Less research has been carried out on *DSCI*, and whether it transports sodium or another ion such as calcium is unclear. It is expressed solely in fly neurons (Castella *et al.*, 2001). Although *DSCI* and *para* have distinct embryonic patterns, they are known to have a parallel expression pattern in the adult and pupal CNS (Hong and Ganetzky, 1994), suggesting that they might serve distinct neuronal functions. Interestingly, in parallel with the *para*^{smellblind} mutations, a smell-impaired *DSCI* mutant has been reported (Kulkarni *et al.*, 2002).

Through sequencing of independently isolated cDNAs, it was discovered that the *para* gene undergoes alternative splicing of the primary transcript (Loughney *et al.*, 1989). This is shown in Figure 4.2. The *para* locus is approximately 64kb, and the transcripts around 6.4kb. Initial analysis uncovered three optional microexons. In some of the microexons the amino acid is almost identical to that of the corresponding alternative, although the DNA sequence differs more significantly. Further analysis (Thackeray and Ganetzky, 1994) has revealed that there may be at least 48 alternative splice variants of *para*. 11 embryonic and 18 adult splice types have already been identified *in vivo*. However, the exact *para* splicing patterns during specific developmental stages has not yet been fully elucidated.

Alternative splicing has already been described for the *Drosophila* potassium ion channel gene *Shaker* (Schwarz *et al.*, 1988). Splicing variation is believed to lead to increased functional diversity in *Drosophila* ion channels (Thackeray and Ganetzky, 1994). The differences between splice variants may allow for an additional site of modification, for example cAMP-dependent phosphorylation, or glycosylation. Putative phosphorylation sites may be of functional importance, as cAMP-dependent phosphorylation reduces the Na⁺ current of sodium channels. Other changes that might alter channel function include changes involving charged residues. Such a substitution might affect the capacity of the S4 domain to act as a voltage sensor, for example.

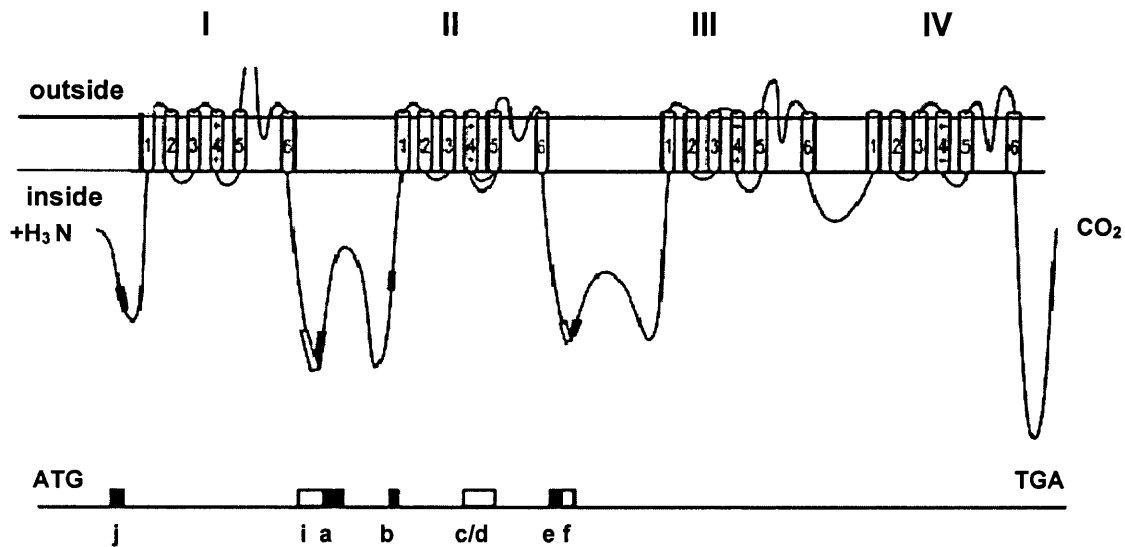


Figure 4.2 Approximate locations of the alternative exons identified in *para*
 Schematic representation of the predicted membrane topology of *para*. The approximate locations of the alternative exons j, i, a, b, c, d, e and f are indicated (Loughney *et al.*, 1989, Thackeray and Ganetzky, 1994, Warmke *et al.*, 1997). Taken from Warmke *et al.*, 1997.

The complete length of the Para protein is between 2071 and 2131 amino acids, depending on which alternative exons are present. The gene is made up of 31 exons in total. A cDNA corresponding to an additional nested transcript has also been isolated (*CG9906*) (Loughney *et al.*, 1989). *CG9906* lies within the first intron of *para*. Although uncharacterised, *CG9906* has a putative role in exocytosis (Flybase: <http://flybase.org>). Whether this transcript has any significance to the expression or function of *para* remains unclear.

The *para* protein has been shown to be modulated by an auxiliary-regulatory 50kDa subunit encoded by *temperature-induced paralytic (tipE)*, also originally identified as a heat-sensitive paralytic mutation (Warmke *et al.*, 1997). This accessory protein enhances *para* sodium channel function in an interaction thought to be similar to that between α and β subunits in vertebrates. Here, *para* is equivalent to the α subunit, and *tipE* is the β subunit counterpart. In *Drosophila* neurons, *tipE* has been demonstrated to control repetitive firing of sodium-dependent action potentials during sustained membrane depolarisation (Hodges *et al.*, 2002).

Insect voltage-gated sodium channels are one of the major targets of conventional pesticides, for example DDT (dichlorodiphenyltrichloroethane) and pyrethroid insecticides. There are two main effects of *para*-specific toxins: the inhibition of ion

transport, and the alteration of gating properties, through the inhibition or persistence of inactivation (reviewed by Zlotkin, 1999). Resistance to such toxins and pesticides in *Drosophila* mutants will be discussed in greater detail in Chapter 5.

4.1.3 Human sodium channel disorders

As mentioned previously, there are at least nine human voltage-gated sodium channel α subunit genes (*SCN1A*, *SCN2A*, etc), mutations in five of which are associated with a variety of disorders. Of the four β subunit genes, only *SCN1B*, a neurally expressed gene, has been directly linked to human disease, namely generalised epilepsy with febrile seizures plus (GEFS+) (Audenaert *et al.*, 2003, Wallace *et al.*, 1998). Sodium channel mutations manifest as either neuronal, cardiac or muscular diseases, depending on where the affected gene is predominantly expressed. A list of disorders associated with sodium channel mutations is displayed in Table 4.1; only some will be discussed in detail. The incidence of such diseases varies considerably according to ethnic origin but they are rare, with an incident rate of approximately one in 100,000. There is a slightly higher incidence in men compared to women. These diseases almost exclusively follow an autosomal dominant mode of inheritance with varying degrees of penetrance (reviewed by Cannon, 1997). In most cases studied, the mutant channels have some defect in channel inactivation, which in turn mediates a dominant negative effect on the wild-type channels. This is because if inactivation is disrupted, some sodium current will be persistently leaked, leading to sustained membrane depolarisation. This sustained depolarisation has the effect of inactivating all channels, wild-type and mutant, leading to a loss of electrical excitability (reviewed by George, 2005).

Neuronal sodium channelopathies are caused by mutations in *SCN1A*, *SCN2A*, *SCN1B*, or *SCN9A*. Such mutations have been shown to be associated with a range of epilepsy and seizure syndromes (reviewed by Lerche *et al.*, 2001). Severe myoclonic epilepsy of infancy (SMEI), for example, is mainly caused by *SCN1A* mutations which give rise to non-functional channels (Lossin *et al.*, 2003). This would suggest that haploinsufficiency is the basis for dominantly inherited SMEI. However, some functional but defective channels have also been identified in cases of SMEI (Rhodes *et al.*, 2004), suggesting a gain-of-function model. GEFS+, also caused by mutations in *SCN1A* (or *SCN1B*) can result in persistent Na⁺ current (Spampanato *et al.*, 2004). Missense mutations in *SCN9A* can lead to painful inherited neuropathy, thought to arise as a result of slow inactivating

channels (Cummins *et al.*, 2004). The neuronal channels are also of particular importance in that they serve as targets for certain drugs such as anaesthetics and anticonvulsants (Catterall, 1999).

	Skeletal Muscle	Cardiac	Neuronal
Gene(s) involved	<i>SCN4A</i>	<i>SCN5A</i>	<i>SCN1A, SCN2A, SCN9A, SCN1B</i>
Disorders	Paramyotonia congenita Hyperkalemic periodic paralysis Hypokalemic periodic paralysis Potassium-aggravated myotonia Painful congenital myotonia Myasthenic syndrome Malignant hyperthermia susceptibility	Long QT syndrome Brugada syndrome Isolated cardiac conduction system disease Atrial standstill Sick sinus syndrome Sudden infant death syndrome Dilated cardiomyopathy, conduction disorder, arrhythmia	Generalised epilepsy with febrile seizures plus Severe myoclonic epilepsy of infancy Intractable childhood epilepsy with frequent generalised tonic-clonic seizures Benign familial neonatal-infantile seizures Familial primary erythralgia

Table 4.1 Inherited sodium channel disorders

The sodium channelopathies fall into three broad categories (muscular, cardiac and neuronal), depending on which gene is affected and therefore the major affected tissue. In some cases however, features of more than one class of disorder may manifest in the same disease (George, 2005).

SCN5A is expressed in the heart and is necessary for the formation of a normal heartbeat, through the propagation of action potentials. Mutations in this gene can cause congenital long QT syndrome (LQTS) and Brugada syndrome (Akai *et al.*, 2000), both associated with ventricular arrhythmias, amongst other symptoms. *SCN5A* mutations can lead to abnormal cardiac events during sleep, and the gene has been implicated in sudden infant death syndrome (Ackerman *et al.*, 2001). In LQTS, channel inactivation is impaired leading to sustained membrane depolarisation (Wang *et al.*, 1996).

Several human disorders associated with myotonia and periodic paralyses are caused by mutations in the skeletal muscle sodium channel *SCN4A* (reviewed by Cannon, 1997, and Caldwell and Schaller, 1992). These include hyperkalemic periodic paralysis (HYPP), paramyotonia congenita (PMC), and potassium-aggravated myotonia (PAM) and hypokalemic periodic paralysis (HOKPP). These diseases are inherited in an autosomal dominant fashion and exhibit high penetrance. The incidence of such disorders is in the

order of one in 100,000. Symptoms are episodic and vary in severity both between and within affected individuals. All of these disorders are associated with mutations in the adult isoform of the skeletal muscle sodium channel alpha subunit (*SCN4A*). This isoform is only expressed at significant levels in skeletal muscle, so there are generally no cardiac or CNS symptoms in the patients. A plethora of *SCN4A* missense mutations have been described with each base change resulting in the substitution of a highly conserved amino acid in the protein. The NCBI Online Mendelian Inheritance in Man database (OMIM: <http://www.ncbi.nlm.nih.gov/entrez/query.fcgi?db=OMIM>) lists 24 allelic variants, with mutations spanning the entire protein (Figure 4.3)

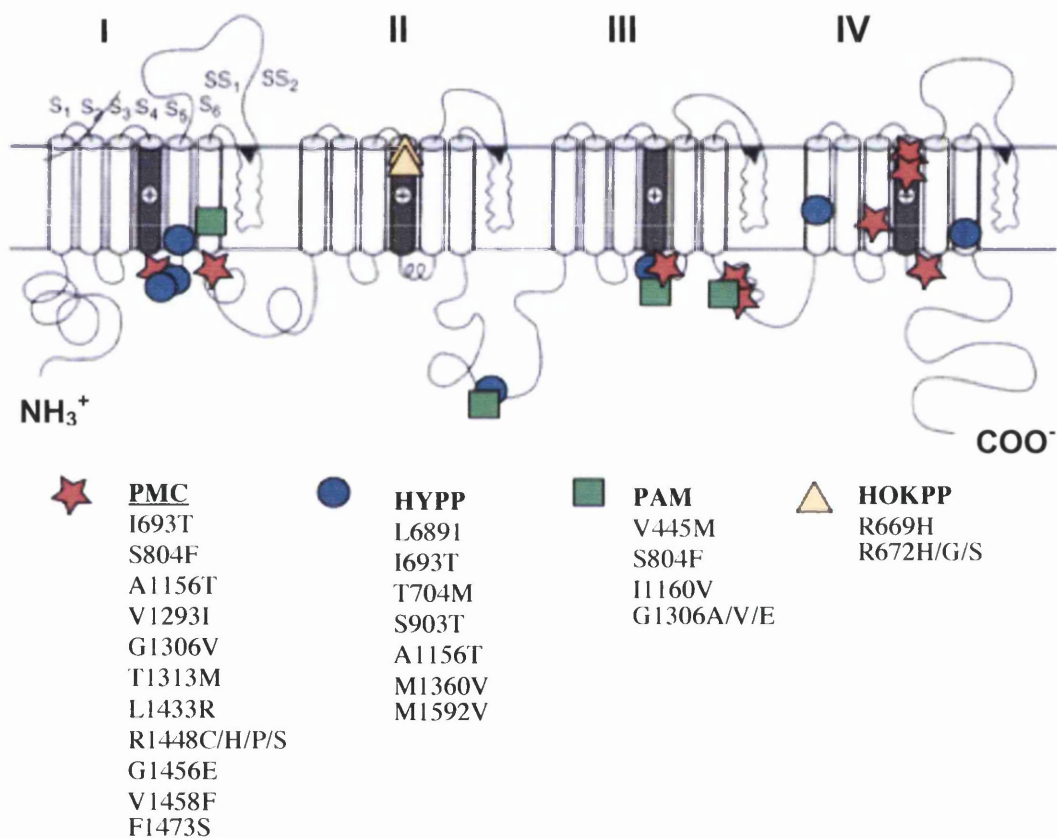


Figure 4.3 Mutations identified in *SCN4A*

Schematic representation of the *SCN4A* skeletal muscle sodium channel, showing positions of missense mutations identified in cases of paramyotonia congenita (PMC), hyperkalemic periodic paralysis (HYPP), potassium-aggravated myotonia (PAM) and hypokalemic periodic paralysis (HOKPP). In some cases, missense mutations were found in patients suffering from overlapping symptoms of more than one disorder. Diagram adapted from Cannon, 1997, Cannon, 2000, and Cannon, 2002.

In these mutant channels, permeation of sodium ions through the channel pore is thought to be normal. The primary defect is instead an alteration in voltage-dependent gating; specifically the disruption of fast inactivation. This manifests itself as aberrant bursts of reopening of the channel and prolonged durations of the open state. Several mutations identified lie in the cytoplasmic loop linking domains III and IV (the proposed 'ball and chain' or inactivation gate). Other mutations lie at the cytoplasmic ends of S5 or S6, which may form part of the inner part of the ionic pore to which the inactivation gate binds (the docking site).

HYPP a dominantly inherited disease, characterised by recurrent attacks of weakness, is associated with elevated serum potassium levels (Gamstorp, 1963). Hypokalemic periodic paralysis (HOKPP) is another disorder associated with *SCN4A* mutations, but does not necessarily involve myotonic attacks. In contrast to HYPP, potassium can be used as a remedy. Two different mutations in *SCN4A*, T704M (Ptacek *et al.*, 1991) and M1592V (Rojas *et al.*, 1991), in domain II S5 and domain IV S6 respectively, have been identified in HYPP patients. Additionally, a case of HYPP in a lineage of quarter horses has been described (Rudolph *et al.*, 1992). This was found to be due to a mutation in domain III transmembrane segment S3 of the equine adult skeletal muscle sodium channel gene.

The main symptom of PMC, first described by von Eulenberg in 1886, is myotonia, which is usually worsened by cold temperatures, although cases of PMC without cold paralysis have also been described (Davies *et al.*, 2000). Also, this myotonia is paradoxically worsened with rapid movement. This is in contrast to myotonia congenita, caused by mutations in the skeletal muscle chloride channel gene *CLCN1* (Koch *et al.*, 1992). PMC is a dominant disorder with high penetrance. Many different mutations within *SCN4A* have been identified in PMC patients. For example, four different substitutions at R1448, a highly conserved residue in the S4 helix of domain IV have been associated with PMC (Ptacek *et al.*, 1992). Two mutations have also been found in the III-IV cytoplasmic loop region of the sodium channel (the proposed location of the channel inactivation gate); G1306V and T1313M (McClatchey *et al.*, 1992b).

Individuals with PAM suffer from myotonia that becomes significantly worse with potassium ingestion. This encompasses a handful of disorders including mild myotonia fluctuans and severe myotonia permanens. As with the previously described sodium channelopathies, the mode of inheritance is dominant. Like PMC, a mutation in domain IV

S4 has been identified, V1589M (Heine *et al.*, 1993). In the family studied, as well as being aggravated by potassium, the myotonia was also worsened by cold. The valine residue is thought to be close to the cytoplasmic surface and putatively forms part of the docking site for the inactivation gate. Also, as in PMC, residue G1306 has been found to be mutated in cases of myotonia fluctuans (Ricker *et al.*, 1994). Here the mutation is G1306A, and is not associated with cold-sensitivity.

At present no cure exists for the sodium channelopathies. Treatments range from the administration of carbonic anhydrase inhibitors and local anaesthetics, to antiarrhythmic or antimyotonic agents. Some side effects of such drugs can however prevent long-term use. For cardiac channelopathies, pacemakers or defibrillators may be fitted. Until recently, channelopathy mutations have been investigated at the channel kinetics level through heterologous expression of mutant channels. Although undoubtedly informative, this *in vitro* method is not ideal for shedding light on the impact of environmental factors on mutant phenotype. A whole animal model is necessary to research the effects of a channel mutation on the whole organism, and in developmental stages and tissues of choice.

To date, murine mutations in two voltage-gated sodium channel genes have been identified. Missense mutations in the mouse gene *Scn8a*, expressed in the brain and spinal cord, have been shown to cause severe neurological phenotypes (Buchner *et al.*, 2004, Kohrman *et al.*, 1996). In addition, transgenic mice carrying a targeted mutation in the S4-S5 linker of domain 2 of the neuronal gene *Scn2a*, analogous to a GEFS+ causing human *SCN2A* mutation, develop a progressive seizure disorder from two months of age (Kearney *et al.*, 2001). Such mouse models will aid research into human channelopathies considerably, particularly neural disorders. Indeed, the *Scn2a* model has been successfully used to map modifiers of the seizure phenotype (Bergren *et al.*, 2005).

However, at present no mammalian model exists for human skeletal muscle (*SCN4A*) disorders. An appropriate genetic model would undoubtedly aid in establishing the mechanisms by which inactivation is disrupted in *SCN4A*-associated sodium channel disorders, and how this disruption may be exacerbated or mitigated by factors such as activity, serum potassium levels, and temperature. Once such interactions are better understood, it should also be possible to develop improved pharmacological treatments.

In addition to the vast array of disorders, there are also pharmacogenomic aspects to sodium channel mutations. Local anaesthetics act by blocking voltage-gated sodium channels (Fozzard *et al.*, 2005). These drugs enter the inner pore and bind to specific amino acids. Their binding affinity is dependent on the activation state of the channel. Because of this, mutant channels can respond very differently to anaesthetics and antiarrhythmic agents, which are often used to treat channelopathies (Desaphy *et al.*, 2004, Lucas *et al.*, 2005). This may be due to mutations affecting binding sites, or alternatively altering channel kinetics. Furthermore, adverse effects may be experienced upon administration of certain therapeutic agents. For example, *SCN4A* mutations, including G1306A, have been implicated in a severe life-threatening reaction to succinylcholine, a commonly used muscle relaxant (Vita *et al.*, 1995). Determining the efficacies or side effects of different drugs on patients presenting with similar disorders but different underlying channel mutations is therefore an important area of research.

4.1.4 Evolutionary aspects

Voltage-gated sodium channels belong to the ion channel superfamily, which also includes voltage-gated potassium channels, voltage-gated calcium channels, transient receptor potential (TRP)-related channels and cyclic-nucleotide-gated channels (Jan and Jan, 1992). While sodium and calcium channels consists of four homologous domains, potassium and cyclic-nucleotide-gated channels are tetramers of single domain subunits. Sodium channels are the most recent of the superfamily to have arisen, and it is widely believed that they evolved from the single-domain channels, via the structurally similar calcium channels (Yu and Catterall, 2003). Sodium channels are believed to have arisen early in the metazoan era, on the basis that they have not been discovered in higher plants, algae or protozoa. They have however been identified in mammalian vertebrates, non-mammalian vertebrates, and invertebrates, and in all these animals their structure, organisation, splicing properties and toxicology is strikingly similar (Plummer and Meisler, 1999). This implies that the voltage-gated sodium channel evolved prior to the evolutionary division of vertebrate and invertebrates.

The use of animal models for human disease relies on the conservation of genes and molecular and cellular systems between seemingly very diverse species. In *Drosophila*, putative structural sodium channels have been identified on the basis of sequence similarity with vertebrate sodium channel genes, the major functional component of which is the

260kDa α subunit. Para bears striking sequence similarity to the rat SCN1A (brain) sodium channel, with 46% amino acid sequence identity. Sequences within the four homology domains are particularly well conserved between fly and rat, ranging from 58% (III) to 66% (II) identity (Loughney *et al.*, 1989). As mentioned previously, the S4 segment of each domain, the voltage sensor, is the most conserved.

Amino acid sequence alignment of Para and the human sodium channels reveals striking similarity. For example, Para is 45% identical to the skeletal muscle gene SCN4A, and the neural genes SCN1A and SCN2A, and 44% identical to the cardiac channel SCN5A. Differences in length of the first cytoplasmic linker, even within species, may reflect differences in expression patterns. For example, the rat brain channel linker is 360 amino acids long compared to that of the rat muscle channel which is 200 residues shorter (Loughney *et al.*, 1989).

Within the protein sequence there are regions that are particularly highly conserved. These segments are likely to confer functionality to the protein. The short cytoplasmic segment between homology domains III and IV is particularly highly conserved (Figure 4.4), sharing 65% amino acid identity between rat and fly, in contrast to the first two linking segments which are more poorly conserved (Loughney *et al.*, 1989).

Domain III-IV linker

<i>Rn SCN1A</i>	1484	DNFNQQKKKFGG-QD	IFMTEE	QKKYYNAMKKLGS	KKPQKPI	PRPGNK	FQGMVFD	1536
<i>Hs SCN1A</i>	1484	DNFNQQKKKFGG-QD	IFMTEE	QKKYYNAMKKLGS	KKPQKPI	PRPGNK	FQGMVFD	1536
<i>Hs SCN5A</i>	1471	DNFNQQKKKLG	QDIFMTEE	QKKYYNAMKKLGS	KKPQKPI	PRPLNK	YQGFIFD	1523
<i>Hs SCN4A</i>	1296	DNFNQQKKKLG	KDIFMTEE	QKKYYNAMKKLGS	KKPQKPI	PRPQNK	IQGMVYD	1348
<i>Dm para</i>	1561	DNFNEQKKKAGGS	LEMFMTE	DQKKYY	SAMKKMG	SKKPLKAI	PRPRWRPQAI	1614

Figure 4.4 Multiple amino acid sequence alignment (ClustalW) of the III-IV cytoplasmic linker

ClustalW amino acid sequence alignment. The sequences displayed are (from top to bottom) rat SCN1A, human SCN1A, human SCN5A, human SCN4A and *Drosophila* Para. Residue numbers are shown. The domain III-IV linker is a particularly highly conserved region of the channel. The hydrophobic four residue motif important for inactivation (IFMT in mammals, MFMT in *Drosophila*) is indicated by a red dotted box. Small hydrophobic amino acids (AVFPMILW) are coloured in red, acidic (DE) in blue, basic (RHK) in magenta, and hydrophilic (STYCNQG) in green.

The high similarity between fly and mammalian sodium channels is very encouraging in terms of developing *Drosophila* as a model for sodium channel disease. If the *Ocd* mutations are point mutations at conserved residues in *para*, it would make the *Ocd* the

ideal model for investigating pathogenesis and for developing novel treatments for human sodium channelopathies.

4.2 Identification of missense mutations in *para*

Selected coding regions of *paralytic* were sequenced and missense mutations were uncovered in lines *Ocd^{1-G}*, *Ocd^{3-G}*, *Ocd^{5-G}* and *Ocd^{7-G}* (Figure 4.5, Table 4.2). The mutations found all lie within the same exon, exon 28, and are in a highly conserved region of the Para protein. *Ocd^{1-G}*, *Ocd^{3-G}* and *Ocd^{5-G}* harbour the same two missense mutations, I1545M and G1571R, caused by an A-G transition and a G-C transversion, respectively. *Ocd^{7-G}* has only one mutation, T1551I, caused by a C-T transition. None of these base changes have been observed in any of the control lines tested, including the original progenitor Oregon-R stock obtained from Leif Søndergaard's laboratory in Copenhagen. The *Ocd* stocks kept by Søndergaard were also sequenced to check for exon 28 mutations (Figure 4.5, Table 4.2).

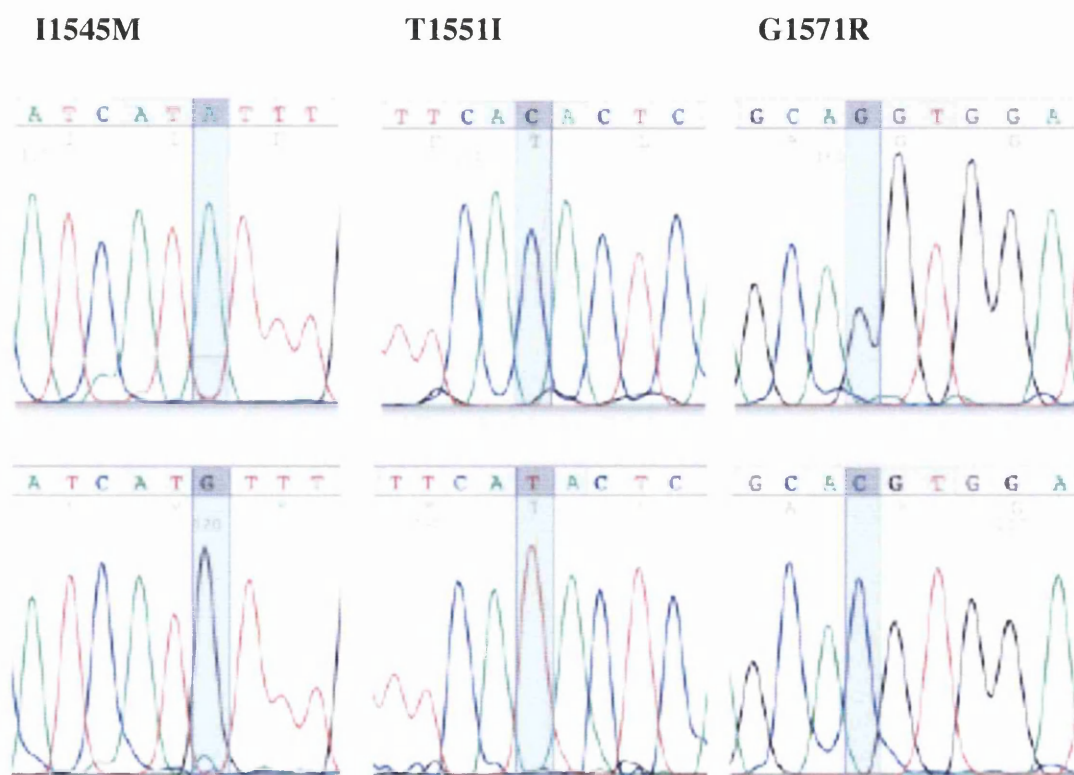


Figure 4.5 *para* coding mutations identified through sequencing of exon 28.

These electropherograms generated from 4peaks software display the DNA sequence of exon 28 in *Ocd* and control fly lines. In each case the top panel shows the wild-type sequence. Three separate mutations were identified, two which exist as a double mutation in certain *Ocd* lines (I1545M and G1571R), and one (T1551I) which exists as a single mutation (see Table 4.2).

Mutant allele(s)	Base change(s)	Coding mutation(s)	Location of mutated residue(s)
$Ocd^{1-S}, Ocd^{1-G},$ $Ocd^{3-S}, Ocd^{3-G},$ $Ocd^{5-S}, Ocd^{5-G},$ Ocd^{6-S}, Ocd^{7-S}	A-G transition G-C transversion	I1545M G1571R	Domain III S6 III-IV linker
Ocd^{4-S}, Ocd^{4-G}	not found	unknown	unknown
Ocd^{2-S}, Ocd^{7-G}	C-T transition	T1551I	Domain III S6

Table 4.2 *para* mutations identified in *Ocd* lines

The *Ocd* mutations identified all lie within *para* exon 28. Mutations were identified in all *Ocd* lines available with the exception of Ocd^4 . All base changes results in a coding mutation. None of the control lines tested harboured any of these base changes. Notably, G1571 is orthologous to human *SCN4A* residue G1306, mutations in which have been associated with cold- and potassium-sensitive periodic paralysis.

Table 4.2 shows the sequence data for both the Glasgow *Ocd* lines and Søndergaard's *Ocd* lines from Copenhagen. In both sets of lines, there are several double mutants and one single mutant, and in both sets, no mutation in Ocd^4 was identified. However, Ocd^{2-S} and Ocd^{7-G} both harbour the T1551I mutation, while Ocd^{7-S} carries the double mutation I1545M and G1571R. This suggests that the stocks may have been mislabelled or mixed up since the two sets have been separated, and that Ocd^{7-G} is actually the original Ocd^2 mutant line.

It is peculiar that several of the alleles share the same double mutant genotype, firstly because they are reported to be independently derived (Søndergaard, 1979a), and secondly because these lines display strong differences in mutant phenotype. It is highly likely that these differences in phenotype are due to the accumulative effects of modifier genes. Each of the mutant lines were found on different days from independently EMS treated batches of male flies (L. Søndergaard, *personal communication*). In this screen, approximately 400,000 F_1 flies were tested. It may be that only a specific conformational change brought about by either the double mutations or the single T1551I mutation is 'required' to generate the *Ocd* phenotype. Alternatively, the fact that more than one line has the same two mutations might be due to one being a polymorphism in the original wild-type stock from which they were derived. However, the progenitor ORR line was sequenced and neither mutation was detectable. If it was present at low levels in the ORR population, it is possible that it might have been diluted out and lost since the discovery of the *Ocd* mutations. For this reason it is important to elucidate whether either one of the mutations in the double mutants is simply a polymorphism, and not necessary for the *Ocd* phenotype. Strategies by which to do this will be discussed in detail later.

In the Para protein, the S6 transmembrane segment of domain III is comprised of residues 1534-1560, and residues 1561-1614 make up the cytoplasmic linker between domains III and IV. The G1571R mutation is located within the cytoplasmic linker, which contains the putative activation gate of the sodium channel. This residue lies very close to the hydrophobic motif MFMT of the inactivation gate (residues 1576-1579) believed to directly interact with the docking site. The I1545M and T1551I mutations both reside at the intracellular phase of segment S6 in domain III (Figure 4.6).

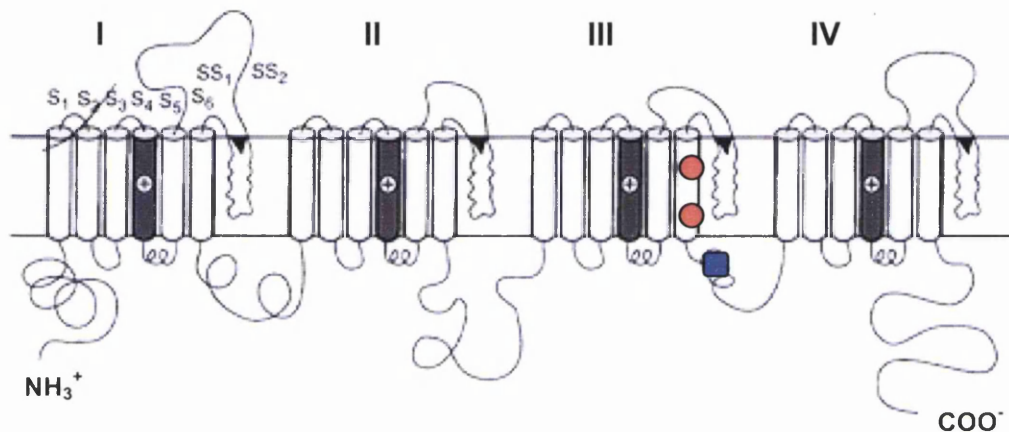


Figure 4.6 Approximate positions of the *Ocd* mutations in the Para sodium channel

The mutations I1545M and G1571R present in the double mutants are represented by circles, and the mutation T1551I by a square. G1571R is located in the III-IV cytoplasmic linker close to the hydrophobic motif required for inactivation I1545M and T1551I are both located in the domain III S6 transmembrane segment.

In the double mutants, the first change at residue 1545 involves methionine being substituted for isoleucine. These amino acids are of a similar size and are both nonpolar and hydrophobic. However, in the second change at residue 1571, arginine, which is large and positively charged (basic), is substituted for glycine, which is very small and hydrophilic, so can confer flexibility to a protein. This may suggest that it is the G1571R mutation that confers the major deleterious effect on sodium channels, although it might also be the case that both mutations are 'necessary' for a viable cold-sensitive paralytic phenotype. The G1571R mutation alone might be completely lethal, but when present with I1545M, there is a subtle rescuing effect. Such hypotheses can be investigated by creating single mutants, the details of which will be described later. In the *Ocd* single mutant, hydrophobic isoleucine at residue T1551 is substituted for threonine, which is hydrophilic.

The differences in polarity between these two amino acids support the notion that this change would exert a phenotypic effect.

The channel sections harbouring the *Ocd* mutations are highly conserved (Figure 4.7). Indeed, all three mutated residues are completely conserved between fly and human. This would suggest that these residues are important for channel function. For example, the G1571R mutation is one of two conserved adjacent glycines. It is possible that this double glycine motif confers flexibility to this part of the protein, perhaps allowing bending for the putative 'ball and chain' inactivation mechanism to work. Because this mutation is also very close to the hydrophobic motif MFMT thought to be important for binding of the 'ball' to its docking site, the G1571R mutation might either hinder the protein bending rendering the channel permanently open, or conversely might cause the channel to be permanently inactivated.

A. Domain III S6

<i>Rn SCN1A</i>	1457	LYMYLYFVIFIIIFGSFFTLNLFIVGVII	1483
<i>Hs SCN1A</i>	1457	LYMYLYFVIFIIIFGSFFTLNLFIVGVII	1483
<i>Hs SCN5A</i>	1444	LYMYLYFVIFIIIFGSFFTLNLFIVGVII	1470
<i>Hs SCN4A</i>	1269	LYMYIYFVIFIIIFGSFFTLNLFIVGVII	1295
<i>Dm para</i>	1534	IYMYLYFVFFIIIFGSFFTLNLFIVGVII	1560

B. Domain III-IV linker

<i>Rn SCN1A</i>	1484	DNFNQOKKKFGS-QDIFMTEEQKKYYNAMKKLGSKKPQKPIPRPGNKFQGMVFD	1536
<i>Hs SCN1A</i>	1484	DNFNQOKKKFGS-QDIFMTEEQKKYYNAMKKLGSKKPQKPIPRPGNKFQGMVFD	1536
<i>Hs SCN5A</i>	1471	DNFNQOKKKLGS-QDIFMTEEQKKYYNAMKKLGSKKPQKPIPRPLNKYQGFIFD	1523
<i>Hs SCN4A</i>	1296	DNFNQOKKKLGS-KDIFMTEEQKKYYNAMKKLGSKKPQKPIPRPQNKIQGMVYD	1348
<i>Dm para</i>	1561	DNFNEQKKKAGSLEMFMTEDQKKYYSAMKKMGSKKPLKAIPRPRWRPQAIVFE	1614

Figure 4.7 The *Ocd* mutations lie in highly conserved regions of Para

A. ClustalW amino acid sequence alignment of domain III S6 (Para residues 1534-1560) in (from top to bottom) rat SCN1A, human SCN1A, SCN5A and SCN4A, and *D. melanogaster* Para. Residue numbers are shown. The locations of *Ocd* mutations I1545M and T1551I are indicated by solid boxes. B. ClustalW alignment of the domain III-IV linker (Para residues 1561-1614) in rat SCN1A, human SCN1A, SCN5A and SCN4A, and *D. melanogaster* Para. The location of the *Ocd* mutation G1571R is indicated by a solid box. The hydrophobic motif believed to be vital in the process of channel inactivation - IFMT in rat and human, MFMT in *Drosophila* - is also indicated by the red dotted box. Small hydrophobic amino acids (AVFPMILW) are coloured in red, acidic (DE) in blue, basic (RHK) in magenta, and hydrophilic (STYHCNQG) in green.

The human skeletal muscle channel *SCN4A* V1293I mutation, which has been found in patients with paramyotonia congenita (but without cold paralysis) lies in the same segment

as *Ocd* mutations I1545M and T1551I (Koch *et al.*, 1995). This is encouraging in terms of developing *Ocd* as a model for such disorders, and demonstrates the validity of such an approach. The fact that mutations located in the same channel section in both humans and flies give rise to such similar phenotypes suggests that the molecular pathogenesis is the same. Therefore, understanding what is happening at the molecular level in *Drosophila* with a view to developing pharmacological treatments should prove fruitful.

Moreover, the G1571R mutation is of particular interest as a mutation in the orthologous residue, G1306, in *SCN4A* has already been found in cases of the human muscle disorder paramyotonia congenita (G1306V), which is cold-sensitive, (McClatchey *et al.*, 1992b). It is remarkable that the mutations at the same residue can result in cold-aggravated paralytic phenotypes in both fruit flies and humans. *SCN4A* G1306 mutations have also been uncovered in two families with potassium-associated myotonia. One family harboured a G1306A substitution (Ricker *et al.*, 1994), the second a G1306E substitution (Lerche *et al.*, 1993). As yet, no G1306R mutation in *SCN4A* has been reported.

It is intriguing that substitution of residues with varying properties can result in such diverse phenotypes, which may or may not be susceptible to environmental effects - either temperature or potassium - to varying degrees. The effect on gating of three classes of G1306 mutation has been investigated; G1306A, G1306E and G1306V (Mitrovic *et al.*, 1995). This revealed inactivation and activation defects in all three channel types which differ in severity, with G1306A being the least and G1306E the most severe. This correlates with the gravity of symptoms observed in patients. A glycine to glutamic acid change would also be predicted to prove most detrimental to the protein. G1306A has also been associated with succinylcholine-induced masseter muscle rigidity, a complication associated with anaesthesia that can be fatal (Vita *et al.*, 1995).

4.3 Rescue of the *Out cold* phenotype by expression of a *para* transgene

4.3.1 The *P{UAS:para}* transgene

In order to confirm that the *Ocd* phenotype is due to mutations in *para*, rescue experiments involving expression of a wild-type *para* transgene in *Ocd* flies were undertaken, taking advantage of the widely used GAL4/UAS system (Brand and Perrimon, 1993).

Fly lines containing insertions of a $P\{UAS:para^+\}$ construct (Figure 4.9) were donated by Dr Richard Baines, University of Warwick (Mee *et al.*, 2004). The construct was created by cloning the *para* cDNA 13.5 (Warmke *et al.*, 1997) into the $pP\{UAST\}$ vector (Brand and Perrimon, 1993). The cDNA encodes a full length protein and corresponds to the third most abundant combination of alternative exons expressed in adult flies (Thackeray and Ganetzky, 1994). It contains exons j, i, b, d, e, but lacks exons a and f (see Figure 4.2).

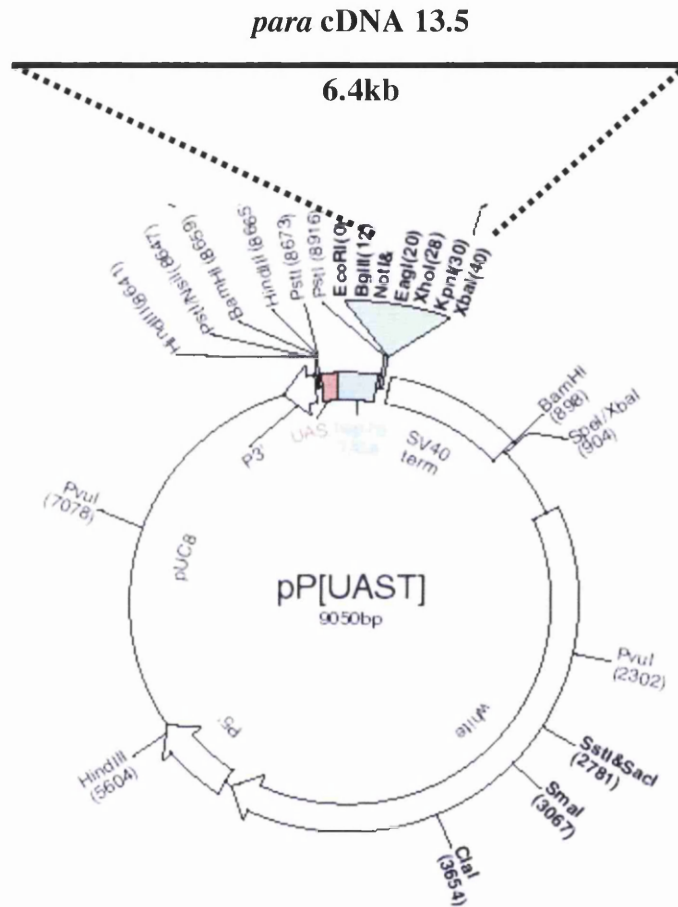


Figure 4.8 The $P\{UAS:para^+\}$ construct

The construct was created in Richard Baines' lab (University of Warwick) by directionally cloning the *para* cDNA 13.5 (Warmke *et al.*, 1997) into the $pP\{UAST\}$ vector (Brand and Perrimon, 1993) using XbaI and NotI restriction sites (Mee *et al.*, 2004).

Because *para* is ubiquitously transcribed throughout the CNS and PNS at all developmental stages (Hong and Ganetzky, 1994), we would predict that the best driver would be pan-neuronal. $P\{1407:GAL4\}$ (Sweeney *et al.*, 1995) is a pan-neuronal CNS driver which has been well characterised with respect to its expression pattern and is known to be a strong driver. In this line, GAL4 is expressed in neuroblasts and throughout development in neurons of the CNS and PNS.

4.3.2 Rescue of *Ocd* semi-lethality

Assuming *para* and *Ocd* are allelic, a GAL4/UAS:*para*⁺ mediated rescue strategy should result in at least partial rescue of the *Ocd* phenotype. However, with respect to cold-sensitivity, all of the *Ocd* mutations are dominant so rescue might be impossible or at least complicated. It is possible that several copies of the wild-type transgene are required, to result in GAL4 driven overexpression of *para*. Also, in the proposed experiment, only one of the many *para* splice forms found in the fly will be expressed. There are at least 48 possible splice variants and in wild-type flies, the expression of different isoforms is developmentally regulated (Thackeray and Ganetzky, 1994).

Although the cold-sensitivity of the *Ocd* mutations is dominant, the *Ocd* males also display semi-lethality that varies between the different mutant lines. Because heterozygous females are viable, this phenotype must be a recessive trait, and it should therefore be possible to rescue male semi-lethality through expression of a wild-type copy of the *para* gene. To this end, heterozygous *Ocd*^{l-G}/*FM7* females homozygous for the $P\{UAS:para^+\}$ on the second chromosome were generated. These females were then crossed to males carrying a $P\{GAL4\}$ driver on a chromosome other than the X, where the *Ocd* mutations are located.

A range of GAL4 driver lines were chosen, including the neural driver *1407*:GAL4, which would be expected to result in rescue. A ubiquitous driver, *da*:GAL4 was also chosen, as well as the muscle driver *dmej2*:GAL4. As negative controls, *hs*:GAL4 and *ey*:GAL4 were used, which express GAL4 in under heat-shock and in the eye imaginal discs, respectively. All crosses were carried out at 25°C.

As a further negative control the female *Ocd*^{l-G}/*FM7* flies with the $P\{UAS:para^+\}$ inserted on the second chromosome, were crossed to wild-type males (i.e. resulting in progeny with no GAL4 driver). Similarly, *Ocd*^{l-G}/*FM7* females were crossed to GAL4 driver males (i.e. resulting in progeny with no $P\{UAS:para^+\}$ construct).

In a cross of these *Ocd* females with a male fly, the expected ratio of *Ocd*^{l-G} males to *FM7* males is 1:1. However, in *Ocd*^{l-G} flies, the ratio is skewed to approximately 1:9. It is therefore possible to assay for any rescue of semi-lethality in the *Ocd*^{l-G} males expressing the wild-type transcript, in order to confirm that *Ocd* and *para* are allelic.

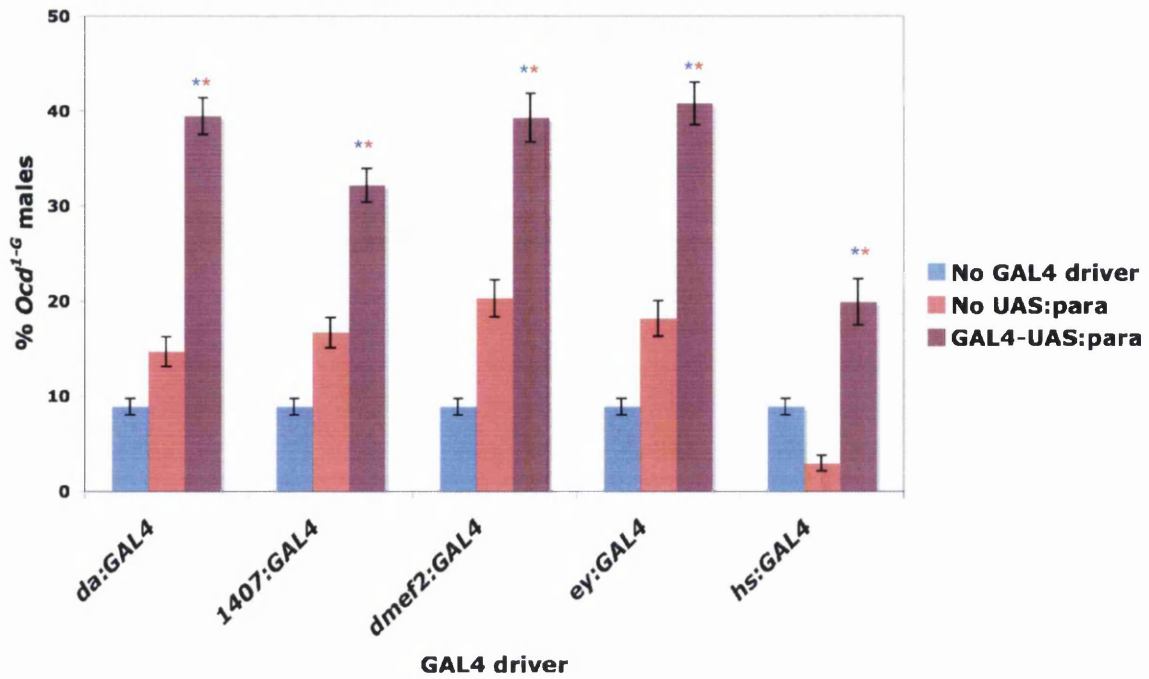


Figure 4.9 Rescue of Ocd^{1-G} semi-lethality by GAL4 driven expression of $para^+$.

The graph shows the percentage of Ocd^{1-G} males eclosing from various crosses. As negative controls, crosses were performed resulting in male offspring harbouring either the $P\{UAS:para^+\}$ construct only (no GAL4 driver), or the specific GAL4 driver only (no $P\{UAS:para^+\}$). To test for rescue of Ocd^{1-G} semi-lethality, $Ocd^{1-G}/FM7$ females carrying the $P\{UAS:para^+\}$ construct on chromosome II were crossed to males carrying a specified GAL4 driver (GAL4-UAS: $para$). This should result in wild-type expression of $para$ in a GAL4 driver-specified manner. Standard error of the proportion in each case is displayed. $2 \times 2 \chi^2$ analysis was used to test for significant deviation from each negative control. Asterisks denote significant deviation from each control (deviation from the “no GAL4 driver” control indicated by blue asterisks; deviation from the “no UAS: $para$ ” control indicated by red asterisks): * $p < 0.001$.

Although reported to be slightly leaky (R. Baines, *personal communication*), no sign of rescue was observed when the $P\{UAS:para^+\}$ construct was crossed into Ocd^{1-G} flies in the absence of a $P\{GAL4\}$ driver. The data presented in Figure 4.9 shows that there is a striking difference between the fraction of eclosing Ocd^{1-G} males in crosses where a $P\{GAL4\}$ element has been crossed in to express $para^+$, and those where one has not. The fraction of Ocd^{1-G} males eclosing from crosses with no driver is always less than 10%. However, except for in the case of $hs:GAL4$, the percentage of Ocd^{1-G} males eclosing is increased upon crossing in a GAL4 driver. Since there should be no exogenous gene expression arising from the presence of a GAL4 driver in the absence of a UAS sequence, this observation suggests that there is a rescuing effect simply from out-crossing the Ocd^{1-G} flies. This would most likely be due to the differences in genetic background between the Ocd^{1-G} line and the GAL4 driver lines.

2x2 χ^2 analysis was used to test for significant deviation from the numbers of *Ocd*^{l-G} males eclosing in each negative control. In the case of each GAL4 driver, there is significant deviation (p<0.001) from each of the negative control experiments. The observed rescue in the remainder of the lines however does not seem to discriminate between the different categories of *P{GAL4}* driver used. *1407:GAL4* driven expression of *para*⁺ pan-neurally results in rescue, as does *da:GAL4* driven expression of *para*⁺ ubiquitously. However, GAL4 driven expression in the muscle (*dme2:GAL4*), and in the eye discs (*ey:GAL4*), also results in significant rescue. *hs:GAL4* driven *para*⁺ can also rescue *Ocd*^{l-G} semi-lethality. There may be an issue with minimal *hs:GAL4* expression even at 25°C; repeating this experiment at lower temperatures, for example at 21°C, might reveal different results. Temperatures lower than this would cause problems due to the cold-sensitivity of the flies.

A preliminary rescue experiment was also carried out using *Ddc:GAL4* (data not shown). The results showed that no rescue of semi-lethality occurred when *para*⁺ was expressed under the control of *Ddc:GAL4*. This is encouraging as *Ddc:GAL4* is only expressed in a subset of serotonergic and dopaminergic neurons. In *Drosophila* larvae, *Ddc* is expressed in only about 150 cells of the CNS (Lundell and Hirsh, 1994).

Unfortunately, some GAL4 lines are better characterised than others, and although the tissues in which there definitely is expression may be well defined, the tissues in which there is no expression may be relatively unknown (Ito *et al.*, 2003). For example, *ey:GAL4* is known to drive strong expression in the eye discs, but characterisation of expression in all tissues of the fly is unpublished. It may be that the *ey* promoter drives expression in the nervous system, and if this driver is particularly strong, it is plausible that it is able to rescue aspects of the *Ocd* phenotype. It would be useful to characterise the GAL4 lines more fully to elucidate exactly where in the fly they drive expression. This could be achieved by driving expression of *P{UAS:lacZ}* and staining sections with X-gal.

Also, crossing more than one insertion into an *Ocd* stock, for example insertions on both the second and third chromosomes, and therefore increasing the dose of *P{UAS:para*⁺} available to be expressed under the control of GAL4, may result in absolute rescue of the semi-lethality.

Although the GAL4/UAS approach clearly demonstrates rescue, an alternative method by which to prove *Ocd* and *para* are allelic is desirable, especially considering the rescue of

semi-lethality, albeit to a lesser extent, observed in the absence of the $P\{UAS:para^+\}$ transgene, which is probably due to genetic background effects. One approach would be to identify the *Ocd* gene via a *P* element revertant screen. The *Ocd* mutations are dominant gain-of-function mutations resulting in cold-sensitivity. If a *P* element was inserted into the causative gene and produced a null allele, the mutant phenotype would be predicted to revert from dominant cold-sensitive to a recessive lethal. Therefore, screening for such revertants then sequencing the *P* element flanking regions by inverse PCR should identify the *Ocd* gene. Although there is already convincing evidence that *Ocd* and *para* are allelic, this might be a worthwhile experiment in the future.

5 Characterisation of the *Ocd* phenotype

5.1 Introduction

In this chapter, experiments to further characterise the mutant phenotype of *Ocd* flies are described. Extensive characterisation of the *Ocd* mutations is necessary for the development of *Ocd* as an animal model for human disease. No animal model at present exists for many periodic paralytic and myotonic disorders associated with sodium channel defects, and the pathogenic mechanisms are not well understood, especially the roles that temperature and serum potassium levels may play. Additionally, identifying downstream effects or modifier genes may lead to the development of novel therapeutic approaches.

Cold-sensitive paralysis and male semi-lethality in *Ocd* lines have been well documented (Søndergaard, 1975, Søndergaard, 1979a), as well as evidence for a mitochondrial role for the gene product (Søndergaard, 1976, Søndergaard, 1986). To gain further information about the effects of the mutation, a comparative proteomics study was carried out. This has also proved useful in elucidating how *Ocd* flies up- or down-regulate protein expression to manage the detrimental intercellular effects of the mutation.

As described in the previous chapters, the *Ocd* mutations have been mapped to *paralytic*, the major fly voltage-gated sodium channel gene. Since voltage-gated sodium channels are essential for the propagation of action potentials, the mutants were analysed at the electrophysiological level. Patch clamping experiments were undertaken at various temperatures to test for any channel gating or inactivation malfunction. This is particularly important because as yet it is unclear why cold temperatures lead to changes in channel activity in the human condition paramyotonia congenita.

Deafness is commonly associated with human mitochondrial disease. In at least one *Drosophila* model of mitochondrial disease, this deafness has been recapitulated in flies (Toivonen *et al.*, 2001). As part of a collaborative project into fly models of mitochondrial disease, *Ocd* flies were tested for any hearing impairment, using the auditory behavioural assay of Eberl *et al.* (1997).

Several human sodium channel disorders, depending on the underlying mutation, are made worse by either increased or decreased serum potassium levels (Cannon, 2002). This

phenomenon has also been observed in a family of quarter horses suffering from hyperkalemic periodic paralysis (Rudolph *et al.*, 1992). The mechanism by which this occurs is unknown. To determine whether the *Ocd* mutations display potassium sensitivity, *Ocd* flies were exposed to potassium chloride. They were also exposed to sodium chloride to test if manipulating sodium levels affects the severity of the *Ocd* phenotype.

Many insecticides specifically target sodium channels (Wang and Wang, 2003, Zlotkin, 1999), and many *para* mutants, both in *Drosophila* as well as numerous other insect species, confer resistance to such chemicals (French-Constant *et al.*, 2004). Mutations may confer resistance either by altering specific binding sites or by changing channel electrophysiological properties. To test whether the *Ocd* mutations confer such resistance, mutant flies were subjected to a DDT contact assay.

5.2 Proteomics

The original objective of the comparative proteomics study between *Ocd* and wild-type was to aid identification of the *Ocd* gene product. An additional aim was to confirm and extend a previous *Ocd* study (Søndergaard, 1986), in which an additional mitochondrial polypeptide was observed upon 2D gel analysis of *Ocd* flies compared to wild-type (see discussion in section 1.4.2). Identifying this extra protein might provide clues to the type of gene product *Ocd* encodes. The original proteomics experiment was undertaken two decades ago, and since then major technological advances have been made in the proteomics field, particularly due to the advent of two dimensional Differential Gel Electrophoresis, or 2D DIGE (Alban *et al.*, 2003, Swatton *et al.*, 2004, Unlu *et al.*, 1997). This technique was developed to overcome problems of reproducibility in 2D gels. In 2D DIGE, samples are labelled with spectrally distinct fluorescent dyes and run together on the same gel. The CyDyes Cy3 and Cy5 that minimally label lysine residues of a protein are widely used. This sample multiplexing circumvents issues of inter-gel variability. Dye reversal is also applied to control for differences in reactivity between dyes. Proteins are resolved on the basis of their charge and molecular weight and differences in expression of proteins between samples can be determined using an analytical software package.

Now that we have identified the gene product of *Ocd*, the effect of the mutations in it on the proteome can be examined. This approach enables the identification of putative suppressors. There may be some pathways or gene families that become up- or down-

regulated in response to the cold-sensitive channel malfunction as part of a 'coping' mechanism. In each of the *Ocd* lines, males are semi-lethal so it follows that those males that do survive to eclosion may do so through the alteration of cellular conditions to counteract problems caused by ion transport imbalance. Additionally, where *Ocd* lines with the same mutation(s) have been kept as isolated stocks, they display striking differences in the severity of their phenotypes, particularly with respect to male viability, suggesting that modifier genes must be acting. However, unless such modifier genes are X-linked to *Ocd*, they would not be identified in this proteomics study. This is because lines used were isogenised prior to analysis, to tightly control for genetic background differences between stocks.

A comparative proteomics study was undertaken in collaboration with Kathryn Lilley at the BBSRC-sponsored Cambridge Centre for Proteomics (Lilley and Griffiths, 2003). 2D DIGE was used to compare the proteomes of wild-type and mutant (*Ocd^{7-G}*) male flies. The *Ocd^{7-G}* mutation (equivalent to *Ocd^{2-S}* and shown to be T1551I) was chosen for analysis as this line yields the most males, and also because these male flies display mutant phenotypes even at the permissive temperature of 25°C. These flies are uncoordinated, hold their wings in a downturned position, are unable to fly and have a decreased lifespan. Because this phenotype is observed even at 25°C, it is highly likely that there are detectable differences between wild-type and mutant proteomes even at the permissive temperature.

So as not to restrict the analysis, protein analysis was performed on whole adult flies and not a mitochondrial preparation, as was used previously (Søndergaard, 1986). Depending on the outcome of the preliminary experiment, samples could subsequently be subfractionated. Indeed, in order to visualize protein species with low copy numbers, subfractionation would be required. Additionally, very small (<10kDa) or very large (>150kDa) proteins (including Para), insoluble membrane proteins and highly basic proteins tend not to be represented on a gel (Nilsson and Davidsson, 2000). The isoelectric point is the pH at which proteins no longer migrate in an electric field due to an equal number of positive and negative ions. Ribosomal proteins, which generally have an isoelectric point greater than 11, tend to run too far on a gel during isoelectric focussing. One way to allow identification of less abundant and highly basic or acidic proteins that are generally underrepresented would be to prefractionate samples prior to electrophoresis according to their charge (Gorg *et al.*, 2002).

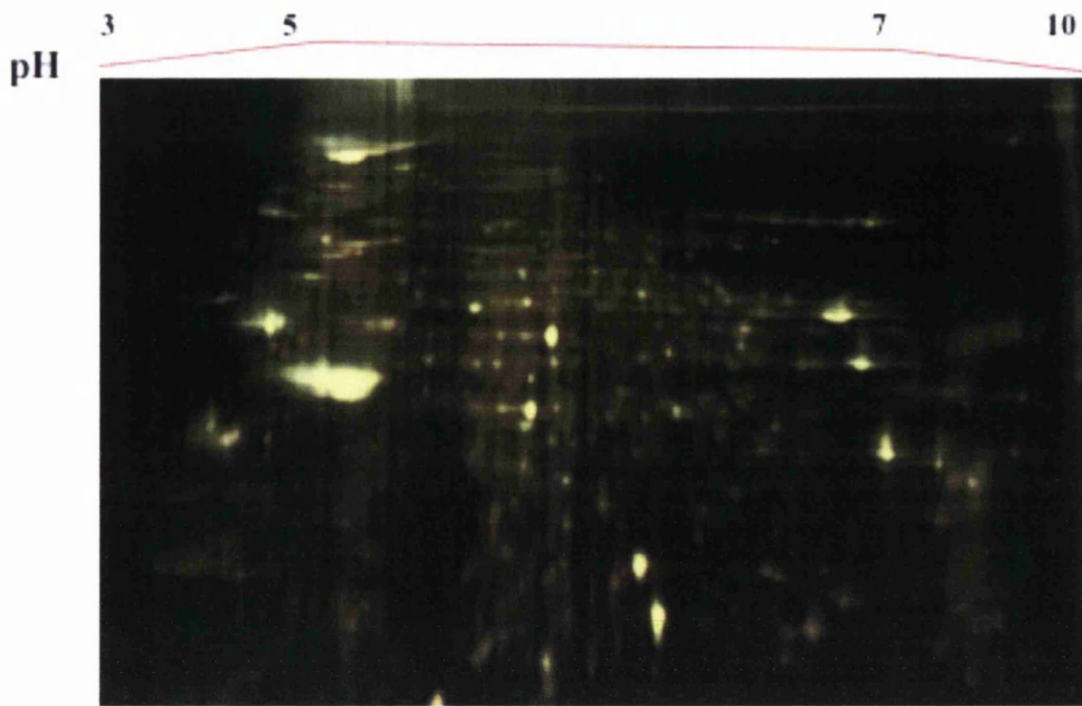


Figure 5.1 Representative example of an overlaid fluorescent cyanine dye image of wild-type and *Ocd* proteomes (2D DIGE)

The wild-type protein sample was labelled with Cy3 (green) and *Ocd* protein with Cy5 (red). Proteins were separated on the basis of molecular weight and charge. Isoelectric points are indicated on the horizontal. Most of the protein spots appear to be yellow, indicating co-localisation of the wild-type and mutant proteins, and therefore very few changes between the proteomes. In this study each biological replicate was run three times on different gels, to compare it to each biological replicate of the opposite sample. This included dye reversal to control for differences in reactivity between the CyDyes. Gels were analysed using DeCyder software and spots recognised as differing significantly between wild-type and *Ocd* were identified using mass spectrometry. CyDye and DeCyder are trademarks of Amersham Biosciences Limited.

Consideration of genetic background is of paramount importance in any *Drosophila* experiment. Subtle changes in genes leading to alterations in genetic pathways and networks have been shown to have a substantial effect on behaviour (Sokolowski, 2001, O'Dell, 2003). If genetic background is not taken into account, misinterpretation of results in a proteomics or transcriptomics experiment may occur, as any changes attributed to a particular mutation may in fact have arisen in the genetic background of two inbred laboratory strains. To address potential problems of genetic background, the *Ocd* flies were crossed into a Canton S (wild-type) background. The *Ocd* flies to be analysed were males selected from progeny of *Ocd*^{7-G}/FM7 females in a Canton-S background crossed with Oregon-R (wild-type) males, i.e. *Ocd*^{7-G} males in a completely mixed Canton-S/Oregon-R background. To control for genetic uniformity, the wild-type control flies were male progeny of Canton-S females crossed with Oregon-R males, so they also had a completely

mixed Canton-S/Oregon-R genetic background. Generating stocks in this way controls for both genetic background and inbreeding. The *Ocd*^{7-G} and wild-type flies were also controlled for all aspects of environment. All flies were grown up at 25°C and protein was extracted in three biological replicates per line (i.e. six in total) from whole adult males aged between one and two days. An example of one of the gels run is shown in Figure 5.1.

Experimental design and method of analysis is critical in proteomics studies. Robust statistical analysis is necessary to verify any possible expression differences. In this study, DeCyder Biological Variance Analysis (BVA) was used (Figure 5.2), which involves using an internal standard, labelled with Cy2, on each gel, again to reduce inter-gel variability and to normalise protein abundance measurements across multiple gels (Alban *et al.*, 2003).

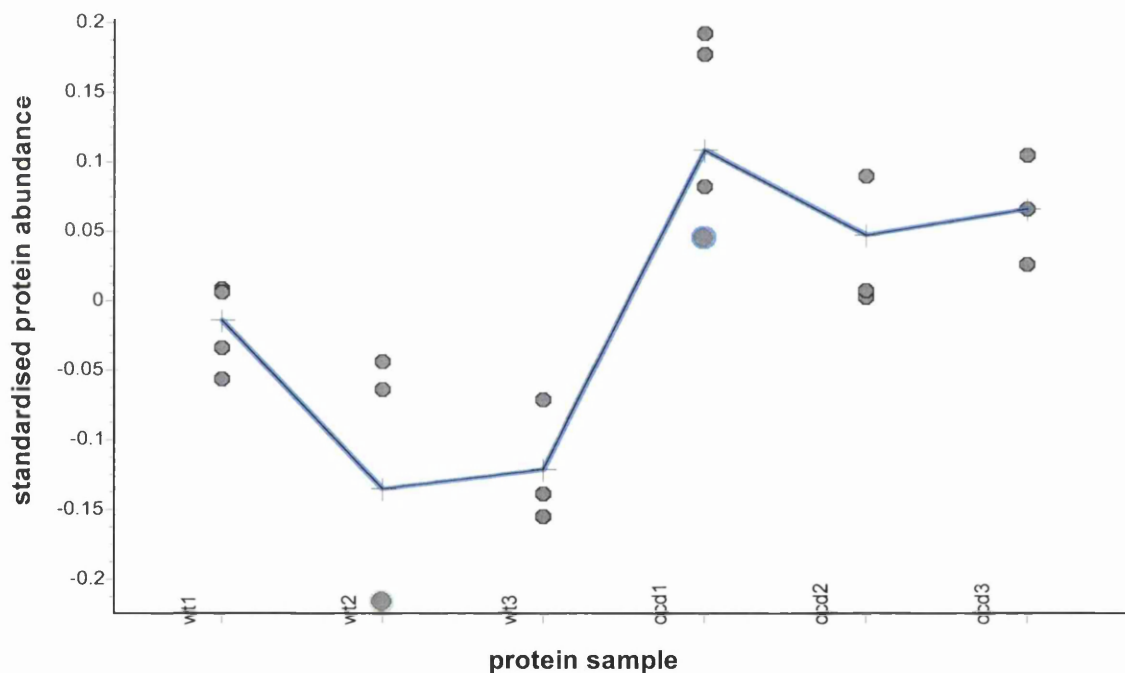


Figure 5.2 Example of a standardised abundance graph generated by DeCyder Biological Variance Analysis (BVA) analysis

Sample descriptions are displayed on the x axis, and standardised protein abundance on the y axis. Each dot plotted on the graph corresponds to the same spot but from a different gel (technical replicates). An internal standard was used to normalise protein abundance measurements across multiple gels. Nested ANOVA using the standardised abundances was then used to determine whether or not a change is significant ($p < 0.05$), and an average ratio change was generated. This graph shows BVA of a protein spot (in three wild-type (wt1-3), and three *Ocd* (ocd1-3) samples) subsequently identified as CG3861, a citrate synthase, which has a ratio change of 1.40 in *Ocd*^{7-G} flies compared to wild-type. The change is statistically significant ($p = 0.0266$).

In a 2D DIGE experiment there are two types of replicates: technical replicates, which refers to running gels using the same samples, and biological replicates, which in this study refers to different samples taken from a single population of flies (wild-type or mutant). To test for significance, a statistical model incorporating a nested analysis of variance (ANOVA) was chosen to allow separation of biological variation between samples and technical variation between experiments (Figure 5.3). This increases the confidence that any spots found to differ between samples are real *in vivo* differences, beyond the biological and technical variation (Karp *et al.*, 2005). This is because commonly used univariate statistic tests, for example the student's t-test, which is equivalent to a one-way ANOVA, make the assumption that all replicates are independent of each other. However, technical replicates from one biological replicate are not independent and will yield similar results so this method of analysis usually results in an excessively high false positive rate.

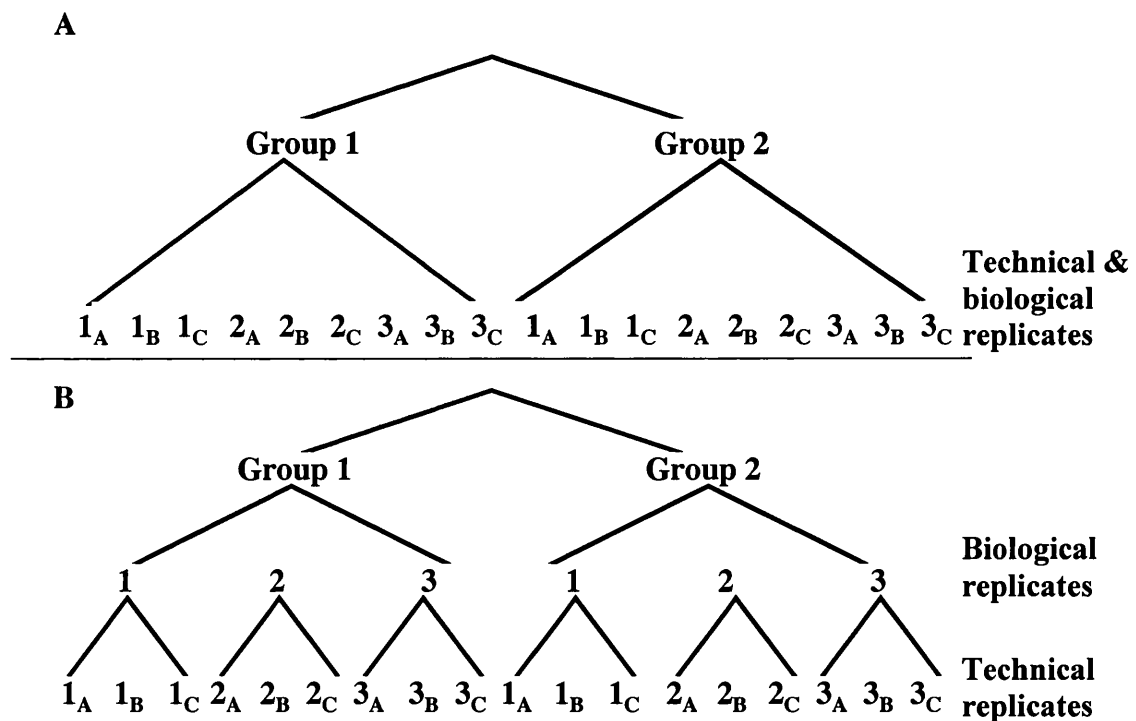


Figure 5.3 Comparison of one-way and nested ANOVA

A: In one-way ANOVA, each replicate is treated as equivalent. B: In a nested ANOVA, technical replicates are nested below their biological replicate. Biological replicates are labelled with numbers (1,2,3) and technical replicates of each biological replicate with a subscript letter (A,B,C). Analysing 2D DIGE data with nested ANOVA has been demonstrated to result in far less false positives compared to analysis with one-way ANOVA (modified from Karp *et al.*, 2005).

Following gel electrophoresis and image analysis using DeCyder software, proteins spots showing changes in abundance between wild-type and *Ocd* were excised from the gel and identified using mass spectrometry. In total, more than 40 protein differences were identified. Of these only 22 were successfully identified by using mass spectrometry data

to search the NCBI database for *Drosophila* matches. Some of the spots corresponded to keratin, which is likely to be due to contamination with human particulates such as skin or hair, and trypsin, which is used for proteolytic cleavage required prior to mass spectrometry. Trypsin also self-digests so trypsin peptide fragments are generated which may be identified in mass spectrometry. Where spots were picked and found to contain a mixture of two or more different proteins, identification was not possible. The 22 spots successfully identified are shown in Tables 5.1 and 5.2 separated according to their cellular localisation.

MW (kDa)	pI (pH)	Corresponding polypeptide(s)	Function	p score from nested ANOVA	Ratio change
58.0	9.1	CG3861-PB	Citrate synthase	0.0026	+1.57
58.3	9.1	CG3861-PA		0.0266	+1.40
		CG3861-PB			
59.0	9.1	CG3612-PA	ATP synthase alpha subunit (Bellwether)	0.00426	+1.39
59.6	9.1	CG3612-PA		0.0147	+1.53
59.6	9.1	CG3612-PA		0.0204	+1.25
59.6	9.1	CG3612-PA		0.0241	+1.45
59.6	9.1	CG3612-PA		0.04951	-1.23
59.6	9.1	CG3612-PA		0.1297	-1.42
86.2	8.5	CG9244-PB	Aconitase	0.01539	+1.40
54.0	8.6	CG4094-PA	Fumarate hydratase	0.0171	+1.28
		CG4094-PB			
41.0	8.8	CG6439-PA	Isocitrate dehydrogenase beta subunit	0.0381	+1.26
53.4	5.2	CG11154	ATP synthase beta subunit	0.0516	-1.74
53.0	7.2	CG7176-PA	Isocitrate dehydrogenase	0.0653	+1.15
		CG7176-PB			
		CG7176-PC			
		CG7176-PD			
38.9	7.0	CG12233-PA	Isocitrate dehydrogenase alpha subunit	0.141	+1.29
		CG12233-PB			

Table 5.1 Mitochondrial proteins differentially expressed in wild-type and *Ocd* flies

Proteins are listed in order of decreasing significance according to ANOVA p scores. Molecular weights (MW) and isoelectric points (pI) are shown. Each entry in the MW column indicates a different spot. Polypeptides are labelled according to Flybase nomenclature. In several cases different spots correspond to the same polypeptide which has migrated to a different position on the gel, due to post-translational modification. Proteins were identified by searching the NCBI database using mass spectrometry data. The corresponding polypeptides and encoding genes are listed. The last two columns list the nested ANOVA p values (those greater than 0.05 are highlighted in red), and the ratio change. Positive values indicate proteins more abundant in *Ocd* flies, negative values indicate those more abundant in wild-type.

MW (kDa)	pI (pH)	Corresponding polypeptide(s)	Function	p score from nested ANOVA	Ratio change
44.6	5.9	enolase	Enolase (<i>Drosophila pseudobscura</i>)	0.0077	-1.20
41.0	6.3	CG6663-PA	Peptidase inhibitor homologue	0.0104	+1.65
74.3	9.2	CG5939-PC	Paramyosin	0.0241	+1.45
61.7	6.1	CG6148-PA CG6148-PB	Putative achaete scute target 1	0.0270	+1.30
39.9	7.6	CG6058	Fructose 1,6-biphosphate aldolase	0.0675	+1.55
51.0	8.0	CG5210-PA	47K glycoprotein Chinitase-like	0.0796	+1.31
31.2	6.6	CG5177-PA	Trehalose phosphatase	0.274	+1.17
97.3	6.1	CG7254-PA	Glycogen phosphorylase	0.3681	-1.25

Table 5.2 Non-mitochondrial proteins differentially expressed in wild-type and *Ocd* flies

Proteins are listed in order of decreasing significance according to ANOVA p scores. Molecular weights (MW) and isoelectric points (pI) are shown. Each entry in the MW column indicates a different spot. Polypeptides are labelled according to Flybase nomenclature. Proteins were identified by searching the NCBI database using mass spectrometry data. The corresponding polypeptides and encoding genes are listed. The last two columns list the nested ANOVA p values (those greater than 0.05 are highlighted in red), and the ratio change. Positive values indicate proteins more abundant in *Ocd* flies, negative values indicate those more abundant in wild-type.

None of the proteins identified are encoded by genes in the *Ocd* critical region, so the protein changes must occur only as a response to the *Ocd* mutation. Although initially performed to help identify the *Ocd* gene product, Para is not represented, and this is likely to be due to its large molecular weight. Also, it is not yet clear whether levels of Para protein are altered in *Ocd* mutants.

In several cases, there is more than one spot corresponding to a particular polypeptide. For example, Bellwether (CG3612-PA) appears several times. Each spot migrates to a slightly different position on the gel, due to post-translational modifications such as phosphorylation or glycosylation. Because these spots differ between wild-type and *Ocd* flies, it would appear that Bellwether is modified in mutant flies in a manner distinct from that of the wild-type animals.

14 of the 22 protein isoforms are mitochondrially localised. Localisation was assessed according to function and also by inclusion in Mitodrome, a database of *Drosophila melanogaster* nuclear genes encoding proteins targeted to the mitochondrion (Sardiello *et al.*, 2003). There is no obvious reason why mitochondrial proteins should be preferentially identified over cytosolic proteins in a comparative proteomics study. 2D DIGE uses CyDyes, which minimally label the lysine residues of a protein. Therefore, proteins with more lysine residues are more heavily labelled. One possibility might be that mitochondrial proteins tend to have more lysine residues, but this does not appear to be the case. At least in echinoderms and hemichordates, proteins encoded by the mitochondrial genome have actually been shown to have a relatively reduced number of lysine residues due to codon reassignment (Castresana *et al.*, 1998), but no comparative study of nuclear encoded mitochondrial proteins has been undertaken.

To date, few *Drosophila* 2D DIGE studies have been published, however one separate study into proteome differences between dichlorodiphenyltrichloroethane (DDT) susceptible and resistant strains identified 21 differentially translated proteins, many of which play a role in glycolysis and the Krebs' cycle (Pedra *et al.*, 2005). These included glycogen phosphorylase and the alpha and beta subunits of ATP synthase, all of which were identified in the *Ocd* proteomics study. This suggests that these proteins in particular may have properties which makes them more susceptible to identification in a 2D gel study. Interestingly however, there is a biological link between *Ocd* and DDT resistant lines so the same proteins might be expected to be identified. This will be discussed in greater detail later in this chapter.

Four of the proteins identified are key enzymes of the tricarboxylic (Krebs') cycle. These are fumarate hydratase, citrate synthase, aconitase, and isocitrate dehydrogenase, which are all up-regulated in the *Ocd* flies (Figure 5.4). This may indicate an increase in ATP synthesis. The remaining two mitochondrial proteins are the core subunits of ATP synthase. Bellwether (Blw), the ATP synthase α subunit, appears to be both up- and down-regulated, depending on the modification state of the protein. The ATP β subunit is down-regulated in mutant flies. Alterations in specific isoforms present in the ATP synthase complex may also be in indication of an increase in ATP synthesis.

Oxidative stress and mitochondrial dysfunction can be a consequence of epileptic seizures in humans (reviewed by Patel *et al.*, 2004). In addition to initiating apoptosis (Henshall *et*

al., 2002), seizure activity is known to have an inactivating effect in susceptible iron-sulphur mitochondrial enzymes such as aconitase, due to the seizure-induced production of oxygen free radicals (Flint *et al.*, 1993). It follows that in *Drosophila*, seizure-like episodes may induce a mitochondrial effect. This may explain why, in *Ocd*^{7-G} mutants, aconitase is up-regulated. Decreased activity or inactivation of aconitase may also disrupt other Krebs' cycle functions, and again, this might explain other Krebs' enzymes up-regulation in *Ocd*^{7-G} as part of a compensatory mechanism.

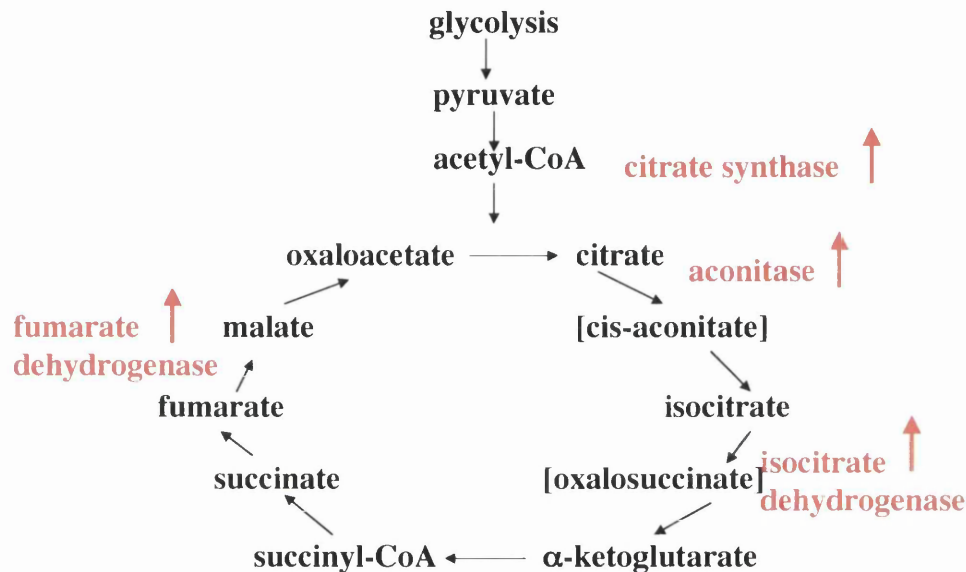


Figure 5.4 Simplified diagram of the TCA (Krebs' cycle)

The reactions in the Krebs' cycle completely oxidise fuel molecules. Fuel is mostly in the form of acetyl-CoA, which is produced from the oxidative decarboxylation of pyruvate following glycolysis. During the cycle, energy is produced which is then carried to the respiratory chain system, where ATP is produced. Stages in the cycle where enzymes are up-regulated in *Ocd* flies are indicated in red. The TCA cycle completely oxidises fuel molecules in ten steps of reactions yielding energy and carbon dioxide.

The observation that approximately two thirds of the polypeptides identified (and half of the corresponding genes) are mitochondrial is especially interesting considering Søndergaard's original finding of an unidentified aberrant protein present in an *Ocd* mitochondrial sample (Søndergaard, 1986). Also, abnormalities in the reaction kinetics of the mitochondrial respiratory chain enzyme complex succinate cytochrome c reductase have been reported in *Ocd* mutants (Søndergaard, 1976, Søndergaard, 1979b). Interestingly, changes in the activation energy of mitochondrial enzymes in *para* mutants have also previously been observed (Søndergaard, 1976). The fact that such a large proportion of the proteins identified in the 2D DIGE study are localised to the mitochondrion is consistent with the original proposal that *Ocd* may play a mitochondrial

role. Alternatively, and in light of the fact that it is known *Ocd* encodes a voltage-gated sodium channel, it may be that mitochondria provide a route by which symptoms induced by the mutation may be alleviated.

Because the *Ocd*^{7-G} males used in the experiment were fairly weak, uncoordinated, and generally unfit even at 25°C, the observed apparent mitochondrial effect may arise as a result of management of the *Ocd* mutation and may not be a direct effect. Because we have now shown that the *Ocd* mutations are alleles of the voltage-gated sodium channel gene *paralytic*, it is possible to draw inferences about why these mutations may have such an impact on the mitochondrion, in addition to the aforementioned seizure-induced oxidative stress mechanism. For example, if the primary effect of the mutations on sodium channel function is to impair fast inactivation, then it might be expected that there will be an increased influx of sodium ions into the cell. The mitochondria may respond to increased sodium ion concentrations by increasing ATP synthesis, specifically by increasing levels of Krebs' cycle enzymes and the ATP synthase complex. This would enable the cell to actively transport sodium ions out of the cell and restore ionic equilibrium. It would be interesting to investigate this further, by examining in detail biochemical aspects of mitochondrial function, specifically the activities of the Krebs' cycle enzymes, the oxidative phosphorylation (OXPHOS) enzymes of the respiratory chain complex, and mitochondrial ATP synthesis. Another worthwhile study would be to investigate proteome changes in response to cold. This would help elucidate whether the mitochondrial protein changes are related to the cold-specific effects of the *Ocd*^{7-G} mutation.

Alternatively, it is possible that any mitochondrial abnormalities observed are not linked to the *Ocd* mutations and have in fact arisen by chance in the genetic background of the *Ocd*^{7-G} line. However, as mentioned previously, this would not be an issue unless such a mutation was tightly linked to *Ocd*. In any case, it would be possible to investigate this by repeating a comparative proteomics study on the other *Ocd* lines, as well as in flies carrying *Ocd*-like transgenes.

Eight spots corresponding to non-mitochondrial proteins were also successfully identified. Those that showed a significant change ($p < 0.05$) were an enolase, a peptidase inhibitor homologue, Paramyosin, and Putative Achaete Scute Target 1. The enolase identified by searching the NCBI database is from a different fly species, *Drosophila pseudoobscura*. The enolases from the two species are more than 90% similar, so it is possible that a few

errors in mass spectrometry identification could lead to identification of the same enzyme from *D. pseudoobscura*. Enolase and fructose 1,6-biphosphate aldolase, two energy metabolism enzymes involved in glycolysis, were identified as being differentially regulated in *Ocd* flies. This might be a further indication of the need for the mutants to alter aspects of ATP production. Interestingly, a *Drosophila* mutation in phosphoglycerate kinase, which results in altered ATP generation, has been shown to lead to temperature-sensitive paralysis (Wang *et al.*, 2004). The fact that Paramyosin, a structural component of muscle, is up-regulated may be a reflection of the observed muscle weakness in some *Ocd^{7-G}* - they are unable to hold their wings up properly, even at room temperature.

The discussion of the relevance of putatively differentially regulated proteins is speculative, and further experiments are required to firstly confirm these initial observations, and secondly to elucidate why these proteins in particular are altered in *Ocd* flies. If the theories of aconitase inactivation or increased ATP synthesis are correct, it is not clear why more or all of the Krebs' cycle or glycolysis enzymes would not be differentially regulated. However this may be due to the rate limiting step in the Krebs' cycle, which is the conversion of isocitrate to α -ketoglutarate, catalysed by isocitrate dehydrogenase (Figure 5.4). This reaction is allosterically inhibited by ATP.

Further evidence of up- or down-regulation could be obtained by running separate 2D gels of wild-type and mutant proteins. The levels of proteins of interest could then be detected with the appropriate antibodies. This could be applied both to already identified proteins and to proteins predicted to display an altered expression pattern. This would require comparing two different gels, however, in contrast to 2D DIGE, and thus the technique has some pitfalls. As mentioned previously, analysis of the Krebs' cycle and OXPHOS enzymes biochemically together with physiological examination of the mitochondria themselves (for example, mtDNA copy numbers) might provide a more fruitful route to understanding exactly what is happening at the mitochondrial level.

5.3 Electrophysiology

To understand how *Ocd* mutations in *para* lead to cold-sensitive changes in channel activity, it is important to first describe the electrophysiology of the mutant channels. Previous analyses of human *SCN4A* derived from myotonic patients indicate that the

inclusion of single amino acid substitutions change the activation threshold and/or rate of fast inactivation (Cannon, 2002). This may also be the case in *Ocd* mutants.

Changes in neuronal excitability often reflect changes in conductance caused by the opening and closing of a variety of ion channels, which can be best measured via voltage clamp (Hodgkin *et al.*, 1952). This technique involves 'clamping' a cell at a set voltage. In order to maintain this voltage, current equal but opposite to current generated by the cell must be injected. Traditionally voltage clamp requires two electrodes to penetrate the cell membrane; one to record voltage and one to pass current. In small neurons, voltage clamping is achieved using a single patch electrode, which simultaneously records voltage and passes current. Whole cell patch clamp involves first isolating a small section of the membrane by withdrawing it into a fire-polished pipette filled with ionically balanced saline (Sakmann and Neher, 1984). In a whole cell recording, applying further suction and a current pulse results in rupture of the isolated membrane and access to the cell cytosol. The saline used to record sodium channel activity contains specific blockers of potassium and calcium channels such that only current generated by the flow of sodium ions is measured. After a reading is taken, it can be verified as being a sodium current by subsequently blocking sodium channels with tetrodotoxin which should eliminate the current.

The major functional sodium channel in *Drosophila* is encoded by *paralytic* (Loughney *et al.*, 1989). Although both *para* and *DSC1*, a putative voltage-gated sodium channel gene, are widely expressed in the CNS and PNS (Hong and Ganetzky, 1994), mutations in *para* are sufficient to block nerve action potentials. For example, the lethal *para* deficiency *Df(1)D34* abolishes sodium current (Baines and Bate, 1998). In *Drosophila para* null embryos, no sodium current can be detected, suggesting that Para is the only functional sodium channel, at least at this stage in development. Therefore, any changes observed in the sodium current can be attributed to the *Ocd* mutations in *para*. Because Para and DSC1 channels coexist in adult neural tissue, it has been proposed that the two channels perform distinct functions (Castella *et al.*, 2001).

A voltage clamp study was undertaken to study the electrophysiological phenotype of *Ocd* mutant larvae. Homozygous *Ocd* flies were used to eliminate problems of sexing larvae. The only homozygous *Ocd* flies available were the original double mutants *Ocd^{5-S}* and *Ocd^{7-S}*, which both harbour the I1545M and G1571R mutations, created in Leif

Søndergaard's laboratory in the 1970s. As these have been kept as a stock ever since, modifiers must be acting to make these flies homozygous viable, though still cold-sensitive. As a control, the wild-type strain Canton-S was used.

Whole cell recordings were taken from wild-type and homozygous mutant first instar larvae at three temperatures: 16°C, 22°C and 28°C, to assess any temperature-sensitivity. Recordings were taken from aCC or RP2 motoneurons, which do not differ in sodium conductance (Baines *et al.*, 2001). These neurons lie close to the midline in abdominal segments A1-A4 (Baines and Bate, 1998). Peak transient sodium current was recorded at a range of voltages from -60 to 45mV in wild-type and *Ocd* larvae. Figure 5.5 shows normal Na⁺ current readings in these neurons, made up of two separate components; transient and persistent current.

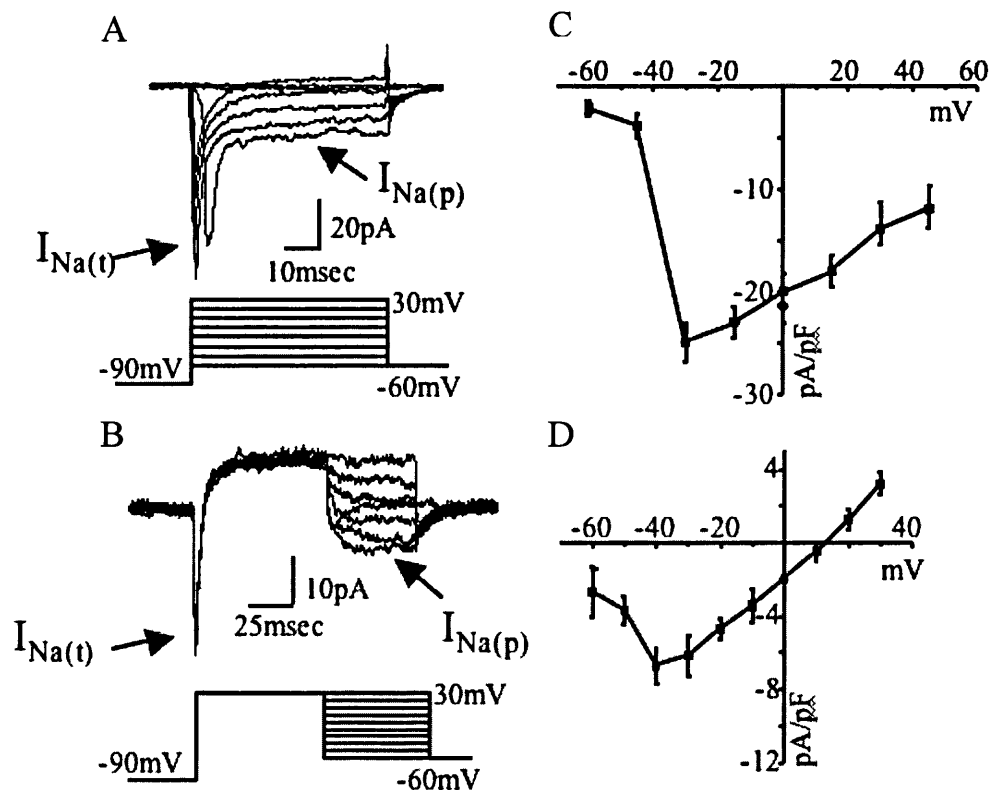


Figure 5.5 Voltage-gated sodium current in wild-type aCC/RP2 motoneurons
 These recordings were taken from wild-type Canton-S larvae at room temperature (22°C-24°C). Voltage-gated Na⁺ current is made up of two major components: A. rapidly inactivating transient Na⁺ current ($I_{Na(t)}$), and B. slow inactivating persistent current ($I_{Na(p)}$). Traces recorded at the voltages indicated are overlaid in each case. C. Transient current is plotted against voltage. D. Persistent current is plotted against voltage. Taken from Mee *et al.*, 2004.

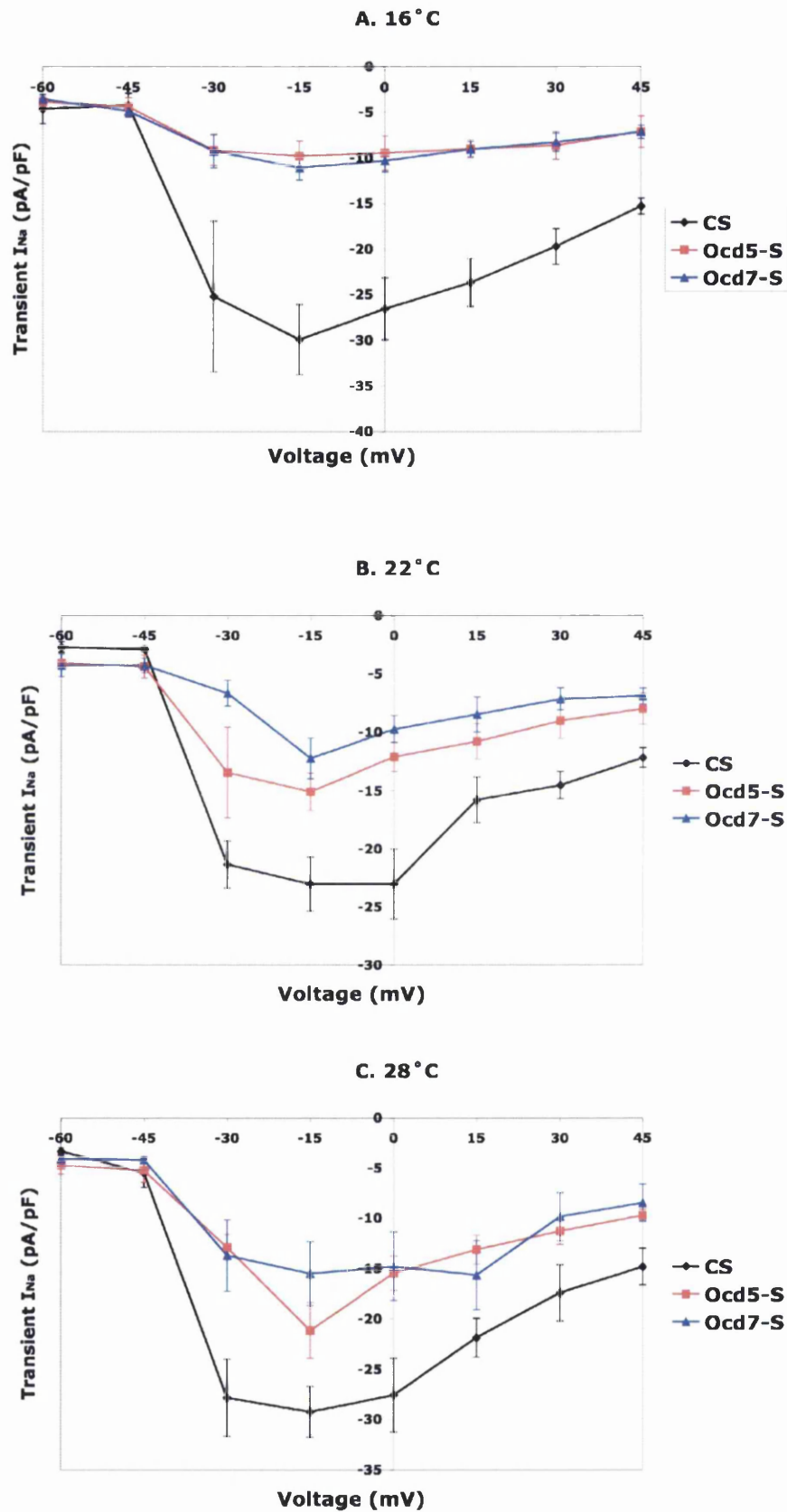


Figure 5.6 Transient current-voltage relationships in Canton-S, *Ocd^{5-S}* and *Ocd^{7-S}*
 Voltage-clamp experiments were conducted at temperatures of 16°C, 22°C and 28°C, shown in separate graphs. The lines tested were Canton-S (wild-type), *Ocd^{5-S}* and *Ocd^{7-S}* (both I1545M+G1571R). Mean transient sodium current was calculated, and standard error of the mean is shown. For each data point, n=4-8.

Figure 5.6 shows the sodium current-voltage relationships for the transient Na⁺ conductance in each fly line tested. At each temperature, transient currents were significantly reduced in *Ocd* flies at voltages greater than -45mV (activation voltage). This reduction is greater at 16°C than at the higher two temperatures, in keeping with the cold-sensitivity of the mutants.

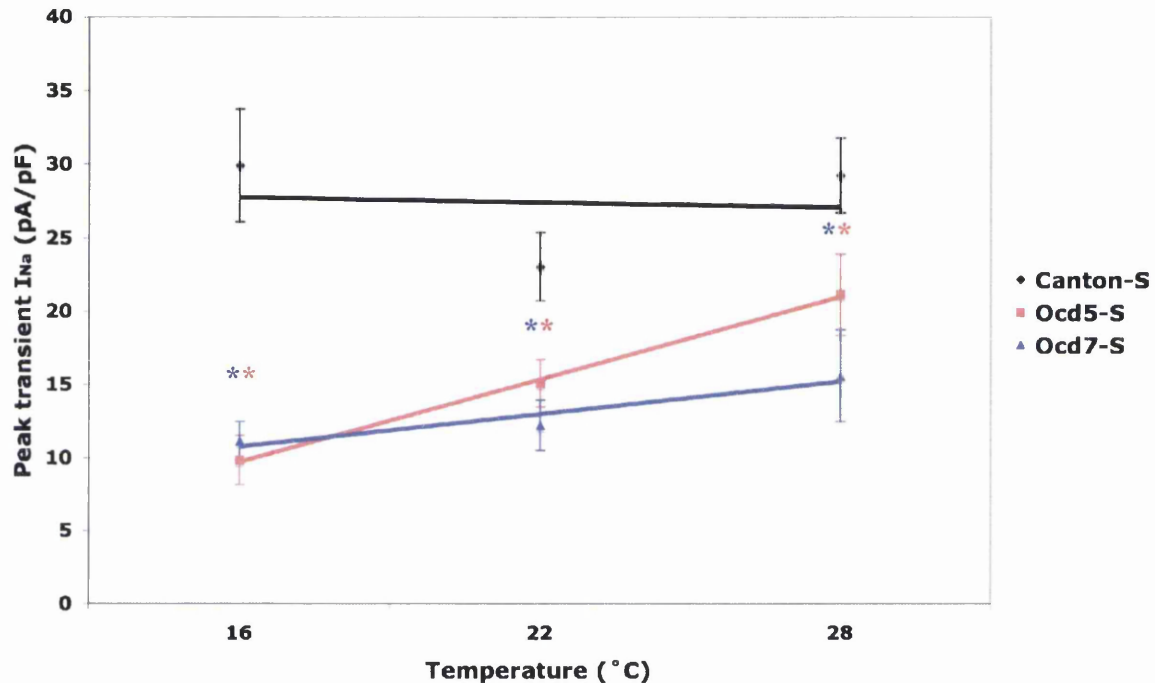


Figure 5.7 Mean peak transient sodium currents (I_{Na}) at -15mV in wild-type and *Ocd* flies

Wild-type (Canton-S) and *Ocd*^{5-S} and *Ocd*^{7-S} (both I1545M + G1571R) larval sodium channels were analysed via whole cell recordings of aCC and RP2 motorneurons. Recordings were taken at three temperatures: 16°C, 22°C and 28°C. Measurements are normalized to cell capacitance, and expressed as current density (pA/pF). Trendlines and standard error of the mean is displayed. The asterisks indicate a significant ($p < 0.05$) reduction in current compared to wild-type, as deduced from student's t-tests.

Peak transient currents of wild-type and *Ocd*^{5-S} and *Ocd*^{7-S} first instar larval sodium channels (measured at -15mV) at all three temperatures are displayed in Figure 5.7. It should be noted that comparison of persistent current between wild-type and mutant channels failed to reveal any clear pattern. Few changes were observed between the two channel types and the *Ocd* persistent current did not appear to display any cold-sensitivity (data not shown).

To analyse the peak transient current, the normality of the data was assessed using Ryan-Joiner tests. The appropriate transformation (log) was then chosen using the Box-Cox plot.

General Linear Model ANOVA was then performed on the normalised data using Minitab software (Figure 5.8). Genotype and temperature account for 44.7% ($p=0.00$) and 11.8% ($p=0.01$) of the variance, respectively, although no interaction was found between fly genotype and temperature ($p=0.12$). The total variance in peak transient current due to both genotype and temperature is therefore 56.5%. This means that the currents in each fly line are significantly different, as are the currents obtained at each temperature.

Source	DF	Seq SS	Adj SS	Adj MS	F	P
Strain	2	0.86216	0.83094	0.41547	23.38	0.000
Temperature	2	0.21082	0.19839	0.09920	5.58	0.008
Interaction between strain and temperature	4	0.14732	0.14732	0.03683	2.07	0.108
Error	32	0.56864	0.56864	0.1777		
Total	40	1.78895				

Figure 5.8 General Linear Model ANOVA for peak transient current data
ANOVA was performed on log transformed values for the peak transient sodium current at all three temperatures (16°C, 22°C and 28°C) in the three strains - Canton-S (CS), *Ocd^{S-S}* and *Ocd^{7-S}*. DF= degrees of freedom. Seq SS= sequential sum of squares. Adj SS= adjusted sum of squares. Adj MS= adjusted mean square.

Student's t-tests were also performed between each mean value, firstly to test for cold-sensitivity. Mean values at 16°C and 28°C in each fly line were compared. Canton-S was found not to be cold-sensitive ($p=0.95$), as would be expected. *Ocd^{S-S}* flies were found to be cold-sensitive ($p=0.01$), in contrast to *Ocd^{7-S}* flies ($p=0.21$). This is interesting given that the two *Ocd* lines harbour the same mutations, and both display a cold-sensitive phenotype. This may be a modifier effect, but further examination of the electrophysiological phenotype would be advantageous, particularly as the sample sizes are relatively small ($n=4-6$).

Student's t-tests between Canton-S and each *Ocd* line at each temperature showed that mutant differed significantly from wild-type at all three temperatures ($p<0.05$). This is also shown in Figure 5.7. The peak transient current (at -15mV) is reduced significantly in *Ocd* mutants at all three temperatures. This is the case in both lines, which contain the same double mutation, but have been kept as isolated stocks for almost 30 years. This data suggests that the mutant channels are compromised in their ability to transport sodium ions. This might be due to a partial blockage of the channel, and is not likely to be due to the initially proposed defect in inactivation where too many sodium ions would be allowed to flow into the cell. This is inconsistent with widely held theories for the basis of human

sodium channelopathies, believed to be caused by impairment in fast inactivation (Caldwell and Schaller, 1992, Cannon, 2002). Alternatively, it might be that the cytoplasmic III-IV linker is permanently held in a half closed position. The G1571 residue is one of two adjacent glycines that may confer flexibility to the linker. Substitution of one glycine for the bulkier arginine could conceivably result in loss of the linker's flexibility.

While temperature does not appear to have a great effect on wild-type currents, as would be expected, *Ocd*⁵⁻⁵ larvae display striking cold-sensitivity, in keeping with the behavioural phenotype. At 16°C, the mean peak transient current in *Ocd*⁵⁻⁵ is only 9.83pA/pF, whereas at 28°C, the value is 21.13pA/pF. This is in contrast to Canton-S, where the values at 16°C and 28°C are 29.92 and 29.24, respectively. *Ocd*⁷⁻⁵ shows an intermediate phenotype, and does not display significant cold-sensitivity, although the peak sodium current is compromised at each temperature. This is intriguing in light of the fact that the two lines harbour identical mutations. In both lines, some sodium current is still present at 16°C. At 16°C both sets of mutants fall to the bottom of vials within a few minutes but some movement remains, including leg stretching. This implies that action potential firing is still occurring at 16°C, but it may be slowed or uncoordinated.

These experiments were only carried out using the *Ocd* double mutants, as homozygous flies were viable. Alternatively, *Ocd* flies could be generated carrying a green fluorescent protein (GFP) balancer chromosome, so that male *Ocd* larvae could be easily distinguished from wild-type. This study should be extended to the single T1551I mutation and also to *Ocd*⁴ flies, where the underlying mutation is unknown. Although *Ocd* I1545M+G1571R mutants display a clear electrophysiological phenotype, further experiments are required to elucidate exactly what is going on at the channel level. It would be interesting to repeat this study at higher temperatures to see if there is a critical temperature where the wild-type and *Ocd* values meet, and where *Ocd* channels might function as normal.

Heterologous expression of *para* using the spherical *Xenopus* oocyte may prove insightful and give a more accurate electrophysiological recording. Using this method, it would be possible to measure activation threshold, inactivation rate and ratio of transient to persistent current. Another useful strategy might be to current clamp motoneurons to study the action potential itself, and to use the cell-attached patch mode to analyse unitary sodium currents. This would allow any inactivation defect(s) to be analysed in detail, and might ascertain if there is any prolonged opening of the channel.

Despite the need for further investigation into the *Ocd* mutants at the electrophysiological level, this work has produced further convincing evidence that the *Ocd* flies are mutant in the voltage-gated sodium channel gene *para*.

5.4 Auditory behavioural assay

Preliminary studies have revealed that *Ocd*^{*5-G*} appear to have some sort of hearing impairment (Figure 5.9). The *Drosophila* behavioural assay to test for deafness is based on the finding that wild-type males will court each other when a recording of the species-specific courtship song is played to them (Eberl *et al.*, 1997). Thus, we can establish if flies are deaf by playing this song to males and measuring any difference in inter-male courtship rates. That is, there should be an increase in courtship if the flies have normal hearing, and no change in courtship rate if the flies are deaf. The deafness test was performed as part of a study into deafness in a range of *Drosophila* mitochondrial mutants. Deafness is a common symptom of human mitochondrial disease, and this phenotype is also recapitulated in the *Drosophila* mitochondrial ribosomal mutant *technical knockout* (Toivonen *et al.*, 2001).

Figure 5.9 clearly shows that the *Ocd*^{*5-G*} flies tested showed a significant decrease in courtship behaviour. If the flies were deaf, no increase or decrease in courtship would be expected. This might indicate that, contrary to being hearing impaired, the mutant flies actually might become paralysed upon exposure to the song, which was played at very high levels. Indeed, the apparent decrease in courtship was stronger when song was played at 100dB. This is particularly interesting as it seems plausible that the *Ocd* flies might undergo sound-induced as well as cold-induced paralysis. However this observation needs to be investigated further, using males from the other *Ocd* lines where possible. The data is interesting in light of the fact that *Ocd*^{*5-G*} flies harbour mutations in a voltage-gated sodium channel. These mutations may cause defects leading to repetitive firing in neurons, and eventually paralysis, not only in response to cold, but to loud noise as well. It could be that the *Ocd* flies are just generally unfit, and are affected adversely by a number of environmental stimuli, including noise and temperature. However, it should be noted that *Ocd* flies are not heat-sensitive, only cold-sensitive (Søndergaard, 1975).

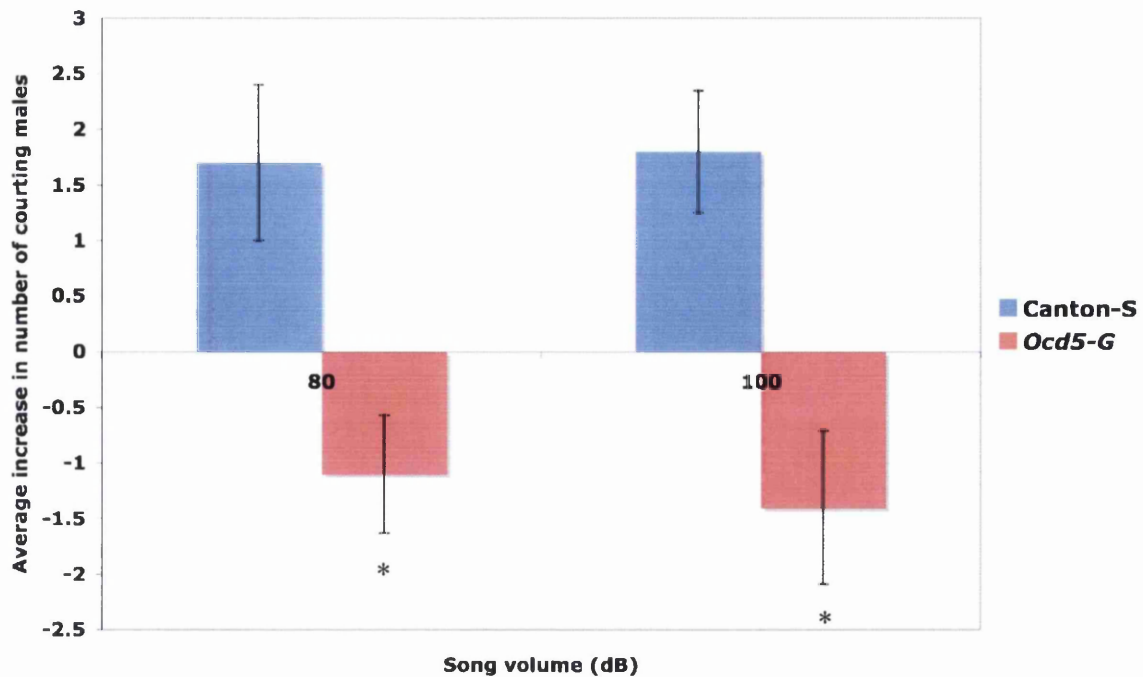


Figure 5.9 Male-male courtship test for deafness in *Ocd^{5-G}* and wild-type flies
 The graph displays increase or decrease in courtship behaviour among *Drosophila* males from *Ocd^{5-G}* and wild-type (Canton-S) lines, after nine minutes, 30 seconds exposure to courtship song played at 80dB and 100dB. An increase in courtship implies the flies can hear. Standard error of the mean is shown for each line. **Ocd^{5-G}* flies differed significantly from wild-type at both 80dB and 100dB (calculated by χ^2 analysis), with $p < 0.001$.

5.5 Sensitivity to potassium and sodium

Mutations in *SCN4A* frequently lead to potassium-sensitivity in an allele-specific manner (reviewed by Cannon, 2002), although the precise mechanism by which this occurs remains unclear. The influx of sodium ions into the cell during membrane depolarisation is followed by the opening of potassium channels that transport potassium ions out of the cell to hyperpolarise the membrane. This forms the basis of the membrane action potential. This synergy between the two channel types is likely to be disrupted upon mutation of a sodium channel domain, so it is reasonable to predict that a membrane might then be defective in potassium ion transport. *SCN4A* residue G1306, orthologous to *para* residue G1571, is known to be associated with periodic paralysis which can be triggered by cold, in paramyotonia congenita (G1306V) (McClatchey *et al.*, 1992b) or by elevated serum potassium levels, in the case of myotonia fluctuans (G1306A) (Ricker *et al.*, 1994). It is

unclear why some sodium channel mutations confer potassium-sensitivity while some do not (reviewed by Cannon, 2002).

To determine any potassium-sensitivity of the *Ocd* (Glasgow) mutant flies, they were grown on food containing various concentrations of potassium chloride. This technique has previously been used to assay viability of *inebriated* mutants on hypertonic media as a measure of the osmotic stress response (Huang *et al.*, 2002). In a parallel experiment, the flies were grown on food containing sodium chloride. If *Ocd* flies are compromised in their ability to transport sodium ions, it might be expected that increasing the intercellular sodium levels may worsen the *Ocd* phenotype. Heterozygous flies were used, but based on knowledge of the human potassium-sensitive disorders, which are mainly inherited in a dominant fashion, it follows that any sensitivity should be apparent even in the heterozygous state. The sensitivity tests were carried out on *Ocd*^{1-G}, *Ocd*^{5-G} (both I1545M+G1571R) and *Ocd*^{7-G} (T1551I) heterozygous females.

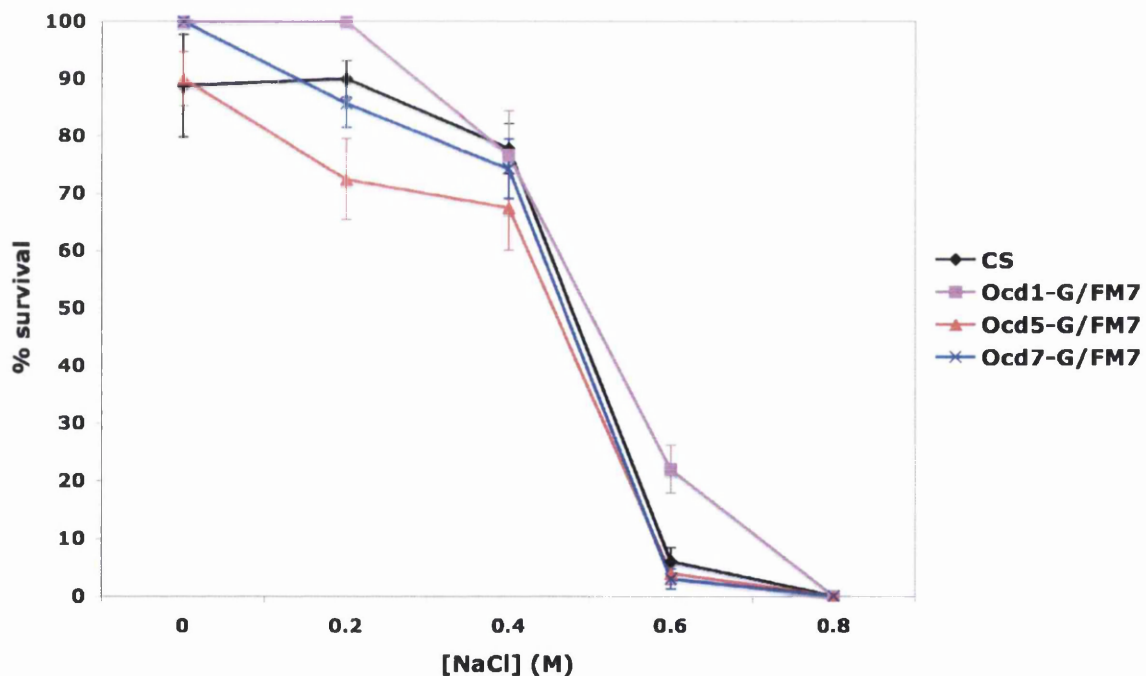


Figure 5.10 NaCl sensitivity assay in heterozygous *Ocd* females and wild-type females

Ocd^{1-G}, *Ocd*^{5-G} (both I1545M+G1571R), *Ocd*^{7-G} (T1551I) and Canton-S (CS) flies were grown on food containing various concentrations on NaCl for four days and survival scored. Standard errors of the proportion are displayed for each value.

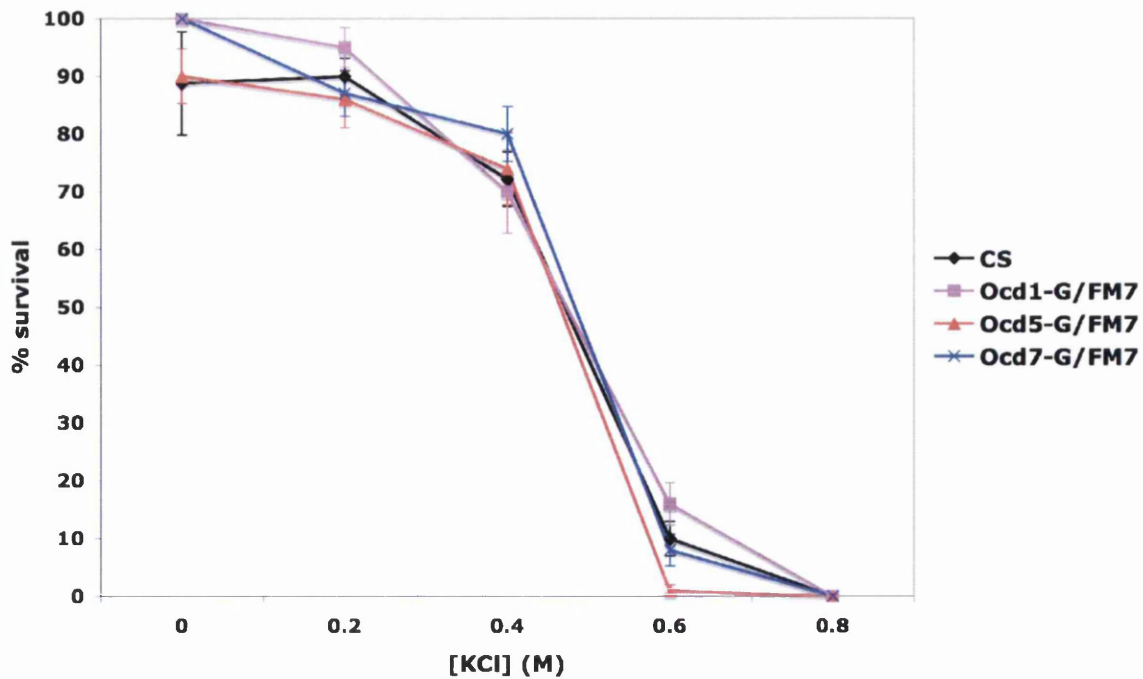


Figure 5.11 KCl sensitivity assay in heterozygous *Ocd* females and wild-type females

Ocd^{1-G}, *Ocd*^{5-G} (both I1545M+G1571R), *Ocd*^{7-G} (T1551I) and Canton-S (CS) flies were grown on food containing various concentrations on NaCl for four days and survival scored. Standard errors of the proportion are displayed for each value.

The results of the NaCl and KCl sensitivity assay are shown in Figures 5.10 and 5.11. All fly lines display sensitivity to increasing concentrations of both salts, and there is no difference between the *Ocd* flies and wild-type, with mortality of each line occurring at similar concentrations. This is the case in both the double mutants *Ocd*^{1-G} and *Ocd*^{5-G}, and the single mutant *Ocd*^{7-G}. Because the *Ocd* flies tested were heterozygous, any recessive tolerance or sensitivity to sodium or potassium ions would not be seen. However, preliminary experiments using both homozygous double mutants and hemizygous male flies were carried out (data not shown) and the survival curve was very similar to those seen here. Therefore it can be concluded that unlike some *SCN4A* mutations, the *Ocd* mutations do not lead to sensitivity to levels of potassium ions. Similarly the flies do not display sodium-sensitivity.

However, because the ions were delivered in salt form, the patterns observed may be due to osmotic (salt) stress, so a different way of delivering sodium or potassium ions might produce different results. The blood-brain barrier in insects and vertebrates maintains the ionic balance of neuronal bathing fluid (reviewed by Carlson *et al.*, 2000). This could pose a problem in these experiments, if excess sodium and potassium ions in the food medium cannot reach the ion channels of the nervous system. Ideally, the effects of excess

potassium could be analysed in *Xenopus* oocytes expressing *Ocd* mutant channels, by adjusting ionic concentrations in the perfusion saline for electrophysiological analysis.

5.6 Pesticide resistance

Resistance to chemical insecticides occurs in field populations via natural selection. Unravelling the molecular basis of resistance is of great importance for understanding the evolution of such mutations. Although extensively studied in houseflies, the genetic model organism *Drosophila* has provided an amenable tool for establishing how pesticides work, and for developing novel insecticides (reviewed by ffrench-Constant *et al.*, 2004). Analysis of resistant *Drosophila* allows targets and modes of action for insecticides to be identified.

Understanding the precise mechanisms underlying sodium channel inactivation has important therapeutic implications. There are at least nine distinct groups of neurotoxins specific to sodium channels, characterised by the site to which they bind (Wang and Wang, 2003). These are shown in Table 5.3. Some toxins block channels, whilst others modify gating. Channel toxicology can provide further information about gating properties and ion transport. Future studies will clearly define the specific molecular interactions involved in the process.

A wide variety of neurotoxins, including DDT (dichlorodiphenyltrichloroethane) and pyrethroids, have been shown to target sodium channels by binding to specific domains within the molecule (Zlotkin, 1999, Wang and Wang, 2003, ffrench-Constant *et al.*, 2004). Several *para* mutants originally isolated on account of their temperature-sensitivity have since been shown to confer insecticide resistance, for example *para*⁷⁴ and *para*^{DN7} (Pittendrigh *et al.*, 1997). Pyrethroids and DDT are known to cause persistent activation of sodium channels (Soderlund and Bloomquist, 1989). Because *Ocd* mutant lines encode sodium channels that differ at single amino acid sites, they may respond to specific neurotoxins in a novel fashion. Strains that are more susceptible or resistant to specific neurotoxins can reveal the specific residues and channel domains that interact with the toxin. This has implications for the design and development of new pesticides.

Receptor site	Neurotoxin(s)	Physiological effects	Putative location
1	Tetrodotoxin Saxitoxin μ -Conotoxin	Inhibition of Na ⁺ permeability	p-loop in all domains
2	Batrachotoxin Veratridine Aconitine Grayanotoxin N-Alkylamides	Persistent activation; depolarisation of resting potentials	S6 in all domains
3	α -Scorpion toxins Sea anemone II toxin	Prolonged channel opening	DIV S3-S4 linker DI S5-S6 linker DIV S5-S6 linker
4	β -Scorpion toxins	Shifts in activation gating; repetitive firings	DII S3-S6 linker
5	Brevetoxins Ciguatoxins	Shifts in activation gating	D1 S6
6	δ -Conotoxins	Prolonged channel opening	Unknown
7	DDT Pyrethroids	Persistent activation; Depolarisation of resting potentials; repetitive firings	DI S6 DII S6 DIII S6
8	Goniopora coral toxin Conus striatus toxin	Prolonged channel opening	Unknown
9	Local anaesthetics Anticonvulsants Antirhythmic Antidepressants	Inhibition of Na ⁺ permeability	DI S6 III S6 IV S6

Table 5.3 Sodium channel neurotoxins and corresponding receptor sites

Neurotoxins targeting voltage-gated sodium channels fall into nine categories, depending on the site they are predicted to bind to. The physiological channel effects differ between categories. The predicted location of each receptor site is indicated. Modified from Wang and Wang, 2003.

There are several neurotoxins which target the S6 segment of domain III in Para (Table 5.3). One of these is DDT. To test for resistance, *Ocd* flies were subjected to a standard DDT contact assay. The lines used were the original lines generated and kept in Søndergaard's lab since the 1970s. A homozygous line, *Ocd*^{S-S}, harbouring the double mutation I1545M and G1571R was analysed, as well as a heterozygous line, *Ocd*^{2-S}, with the single T1551I change balanced over FM7. The wild-type strain used as a control was Søndergaard's original *Ocd* progenitor Oregon-R line.

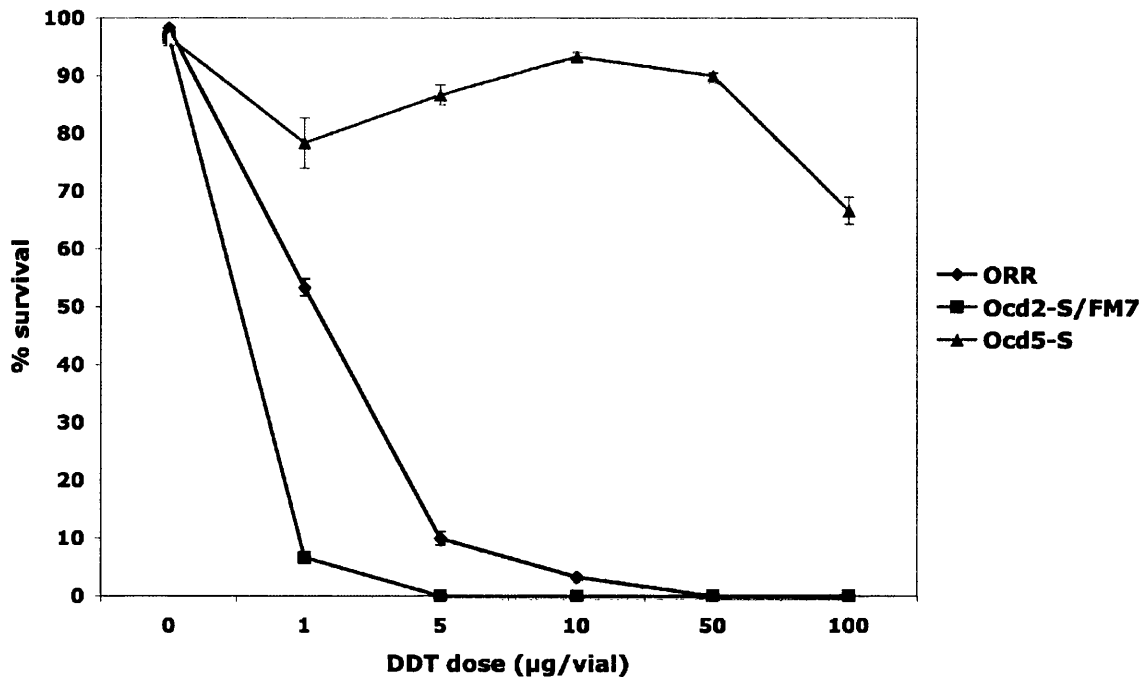


Figure 5.12 Preliminary data from DDT contact assay

The graph shows the percentage of female flies which survive at selected DDT doses of between 0 and 100µg/vial. The lines used were wild-type Oregon-R (ORR), *Ocd^{2-S}/FM7* (T1551I) heterozygotes and *Ocd^{5-S}* (I1545M+G1571R) homozygotes. Standard error of each mean is displayed. For each data point, n=60

Figure 5.12 shows preliminary data from the DDT contact assay at DDT doses of between 0 and 100µg/vial. It is clear from the graph that *Ocd^{5-S}* females display striking resistance to DDT compared to wild-type. In contrast, *Ocd^{2-S}/FM7* females, appear to show slight sensitivity to DDT. To analyse the extent of the resistance, *Ocd^{5-S}* flies were grown on increasing concentrations of DDT, up to 1000µg/vial. Probit (probability unit) analysis was applied to each of the lines tested. Probit regression is typically used to analyse dose-response data (Finney, 1971). The results are plotted in Figure 5.13. The lethal dose LD₅₀ and resistance ratio were calculated for each genotype (Table 5.4). LD₅₀ represents the amount of DDT that causes the death of 50% of a group of test animals.

Figures 5.12, 5.13 and Table 5.4 show the DDT bioassay data. While heterozygous *Ocd* flies with the T1551I mutation (*Ocd^{2-S}*) appear to show a mild sensitivity (0.19 resistance compared to Oregon-R), the most striking result is that of the homozygous double mutants (*Ocd^{5-S}*). These flies display a marked increase in resistance to DDT compared to wild-type. In both males and females there is more than a thousand-fold difference in DDT resistance compared to Oregon-R (Table 5.4).

Line	Sex	LD ₅₀ (µg/vial) (95% CI)	Resistance ratio
Oregon-R	Male	0.38 (0.21-0.54)	1.00
	Female	0.62 (0.31-1.00)	1.00
<i>Ocd</i> ^{2-S} /FM7	Female	0.12 (0.08-0.16)	0.19
<i>Ocd</i> ^{5-S}	Male	432.72 (330-530)	1138.74
	Female	801.67 (550-1720)	1293.02

Table 5.4 Resistance levels of wild-type and *Ocd* lines to DDT

LD50 represents the amount of DDT, given all at once, which causes the death of 50% of a group of test animals. This was calculated for wild-type Oregon-R males and females, heterozygous *Ocd*^{2-S} females (T1551I), and homozygous *Ocd*^{5-S} males and females (I1545M+G1571R). *Ocd*^{2-S} homozygous females and hemizygous males are lethal, so no data is available. 95% confidence intervals are displayed. For each test group, n=360. Resistance ratio with reference to Oregon-R is also shown.

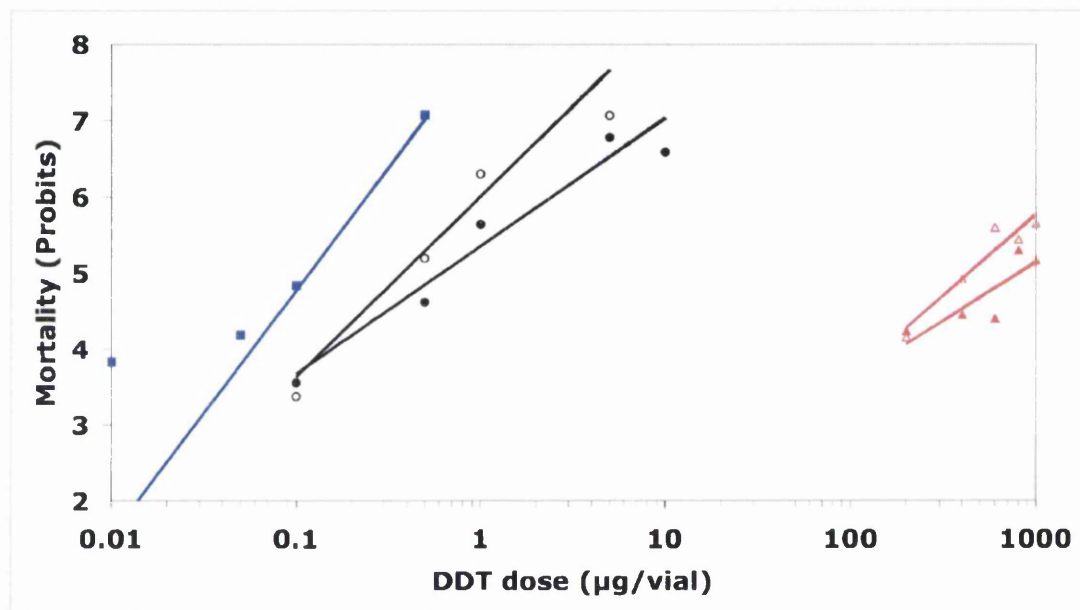


Figure 5.13 DDT lethality assay in wild-type and *Ocd*

Probit analysis of DDT dose-response relationships for wild-type and *Ocd* mutants. Wild-type (ORR) is represented by black circles, *Ocd*^{2-S}/FM7 (T11551I) by blue squares, and *Ocd*^{5-S} (I1545M+G1571R) by red triangles. Open shapes represent male data; closed shapes represent female data. Regression lines are shown. No data was available from homozygous or hemizygous *Ocd*^{2-S} flies, due to lethality.

The I1545M mutation lies within domain III S6, and the G1571R substitution in the domain III-IV linker. DDT and pyrethroid insecticides are believed to target domain III S6 (Pauron *et al.*, 1989). Indeed, a *para* heat sensitive paralytic mutation, *para*⁷⁴ (M1536I), which also resides in domain III S6, is known to confer resistance to these insecticides (Pittendrigh *et al.*, 1997, Martin *et al.*, 2000). This new finding however suggests that the I1545 and/or G1571 residue may be crucial targets for DDT. It may well be that mutations at residue T1551 confer resistance when homozygous. However, these flies have only been tested in the heterozygous state so unless this resistance was a dominant trait, it would be masked.

The fact that a double mutant gives such a high resistance ratio is very interesting. In houseflies, a double mutant (*super-kdr*) is known to exist which also confers high resistance to DDT and pyrethroids. In this case, one mutation is the *knockdown resistant* (*kdr*) amino acid replacement in domain II S6 of the housefly *para* homologue, and the second is found in the intracellular loop between domain II segments S4 and S5. The *super-kdr* type mutation has thus far only been found in houseflies (Williamson *et al.*, 1996) and horn flies (Guerrero *et al.*, 1997) whereas the *kdr*-like substitution has been found in a broader range of insects, including the mosquito (Martinez-Torres *et al.*, 1998) and the cockroach (Dong, 1997).

In a comparative proteomics study comparing selected DDT resistant and sensitive lines, several proteins involved in metabolic pathways such as glycolysis and the Krebs' cycle were identified as being differentially translated (Pedra *et al.*, 2005). Intriguingly, this draws parallels with the *Ocd* proteomics data. Given that at least one of the *Ocd* mutants shows a remarkable degree of DDT resistance, this highlights an alternative explanation for why so many mitochondrial proteins were identified in *Ocd* 2D DIGE. Sodium channels provide the primary target for DDT, but metabolic pathways are also affected. Indeed, DDT has been shown to affect glucose utilisation in both insects and mammals (Ela *et al.*, 1970, Okazaki and Katayama, 2003). It is possible that alterations in mitochondrial metabolic pathways as a consequence of the *Ocd* mutation, together with the *para* mutations uncovered, may result in the exceptionally high resistance observed.

Dissecting sites of insect resistance is crucial for the development of novel insecticides. However, although resistance associated mutations may give clues to insecticide binding sites, this is not necessarily always the case. Many sodium channel targeting toxins alter channel properties, for example fast inactivation. If mutations resulting in resistance also confer functional changes to the channel, then they may also alleviate detrimental effects caused by certain toxins. This might be the case with the *Ocd* mutations, and further investigation would be required to see whether DDT actually binds to the mutated residues.

At least one *Ocd* mutant is highly resistant to the sodium channel-targeting chemical DDT. This is further convincing evidence that *Ocd* is allelic to *para*, the major *Drosophila* voltage-gated sodium channel gene. Future experiments should elucidate whether the remainder of the *Ocd* mutant lines share this striking phenotype, and reveal which, if any, of the substituted residues are important for DDT binding. It would also be interesting to

analyse the electrophysiological phenotype of *Ocd* flies, during or following exposure to DDT, and other toxins.

6 Discussion

6.1 Project summary

The primary aim of this project was to identify the *Ocd* gene and gene product. Through two complementary mapping techniques, *Ocd* was found to map to the voltage-sodium channel gene *paralytic*. Complementation data compiled between *Ocd* and the *para* null allele *Df(1)D34* supports this. Sequence analysis of *para* in *Ocd* flies revealed missense mutations in all but one of the seven *Ocd* alleles. These mutations - I1545M, T1551I and G1571R - lie in highly conserved and functionally important regions of the sodium channel.

Subsequent characterisation of these novel alleles of *para* revealed that in the double mutants (I1545M and G1571R), peak transient sodium current is significantly reduced, and this effect is more pronounced at lower temperatures (16°C), suggesting a physiological basis for the cold-sensitivity. A DDT bioassay revealed that the double mutants also display striking DDT resistance. The LD₅₀ of *Ocd*^{S-S} (I1545M and G1571R) adults is over a thousand times higher than that of wild-type adults. This is in keeping with *Ocd* and *para* being allelic, as several *para* mutants display resistance to several pesticides (ffrench-Constant *et al.*, 2004, Pittendrigh *et al.*, 1997).

Upon 2D proteomic analysis of *Ocd*^{I-G} T1551I mutants, several mitochondrial proteins were shown to be differentially regulated compared to wild-type. This is interesting in light of early evidence that *Ocd* may perform a mitochondrial role. However, it is possible that this apparent mitochondrial phenotype is an indirect effect of the mutations, possibly induced by the onset of seizures.

Investigations undertaken in this project have shown conclusively that the *Ocd* mutations are allelic to *para*. In light of this, it is now possible to further develop *Ocd* as a model for human sodium channel disease, in which issues of pathogenesis and therapeutic development can be addressed.

6.2 *Ocd* as a model for human sodium channelopathies

Many human sodium channelopathies have been described (reviewed by George, 2005 and Cannon, 2000), but for most no effective treatment exists. Animal models can provide a route via which therapies can be developed and tested, and can also allow the cellular and molecular basis of disease to be dissected. As yet, for the majority of seizure disorders, no tractable whole animal model has been described, although mammalian cell lines are routinely used, particularly to measure electrophysiological properties of mutant human sodium channels. In the absence of a vertebrate model, using an invertebrate whole organism model would prove extremely useful. The advantages of using a whole animal include being able to investigate the effects of endogenous factors such as serum potassium levels and temperature. At the moment, the precise mechanisms by which channel inactivation is disrupted in the channelopathies is not known, nor are the mechanisms by which cold and potassium trigger attacks.

As described previously, all of the newly discovered *Ocd* mutations lie in conserved regions of the sodium channel. Additionally, one of the mutations is located at *para* residue G1571, which is analogous to the human skeletal muscle sodium channel *SCN4A* residue G1306, mutations of which cause paramyotonia congenita and potassium-aggravated myotonia, depending on which residue is substituted (Lerche *et al.*, 1993, McClatchey *et al.*, 1992a, Ricker *et al.*, 1994). It is remarkable that mutations in the same conserved residue in flies and humans can give rise to such strikingly similar phenotypes, particularly in the case of cold-sensitive paramyotonia congenita. This is encouraging in terms of developing *Ocd* as a model for human disease, particularly with respect to disorders caused by *SCN4A* mutations, as it strongly implies that the molecular pathogenesis of the respective disorders are conserved from fly to human. Further characterisation of the *Ocd* lines should clarify how the mutations uncovered lead to the associated mutant phenotypes, and it is likely that the pathogenic mechanism is similar to that in humans. The *Ocd* lines may also be of great use in identifying specific chemicals and pharmaceutical products that may be able to alleviate symptoms of sodium channel dysfunction.

6.3 Future directions

The *Ocd* mutations have been successfully mapped to *paralytic*, and promise to provide an invaluable system in which to study human sodium channelopathies. However, before *Ocd*

is established as a model for specific disorders, further investigations and characterisation is required.

6.3.1 Creation of *Ocd*-like and other novel *para* mutations

Several lines of evidence point towards *Ocd* and the *para* being allelic. *Ocd* maps very close to *para*; *para* and *Ocd* do not complement; missense mutations in *para* have been uncovered in *Ocd* lines; expression of wild-type *para* in *Ocd* lines results in rescue of the male semi-lethality; Na⁺ current is significantly reduced in *Ocd* larval motorneurons, and at least one *Ocd* line shows remarkably high levels of resistance to the sodium channel-targeting chemical DDT. However, it remains necessary to prove that the precise mutations uncovered during sequencing *para* are the underlying cause of the mutant phenotypes.

In order to demonstrate that the *Ocd* mutations discovered are indeed the basis of the *Ocd* phenotype, and to identify which residues mediate each phenotype, the three *Ocd* mutations could be re-created via site-directed mutagenesis of the *para* 13.5 cDNA (Warmke *et al.*, 1997) and cloned into the *pP*{UAST} vector (Brand and Perrimon, 1993). Rescue of the *Ocd*^{*l-G*} male semi-lethality by wild-type *para* has been demonstrated using the GAL4/UAS system. It is likely that introducing *Ocd*-like transgenes using this approach would induce some or all of the *Ocd* phenotypes. Cold-sensitive paralysis is a dominant trait, so it is reasonable to assume that an *Ocd* transgene would generate cold-sensitivity regardless of the presence of one or more wild-type *para* alleles. The two *Ocd*^{*l*} mutations, I1545M and G1571R, could be created in one transgene as a double mutation, and also separately as single mutations. This would identify whether both are necessary for the *Ocd* phenotype, or if either alone is sufficient. The *Ocd*^{*2-S*} and *Ocd*^{*7-G*} mutation T1551I could be introduced as a single mutation to confirm it is the basis of the *Ocd* phenotype.

Creating fly lines containing *Ocd*-like transgenes is a relatively quick way to ascertain whether one of the *Ocd*^{*l*} mutations is sufficient to generate the *Ocd* phenotype. However, the GAL4/UAS transgenic approach may prove problematic, largely because the transgene will only represent one of the many alternative *para* splice variants, and so cannot recapitulate the transcriptional complexity of the *para* expression. Problems in establishing tissue-specificity and appropriate levels of expression in many *P*{GAL4} drivers are well documented (Ito *et al.*, 2003). It is also possible that gene dosage would prove an issue. However, this could be addressed by adjusting dosage by using the lethal *para* deletion

line *Df(1)D34*, and also by altering the number of *Ocd* transgenes. Expression of the transgenes could also be adjusted by using different *P{GAL4}* drivers.

Nevertheless, given the limitations associated with the GAL4/UAS approach, an alternative method would be advantageous. Recent innovations have made targeted mutagenesis possible in *Drosophila*, using homologous recombination (Gong and Rong, 2003, Rong and Golic, 2000). At least 17 different endogenous *Drosophila* genes have been successfully modified using the 'ends-in' or 'insertional gene targeting' technique (reviewed by Venken and Bellen, 2005). This strategy could be used to create novel missense mutations in *para*. Because the chromosomal *para* gene is being manipulated, every transcript would be produced, and would undergo normal RNA editing and splicing, assuming the mutations do not affect these processes. This method, although more laborious and time-consuming, circumvents all the issues raised with the GAL4/UAS approach.

In addition to recreating the *Ocd* mutations themselves, it would be interesting to recreate novel *para* mutations, based upon knowledge of human disease-causing mutations, particularly those within the skeletal muscle sodium channel gene *SCN4A*. These will help develop a new understanding of the pathogenesis of such diseases, and also provide a model in which to develop and test novel pharmacological agents. This should prove fruitful as it is already known that the *Ocd* G1571 mutation in flies, analogous to the disease-causing G1306 mutations in humans, can lead to a strikingly similar cold-sensitive phenotype in both organisms.

The GAL4/UAS approach would identify which, if either, of the double mutations, I1545M or G1571R, is solely responsible for the *Ocd* phenotype. The causative mutation could then be introduced alone via homologous recombination. Additionally, a human cold-sensitive mutation, for example T1313M, which causes paramyotonia congenita (McClatchey *et al.*, 1992b) and a potassium-sensitive mutation, for example M1360V, associated with hyperkalemic periodic paralysis (Wagner *et al.*, 1997), could be introduced as the equivalent *Drosophila* mutations T1579M and M1626V, respectively.

Once produced, experiments would have to be undertaken to confirm these mutations cause a discernible *Ocd*-like phenotype in flies. An important factor to consider when developing genetic model organisms for human disease is whether the disease phenotype is

recapitulated to at least some extent in the model. Phenotypic characterisation of the fly strains would include tests for cold-sensitivity, potassium-sensitivity, toxin resistance and any electrophysiological defects. As has been described, these assays are relatively simple to perform the fly. This analysis could be extended to the *Ocd* alleles already described, as well as several other alleles of *para*, which have yet to be fully characterised in this respect. Thorough characterisation would lead to a comprehensive understanding of which mutations lead to which periodic paralyses induced by specific chemical or environmental challenges, and this in turn would be likely to lead to the identification of chemicals that can alleviate these phenotypes, in both flies and humans.

This also paves the way for the development of *Drosophila* as a diagnostic tool: suspected disease-causing *SCN4A* mutations from affected families could be recreated in the fly. Successfully replicating the mutant phenotype in *Drosophila*, particularly at the electrophysiological level, would confirm the mutations are causative.

6.3.2 Characterisation of pre-existing and novel *para* strains

6.3.2.1 Testing for sensitivity to cold, potassium, and rest after exercise

Robust tests for cold and potassium-sensitivity have already been established and have been described previously. These could be applied to each of the newly created *para* lines. Although no potassium-sensitivity in terms of viability has been observed in *Ocd* flies, it is highly likely that a potassium-sensitive *SCN4A* mutation would give rise to potassium-sensitivity in flies. Aside from lethality, any behavioural defects, including paralysis susceptibility, associated with potassium ingestion could be measured. In addition to temperature and serum potassium levels, rest after exercise is also known to exacerbate certain *SCN4A*-associated disorders (reviewed by Cannon, 2002). As yet, a robust test for sensitivity to rest after exercise in *Drosophila* has not been established. A novel test might involve forcing flies to run continuously within tubes in a rotating wheel for defined periods of time, and subsequently paralysis susceptibility would be measured.

6.3.2.2 Chemical challenge

Many different chemicals, including neurotoxins and pesticides, exert their effect on voltage-gated sodium channels (Wang and Wang, 2003, Zlotkin, 1999). Much research has

focussed on which channel domains specifically are the targets of such chemicals. Targeting *Ocd* and novel *para* flies with different neurotoxins, and simultaneously analysing inducible paralytic phenotypes would determine which channel domains mediate cold- and potassium-sensitivity, and may also isolate chemicals that can mitigate or exacerbate these phenotypes.

*Ocd*¹ I1545M and G1571R double mutants are over a thousand times more resistant to DDT than wild-type (section 5.5). The novel *para* lines, which would all contain single amino acid substitutions, may also respond in a unique fashion to various neurotoxin and pesticides. Pesticide resistance assays akin to those described previously could be conducted using a range of chemicals with known and unknown molecular targets within voltage-gated sodium channels. Primarily, this may pinpoint domains and specific residues that are vital for toxin binding. This has important implications for the design and development of novel pesticides. Moreover, any chemical which instigates a rescuing effect may identify a route via which human disorders caused by specific mutations can be treated.

6.3.2.3 Investigation into the electrophysiological phenotype of *Ocd*

Further characterisation of the electrophysiological phenotype of *Ocd* flies is required to establish how the mutations lead to cold-sensitive sodium channel dysfunction. Electrophysiological properties, particularly any inactivation defects, of individual *Ocd* sodium channels, can be investigated using patch clamping. Patch clamping can be performed under a variety of conditions, meaning that the effect of cold, potassium, neurotoxins, and rest after exercise can be analysed.

Analyses of *SCN4A* derived from myotonic patients show that single amino acid substitutions alter the activation threshold and/or rate of fast inactivation (Cannon, 2002, Wu *et al.*, 2005). If the same is observed in *Ocd* channels, the validity of using *Ocd* as a model is further enhanced. This can be investigated using heterologous expression of *Ocd* channels in *Xenopus laevis* oocytes. Heterologous expression is favourable as it overcomes problems created by voltage clamping in *Drosophila* intact motorneurons, the morphological properties of which are not ideal for electrophysiological studies. The *Xenopus* oocyte is large, easy to handle, expresses few endogenous membrane transport systems, and is almost spherical, compared to neurons that have extensive axo-dendritic

regions. This makes voltage clamping much easier, and *Xenopus* oocytes are routinely used in electrophysiology, allowing the subtlest changes in channel kinetics to be detected (reviewed by Wagner *et al.*, 2000).

To enable this to work, for each channel variant, *para* cRNA and cRNA of the accessory protein *tipE* would need to be injected into oocytes. The two electrode voltage clamp technique (reviewed by Wagner *et al.*, 2000) could be used to measure whole cell currents through sodium channels. This would also allow activation threshold, inactivation rate, and ratio of transient to persistent current to be measured. Exogenous factors such as temperature and potassium could be manipulated in the perfusion saline to test for any cold- and potassium-sensitivity of different mutant channels.

The clear limitation of using *Xenopus* oocytes as an expression system is that the endogenous environment is very different from that of a *Drosophila* neuron. Differences in signalling pathways and, crucially, membrane composition exist between oocytes and the tissues or cells of flies, and ultimately expression in a fly cell line would be desirable. To address this, the various mutant *para* cRNAs would also need to be expressed in *Drosophila* S2 cells, a cell line derived from phagocytic haematopoietic cells (Schneider, 1972). Although uncharacterised for sodium channel expression, S2 cells have already been successfully used to stably express several types of *Drosophila* transmembrane proteins such as GABA receptors, acetylcholine receptors, and dopamine receptors (Millar *et al.*, 1995, Millar *et al.*, 1994, Han *et al.*, 1996).

6.3.3 Identification of genes that suppress the *Ocd* phenotype

Separate *Ocd* stocks harbouring the same *para* missense mutations vary greatly in terms of the severity of the phenotype (for example, sections 3.2 and 5.3). This implies that different stocks have acquired modifier (suppressor) mutations over time, which alleviate the mutant phenotype. This has implications for therapeutical developments in human sodium channelopathy research. If such suppressors can be identified, they may pinpoint cellular pathways that could be exploited to effectively treat channel disorders.

In order to identify modifier genes of *Ocd*, replicates of an isogenised *Ocd* line could be subject to selection against the *Ocd* cold-sensitive paralytic phenotype. This could be achieved by breeding from the most cold-tolerant males and females. After about 20

generations, it would be anticipated that some or all of the replicate lines would have gradually become cold tolerant. A gradual change in tolerance would suggest the combinatorial effects of many modifiers. Genes contributing to this cold-tolerance, and therefore directly modifying the *Ocd* phenotype, could be identified using transcriptomic methodologies. Microarray analysis would identify genes in the selected *Ocd* lines that are differentially expressed compared to a wild-type control and the original isogenised *Ocd* strain. Issues of inbreeding and genetic background should be addressed to tightly control this experiment.

Additionally, an abrupt change in cold-tolerance observed in a single generation would suggest that there has been a single gene suppressor of *Ocd*. Such suppressors could be mapped using SNPs and molecularly defined *P* elements. Once their identity is known, investigations into how they exert the suppression effect could be carried out.

This modifier screen should identify specific pathways by which the *Ocd* phenotype may be suppressed, and this information could be extrapolated to human sodium channel disorders, in terms of therapeutic development. This approach has been used successfully to identify suppressor lines of the *technical knockout (tko)* phenotype (Moreno, Kemppainen, Jacobs and O'Dell, *unpublished*).

6.3.4 The role of mitochondria in the *Ocd* mutant phenotype

Several lines of evidence support the notion that *Ocd* plays a role in the mitochondrion. Early work by Søndergaard (1975, 1976, 1979, 1986) showed that the enzyme kinetics of succinate cytochrome c reductase was affected by the *Ocd* mutations, and that the 2D electrophoretic pattern of the mitochondrial proteome was altered. Because *Ocd* males are semi-lethal, those males that do survive to adulthood must do so via some mechanism that allows them to cope with malfunctioning sodium channels. 2D proteomic analysis of *Ocd^{7-G}* (T1551I) revealed 16 proteins with altered expression levels compared to wild-type, eight of which were mitochondrial (section 5.2). This high proportion of mitochondrial proteins strongly implies that the *Ocd* mutations affect mitochondrial function in some way. This mitochondrial effect could be part of a strategy to cope with effects of mutant channels, or alternatively could be the consequence of seizure episodes induced by cold.

In light of the fact that *Ocd* and *para* are allelic, it is also important to note the activation energy of succinate cytochrome c reductase was altered upon temperature increase to 25°C in both *para^{ts1}* and *shibire^{ts}*, two heat-sensitive paralytic mutants (Søndergaard, 1976). This shows that this effect is not exclusive to *Ocd*, and because the effect is seen in three separate paralytic mutants - two sodium channel mutants and one dynamin mutant (van der Blik and Meyerowitz, 1991) - it is more likely that mitochondrial function in these flies is affected by paralytic or seizure episodes, rather than *Ocd* having a direct mitochondrial role. Nevertheless, this is interesting in terms of developing treatments to alleviate all aspects of the human channelopathy phenotype, including any possible mitochondrial effect.

The 2D proteomics data should be verified using comparative 2D western blotting techniques, in case there is a reason why mitochondrial proteins are more susceptible to identification in 2D DIGE. Subsequent biochemical analysis of Krebs' cycle enzymes, OXPHOS enzymes and of mitochondrial ATP synthesis could confirm that mitochondrial function is indeed altered in *Ocd* flies. Further investigation would be required to explain exactly how the *Ocd* mutations, or the associated phenotype(s) cause mitochondrial damage. It would also be interesting to extend this study to other conditional paralytic mutants.

6.4 Conclusions

The *Drosophila Out cold* mutations have been shown to be missense mutations in the major voltage-gated sodium channel gene *paralytic*. Characterisation of the mutations has revealed that they provide a valid and tractable model for studying human sodium channel disorders. Future developments of *Ocd* as a model will undoubtedly lead to a greater understanding of the pathogenic mechanisms underlying such diseases, and will aid in the identification of novel treatments.

List of references

- Ackerman, M. J., Siu, B. L., Sturner, W. Q., Tester, D. J., Valdivia, C. R., Makielski, J. C. & Towbin, J. A. (2001). Postmortem molecular analysis of *SCN5A* defects in sudden infant death syndrome. *Jama*, 286, 2264-2269.
- Adams, M. D. & Sekelsky, J. J. (2002). From sequence to phenotype: reverse genetics in *Drosophila melanogaster*. *Nat Rev Genet*, 3, 189-198.
- Akai, J., Makita, N., Sakurada, H., Shirai, N., Ueda, K., Kitabatake, A., Nakazawa, K., Kimura, A. & Hiraoka, M. (2000). A novel *SCN5A* mutation associated with idiopathic ventricular fibrillation without typical ECG findings of Brugada syndrome. *FEBS Lett*, 479, 29-34.
- Alban, A., David, S. O., Bjorkesten, L., Andersson, C., Sloge, E., Lewis, S. & Currie, I. (2003). A novel experimental design for comparative two-dimensional gel analysis: two-dimensional difference gel electrophoresis incorporating a pooled internal standard. *Proteomics*, 3, 36-44.
- Alvarez de la Rosa, D., Canessa, C. M., Fyfe, G. K. & Zhang, P. (2000). Structure and regulation of amiloride-sensitive sodium channels. *Annu Rev Physiol*, 62, 573-594.
- Anderson, S., Bankier, A. T., Barrell, B. G., de Bruijn, M. H., Coulson, A. R., Drouin, J., Eperon, I. C., Nierlich, D. P., Roe, B. A., Sanger, F., Schreier, P. H., Smith, A. J., Staden, R. & Young, I. G. (1981). Sequence and organization of the human mitochondrial genome. *Nature*, 290, 457-465.
- Ashburner, M. (1989). *Drosophila: a laboratory manual*, Cold Spring Harbour Press.
- Audenaert, D., Claes, L., Ceulemans, B., Lofgren, A., Van Broeckhoven, C. & De Jonghe, P. (2003). A deletion in *SCN1B* is associated with febrile seizures and early-onset absence epilepsy. *Neurology*, 61, 854-856.
- Baines, R. A. & Bate, M. (1998). Electrophysiological development of central neurons in the *Drosophila* embryo. *J Neurosci*, 18, 4673-4683.

- Baines, R. A., Uhler, J. P., Thompson, A., Sweeney, S. T. & Bate, M. (2001). Altered electrical properties in *Drosophila* neurons developing without synaptic transmission. *J Neurosci*, 21, 1523-1531.
- Ballard, J. W. (2005). *Drosophila simulans* as a novel model for studying mitochondrial metabolism and aging. *Exp Gerontol*, 40, 763-773.
- Baulac, S., Gourfinkel-An, I., Nabbout, R., Huberfeld, G., Serratosa, J., Leguern, E. & Baulac, M. (2004). Fever, genes, and epilepsy. *Lancet Neurol*, 3, 421-430.
- Bayliss, F. T. & Ingrahm, J. L. (1974). Mutation in *Saccharomyces cerevisiae* conferring streptomycin and cold sensitivity by affecting ribosome formation and function. *J Bacteriol*, 118, 319-328.
- Bellen, H. J., Levis, R. W., Liao, G., He, Y., Carlson, J. W., Tsang, G., Evans-Holm, M., Hiesinger, P. R., Schulze, K. L., Rubin, G. M., Hoskins, R. A. & Spradling, A. C. (2004). The BDGP gene disruption project: single transposon insertions associated with 40% of *Drosophila* genes. *Genetics*, 167, 761-781.
- Bentley, A., MacLennan, B., Calvo, J. & Dearolf, C. R. (2000). Targeted recovery of mutations in *Drosophila*. *Genetics*, 156, 1169-1173.
- Berger, J., Suzuki, T., Senti, K. A., Stubbs, J., Schaffner, G. & Dickson, B. J. (2001). Genetic mapping with SNP markers in *Drosophila*. *Nat Genet*, 29, 475-481.
- Bergren, S. K., Chen, S., Galecki, A. & Kearney, J. A. (2005). Genetic modifiers affecting severity of epilepsy caused by mutation of sodium channel *Scn2a*. *Mamm Genome*, 16, 683-690.
- Biervert, C. & Steinlein, O. K. (1999). Structural and mutational analysis of *KCNQ2*, the major gene locus for benign familial neonatal convulsions. *Hum Genet*, 104, 234-240.
- Bonini, N. M., Bui, Q. T., Gray-Board, G. L. & Warrick, J. M. (1997). The *Drosophila eyes absent* gene directs ectopic eye formation in a pathway conserved between flies and vertebrates. *Development*, 124, 4819-4826.

- Bonnot, G., Peypelut, L., Gerard, F., Lavenseau, L., Fleurat-Lessard, F. & Fields, P. G. (1998). The effect of cold acclimation and deacclimation on cold tolerance, trehalose and free amino acid levels in *Sitophilus granarius* and *Cryptolestes ferrugineus* (Coleoptera). *J Insect Physiol*, 44, 955-965.
- Brand, A. H. & Perrimon, N. (1993). Targeted gene expression as a means of altering cell fates and generating dominant phenotypes. *Development*, 118, 401-415.
- Broadie, K. & Bate, M. (1993). Activity-dependent development of the neuromuscular synapse during *Drosophila* embryogenesis. *Neuron*, 11, 607-619.
- Brumby, A. M. & Richardson, H. E. (2005). Using *Drosophila melanogaster* to map human cancer pathways. *Nat Rev Cancer*, 5, 626-639.
- Buchner, D. A., Seburn, K. L., Frankel, W. N. & Meisler, M. H. (2004). Three ENU-induced neurological mutations in the pore loop of sodium channel *Scn8a* (Na(v)1.6) and a genetically linked retinal mutation, *rd13*. *Mamm Genome*, 15, 344-351.
- Caldwell, J. H. & Schaller, K. L. (1992). Opening the gates on ion channel diseases. *Nat Genet*, 2, 87-89.
- Cannon, S. C. (1997). From mutation to myotonia in sodium channel disorders. *Neuromuscul Disord*, 7, 241-249.
- Cannon, S. C. (2000). Spectrum of sodium channel disturbances in the nondystrophic myotonias and periodic paralyses. *Kidney Int*, 57, 772-779.
- Cannon, S. C. (2002). An expanding view for the molecular basis of familial periodic paralysis. *Neuromuscul Disord*, 12, 533-543.
- Carlson, S. D., Juang, J. L., Hilgers, S. L. & Garment, M. B. (2000). Blood barriers of the insect. *Annu Rev Entomol*, 45, 151-174.

- Castella, C., Amichot, M., Berge, J. B. & Pauron, D. (2001). *DSCI* channels are expressed in both the central and the peripheral nervous system of adult *Drosophila melanogaster*. *Invert Neurosci*, 4, 85-94.
- Castresana, J., Feldmaier-Fuchs, G. & Paabo, S. (1998). Codon reassignment and amino acid composition in hemichordate mitochondria. *Proc Natl Acad Sci U S A*, 95, 3703-3707.
- Catterall, W. A. (1999). Molecular properties of brain sodium channels: an important target for anticonvulsant drugs. *Adv Neurol*, 79, 441-456.
- Cherbas, L., Hu, X., Zhimulev, I., Belyaeva, E. & Cherbas, P. (2003). EcR isoforms in *Drosophila*: testing tissue-specific requirements by targeted blockade and rescue. *Development*, 130, 271-284.
- Chomyn, A. & Attardi, G. (2003). MtDNA mutations in aging and apoptosis. *Biochem Biophys Res Commun*, 304, 519-529.
- Claes, L., Del-Favero, J., Ceulemans, B., Lagae, L., Van Broeckhoven, C. & De Jonghe, P. (2001). De novo mutations in the sodium-channel gene *SCN1A* cause severe myoclonic epilepsy of infancy. *Am J Hum Genet*, 68, 1327-1332.
- Clary, D. O. & Wolstenholme, D. R. (1985). The mitochondrial DNA molecular of *Drosophila yakuba*: nucleotide sequence, gene organization, and genetic code. *J Mol Evol*, 22, 252-271.
- Coyle, I. P., Koh, Y. H., Lee, W. C., Slind, J., Fergestad, T., Littleton, J. T. & Ganetzky, B. (2004). Nervous wreck, an SH3 adaptor protein that interacts with Wsp, regulates synaptic growth in *Drosophila*. *Neuron*, 41, 521-534.
- Cummins, T. R., Dib-Hajj, S. D. & Waxman, S. G. (2004). Electrophysiological properties of mutant Nav1.7 sodium channels in a painful inherited neuropathy. *J Neurosci*, 24, 8232-8236.
- D'Elia, D., Catalano, D., Licciulli, F., Turi, A., Tripoli, G. & Caggese, C. (2004). MitoDrome: a specialized resource of nuclear genes encoding mitochondrial

proteins of *D. melanogaster*, *D. pseudoobscura*, and *A. gambiae*
<http://www2.ba.itb.cnr.it/mitodrome/>.

Davies, N. P., Eunson, L. H., Gregory, R. P., Mills, K. R., Morrison, P. J. & Hanna, M. G. (2000). Clinical, electrophysiological, and molecular genetic studies in a new family with paramyotonia congenita. *J Neurol Neurosurg Psychiatry*, 68, 504-507.

de Bono, S., Riechmann, L., Girard, E., Williams, R. L. & Winter, G. (2005). A segment of cold shock protein directs the folding of a combinatorial protein. *Proc Natl Acad Sci U S A*, 102, 1396-1401.

de Vries, D. D., van Engelen, B. G., Gabreels, F. J., Ruitenbeek, W. & van Oost, B. A. (1993). A second missense mutation in the mitochondrial *ATPase 6* gene in Leigh's syndrome. *Ann Neurol*, 34, 410-412.

Dellinger, B., Felling, R. & Ordway, R. W. (2000). Genetic modifiers of the *Drosophila* NSF mutant, *comatose*, include a temperature-sensitive paralytic allele of the calcium channel alpha1-subunit gene, *cacophony*. *Genetics*, 155, 203-211.

Desaphy, J. F., De Luca, A., Didonna, M. P., George, A. L., Jr. & Camerino Conte, D. (2004). Different flecainide sensitivity of hNav1.4 channels and myotonic mutants explained by state-dependent block. *J Physiol*, 554, 321-334.

Dong, K. (1997). A single amino acid change in the *para* sodium channel protein is associated with knockdown-resistance (*kdr*) to pyrethroid insecticides in German cockroach. *Insect Biochem Mol Biol*, 27, 93-100.

Doyle, D. A., Morais Cabral, J., Pfuetzner, R. A., Kuo, A., Gulbis, J. M., Cohen, S. L., Chait, B. T. & MacKinnon, R. (1998). The structure of the potassium channel: molecular basis of K⁺ conduction and selectivity. *Science*, 280, 69-77.

Duffy, J. B. (2002). GAL4 system in *Drosophila*: a fly geneticist's Swiss army knife. *Genesis*, 34, 1-15.

- Duncan, R. F., Cavener, D. R. & Qu, S. (1995). Heat shock effects on phosphorylation of protein synthesis initiation factor proteins eIF-4E and eIF-2 alpha in *Drosophila*. *Biochemistry*, 34, 2985-2997.
- Eberl, D. F., Duyk, G. M. & Perrimon, N. (1997). A genetic screen for mutations that disrupt an auditory response in *Drosophila melanogaster*. *Proc Natl Acad Sci U S A*, 94, 14837-14842.
- Ela, R., Chefurka, W. & Robinson, J. R. (1970). In vivo glucose metabolism in the normal and poisoned cockroach, *Periplaneta americana*. *J Insect Physiol*, 16, 2137-2156.
- Enerback, S., Jacobsson, A., Simpson, E. M., Guerra, C., Yamashita, H., Harper, M. E. & Kozak, L. P. (1997). Mice lacking mitochondrial uncoupling protein are cold-sensitive but not obese. *Nature*, 387, 90-94.
- Escayg, A., MacDonald, B. T., Meisler, M. H., Baulac, S., Huberfeld, G., An-Gourfinkel, I., Brice, A., LeGuern, E., Moulard, B., Chaigne, D., Buresi, C. & Malafosse, A. (2000). Mutations of *SCN1A*, encoding a neuronal sodium channel, in two families with GEFS+2. *Nat Genet*, 24, 343-345.
- Falke, E. V. & Wright, T. R. (1975a). Cold-sensitive mutants of *Drosophila melanogaster* defective in ribosome assembly. *Genetics*, 81, 655-682.
- Falke, E. V. & Wright, T. R. (1975b). Cold-sensitive mutants of *Drosophila melanogaster* defective in ribosome assembly. *Genetics*, 81, 655-682.
- Feng, Y., Huynh, L., Takeyasu, K. & Fambrough, D. M. (1997). The *Drosophila* Na,K-ATPase alpha-subunit gene: gene structure, promoter function and analysis of a cold-sensitive recessive-lethal mutation. *Genes Funct*, 1, 99-117.
- French-Constant, R. H., Daborn, P. J. & Le Goff, G. (2004). The genetics and genomics of insecticide resistance. *Trends Genet*, 20, 163-170.
- Finney, D. J. (1971). *Probit Analysis*, Cambridge, Cambridge University Press.

- Flint, D. H., Tuminello, J. F. & Emptage, M. H. (1993). The inactivation of Fe-S cluster containing hydro-lyases by superoxide. *J Biol Chem*, 268, 22369-22376.
- Fortini, M. E. & Bonini, N. M. (2000). Modeling human neurodegenerative diseases in *Drosophila*: on a wing and a prayer. *Trends Genet*, 16, 161-167.
- Fozzard, H. A., Lee, P. J. & Lipkind, G. M. (2005). Mechanism of local anesthetic drug action on voltage-gated sodium channels. *Curr Pharm Des*, 11, 2671-2686.
- Fyrberg, E., Kelly, M., Ball, E., Fyrberg, C. & Reedy, M. C. (1990). Molecular genetics of *Drosophila alpha-actinin*: mutant alleles disrupt Z disc integrity and muscle insertions. *J Cell Biol*, 110, 1999-2011.
- Gamo, S., Dodo, K., Matakatsu, H. & Tanaka, Y. (1998). Molecular genetical analysis of *Drosophila* ether sensitive mutants. *Toxicol Lett*, 100-101, 329-337.
- Gamstorp, I. (1963). Adynamia episodica hereditaria and myotonia. *Acta Neurol Scand*, 39, 41-58.
- Ganetzky, B. (1984). Genetic studies of membrane excitability in *Drosophila*: lethal interaction between two temperature-sensitive paralytic mutations. *Genetics*, 108, 897-911.
- Ganetzky, B. & Wu, C. F. (1982). *Drosophila* mutants with opposing effects on nerve excitability: genetic and spatial interactions in repetitive firing. *J Neurophysiol*, 47, 501-514.
- Garesse, R. & Kaguni, L. S. (2005). A *Drosophila* model of mitochondrial DNA replication: proteins, genes and regulation. *IUBMB Life*, 57, 555-561.
- George, A. L. (2005). Inherited disorders of voltage-gated sodium channels. *J Clin Invest*, 115, 1990-1999.
- Glasscock, E., Singhania, A. & Tanouye, M. A. (2005). The *mei-P26* Gene Encodes a RING Finger B-box Coiled-Coil-NHL Protein That Regulates Seizure Susceptibility in *Drosophila*. *Genetics*, 170, 1677-1689.

- Goldin, A. L. (2003). Mechanisms of sodium channel inactivation. *Curr Opin Neurobiol*, 13, 284-290.
- Gong, M. & Rong, Y. S. (2003). Targeting multi-cellular organisms. *Curr Opin Genet Dev*, 13, 215-220.
- Gorg, A., Boguth, G., Kopf, A., Reil, G., Parlar, H. & Weiss, W. (2002). Sample prefractionation with Sephadex isoelectric focusing prior to narrow pH range two-dimensional gels. *Proteomics*, 2, 1652-1657.
- Goto, S. G. (2001). A novel gene that is up-regulated during recovery from cold shock in *Drosophila melanogaster*. *Gene*, 270, 259-264.
- Goto, Y., Nonaka, I. & Horai, S. (1990). A mutation in the tRNA(Leu)(UUR) gene associated with the MELAS subgroup of mitochondrial encephalomyopathies. *Nature*, 348, 651-653.
- Gracey, A. Y., Fraser, E. J., Li, W., Fang, Y., Taylor, R. R., Rogers, J., Brass, A. & Cossins, A. R. (2004). Coping with cold: An integrative, multitissue analysis of the transcriptome of a poikilothermic vertebrate. *Proc Natl Acad Sci U S A*, 101, 16970-16975.
- Guerrero, F. D., Jamroz, R. C., Kammlah, D. & Kunz, S. E. (1997). Toxicological and molecular characterization of pyrethroid-resistant horn flies, *Haematobia irritans*: identification of kdr and super-kdr point mutations. *Insect Biochem Mol Biol*, 27, 745-755.
- Guerrini, R., Belmonte, A. & Genton, P. (1998). Antiepileptic drug-induced worsening of seizures in children. *Epilepsia*, 39 Suppl 3, S2-10.
- Gupta, V. & Oliver, B. (2003). *Drosophila* microarray platforms. *Brief Funct Genomic Proteomic*, 2, 97-105.
- Guthrie, C., Nashimoto, H. & Nomura, M. (1969). Structure and function of *E. coli* ribosomes. 8. Cold-sensitive mutants defective in ribosome assembly. *Proc Natl Acad Sci U S A*, 63, 384-391.

- Gutierrez-Delicado, E. & Serratosa, J. M. (2004). Genetics of the epilepsies. *Curr Opin Neurol*, 17, 147-153.
- Han, K. A., Millar, N. S., Grotewiel, M. S. & Davis, R. L. (1996). DAMB, a novel dopamine receptor expressed specifically in *Drosophila* mushroom bodies. *Neuron*, 16, 1127-1135.
- Hanak, P. & Jezek, P. (2001). Mitochondrial uncoupling proteins and phylogenesis--UCP4 as the ancestral uncoupling protein. *FEBS Lett*, 495, 137-141.
- Hare, P. D. & Cress, W. A. (1997). Metabolic implications of stress-induced proline accumulation in plants. *Plant Growth Regulation*, 21, 79-102.
- Haug, K., Warnstedt, M., Alekov, A. K., Sander, T., Ramirez, A., Poser, B., Maljevic, S., Hebeisen, S., Kubisch, C., Rebstock, J., Horvath, S., Hallmann, K., Dullinger, J. S., Rau, B., Haverkamp, F., Beyenburg, S., Schulz, H., Janz, D., Giese, B., Muller-Newen, G., Propping, P., Elger, C. E., Fahlke, C., Lerche, H. & Heils, A. (2003). Mutations in *CLCN2* encoding a voltage-gated chloride channel are associated with idiopathic generalized epilepsies. *Nat Genet*, 33, 527-532.
- Heine, R., Pika, U. & Lehmann-Horn, F. (1993). A novel *SCN4A* mutation causing myotonia aggravated by cold and potassium. *Hum Mol Genet*, 2, 1349-1353.
- Henshall, D. C., Araki, T., Schindler, C. K., Lan, J. Q., Tiekoter, K. L., Taki, W. & Simon, R. P. (2002). Activation of Bcl-2-associated death protein and counter-response of Akt within cell populations during seizure-induced neuronal death. *J Neurosci*, 22, 8458-8465.
- Hirose, S., Zenri, F., Akiyoshi, H., Fukuma, G., Iwata, H., Inoue, T., Yonetani, M., Tsutsumi, M., Muranaka, H., Kurokawa, T., Hanai, T., Wada, K., Kaneko, S. & Mitsudome, A. (2000). A novel mutation of *KCNQ3* (c.925T-->C) in a Japanese family with benign familial neonatal convulsions. *Ann Neurol*, 47, 822-826.
- Hodges, D. D., Lee, D., Preston, C. F., Boswell, K., Hall, L. M. & O'Dowd, D. K. (2002). *tipE* regulates Na⁺-dependent repetitive firing in *Drosophila* neurons. *Mol Cell Neurosci*, 19, 402-416.

- Hodgkin, A. L., Huxley, A. F. & Katz, B. (1952). Measurement of current-voltage relations in the membrane of the giant axon of *Loligo*. *J Physiol*, 116, 424-448.
- Holt, I. J., Harding, A. E., Petty, R. K. & Morgan-Hughes, J. A. (1990). A new mitochondrial disease associated with mitochondrial DNA heteroplasmy. *Am J Hum Genet*, 46, 428-433.
- Homyk, T., Jr. & Pye, Q. (1989). Some mutations affecting neural or muscular tissues alter the physiological components of the electroretinogram in *Drosophila*. *J Neurogenet*, 5, 37-48.
- Hong, C. S. & Ganetzky, B. (1994). Spatial and temporal expression patterns of two sodium channel genes in *Drosophila*. *J Neurosci*, 14, 5160-5169.
- Hoskins, R. A., Phan, A. C., Naeemuddin, M., Mapa, F. A., Ruddy, D. A., Ryan, J. J., Young, L. M., Wells, T., Kopczynski, C. & Ellis, M. C. (2001). Single nucleotide polymorphism markers for genetic mapping in *Drosophila melanogaster*. *Genome Res*, 11, 1100-1113.
- Huang, X., Huang, Y., Chinnappan, R., Bocchini, C., Gustin, M. C. & Stern, M. (2002). The *Drosophila inebriated*-encoded neurotransmitter/osmolyte transporter: dual roles in the control of neuronal excitability and the osmotic stress response. *Genetics*, 160, 561-569.
- Ito, K., Okada, R., Tanaka, N. K. & Awasaki, T. (2003). Cautionary observations on preparing and interpreting brain images using molecular biology-based staining techniques. *Microsc Res Tech*, 62, 170-186.
- Jacobs, H. T., Fernandez-Ayala, D. J., Manjiry, S., Kemppainen, E., Toivonen, J. M. & O'Dell, K. M. (2004). Mitochondrial disease in flies. *Biochim Biophys Acta*, 1659, 190-196.
- Jan, L. Y. & Jan, Y. N. (1992). Tracing the roots of ion channels. *Cell*, 69, 715-718.

- Jarman, A. P., Grau, Y., Jan, L. Y. & Jan, Y. N. (1993). *atonal* is a proneural gene that directs chordotonal organ formation in the *Drosophila* peripheral nervous system. *Cell*, 73, 1307-1321.
- Jensen, F. E. & Baram, T. Z. (2000). Developmental seizures induced by common early-life insults: short- and long-term effects on seizure susceptibility. *Ment Retard Dev Disabil Res Rev*, 6, 253-257.
- Jiang, W., Hou, Y. & Inouye, M. (1997). CspA, the major cold-shock protein of *Escherichia coli*, is an RNA chaperone. *J Biol Chem*, 272, 196-202.
- Karp, N. A., Spencer, M., Lindsay, H., O'Dell, K. & Lilley, K. S. (2005a). Impact of Replicate Types on Proteomic Expression Analysis. *J Proteome Res*, 4, 1867-1871.
- Kawasaki, F., Felling, R. & Ordway, R. W. (2000). A temperature-sensitive paralytic mutant defines a primary synaptic calcium channel in *Drosophila*. *J Neurosci*, 20, 4885-4889.
- Kearney, J. A., Plummer, N. W., Smith, M. R., Kapur, J., Cummins, T. R., Waxman, S. G., Goldin, A. L. & Meisler, M. H. (2001). A gain-of-function mutation in the sodium channel gene *Scn2a* results in seizures and behavioral abnormalities. *Neuroscience*, 102, 307-317.
- Kim, Y. J. & Baker, B. S. (1993). Isolation of RRM-type RNA-binding protein genes and the analysis of their relatedness by using a numerical approach. *Mol Cell Biol*, 13, 174-183.
- Koch, M. C., Baumbach, K., George, A. L. & Ricker, K. (1995). Paramyotonia congenita without paralysis on exposure to cold: a novel mutation in the *SCN4A* gene (Val1293Ile). *Neuroreport*, 6, 2001-2004.
- Koch, M. C., Steinmeyer, K., Lorenz, C., Ricker, K., Wolf, F., Otto, M., Zoll, B., Lehmann-Horn, F., Grzeschik, K. H. & Jentsch, T. J. (1992). The skeletal muscle chloride channel in dominant and recessive human myotonia. *Science*, 257, 797-800.

- Kohrman, D. C., Smith, M. R., Goldin, A. L., Harris, J. & Meisler, M. H. (1996). A missense mutation in the sodium channel *Scn8a* is responsible for cerebellar ataxia in the mouse mutant *jolting*. *J Neurosci*, 16, 5993-5999.
- Kornberg, T. B. & Krasnow, M. A. (2000). The *Drosophila* genome sequence: implications for biology and medicine. *Science*, 287, 2218-2220.
- Kuebler, D. & Tanouye, M. A. (2000). Modifications of seizure susceptibility in *Drosophila*. *J Neurophysiol*, 83, 998-1009.
- Kuebler, D., Zhang, H., Ren, X. & Tanouye, M. A. (2001). Genetic suppression of seizure susceptibility in *Drosophila*. *J Neurophysiol*, 86, 1211-1225.
- Kulkarni, N. H., Yamamoto, A. H., Robinson, K. O., Mackay, T. F. & Anholt, R. R. (2002). The DSC1 channel, encoded by the *smi60E* locus, contributes to odor-guided behavior in *Drosophila melanogaster*. *Genetics*, 161, 1507-1516.
- Leegwater, P. A., Vermeulen, G., Konst, A. A., Naidu, S., Mulders, J., Visser, A., Kersbergen, P., Mobach, D., Fonds, D., van Berkel, C. G., Lemmers, R. J., Frants, R. R., Oudejans, C. B., Schutgens, R. B., Pronk, J. C. & van der Knaap, M. S. (2001). Subunits of the translation initiation factor eIF2B are mutant in leukoencephalopathy with vanishing white matter. *Nat Genet*, 29, 383-388.
- Lerche, H., Heine, R., Pika, U., George, A. L., Jr., Mitrovic, N., Browatzki, M., Weiss, T., Rivet-Bastide, M., Franke, C., Lomonaco, M. & et al. (1993). Human sodium channel myotonia: slowed channel inactivation due to substitutions for a glycine within the III-IV linker. *J Physiol*, 470, 13-22.
- Lerche, H., Jurkat-Rott, K. & Lehmann-Horn, F. (2001). Ion channels and epilepsy. *Am J Med Genet*, 106, 146-159.
- Lerche, H., Weber, Y. G., Jurkat-Rott, K. & Lehmann-Horn, F. (2005). Ion channel defects in idiopathic epilepsies. *Curr Pharm Des*, 11, 2737-2752.

- Li, H., Chaney, S., Roberts, I. J., Forte, M. & Hirsh, J. (2000). Ectopic G-protein expression in dopamine and serotonin neurons blocks cocaine sensitization in *Drosophila melanogaster*. *Curr Biol*, 10, 211-214.
- Lilley, K. S. & Griffiths, D. R. (2003). Proteomics in *Drosophila melanogaster*. *Brief Funct Genomic Proteomic*, 2, 106-113.
- Lilly, M. & Carlson, J. (1990). *smellblind*: a gene required for *Drosophila* olfaction. *Genetics*, 124, 293-302.
- Lilly, M., Kreber, R., Ganetzky, B. & Carlson, J. R. (1994a). Evidence that the *Drosophila* olfactory mutant *smellblind* defines a novel class of sodium channel mutation. *Genetics*, 136, 1087-1096.
- Lilly, M., Riesgo-Escovar, J. & Carlson, J. (1994b). Developmental analysis of the *smellblind* mutants: evidence for the role of sodium channels in *Drosophila* development. *Dev Biol*, 162, 1-8.
- Lossin, C., Rhodes, T. H., Desai, R. R., Vanoye, C. G., Wang, D., Carniciu, S., Devinsky, O. & George, A. L., Jr. (2003). Epilepsy-associated dysfunction in the voltage-gated neuronal sodium channel *SCN1A*. *J Neurosci*, 23, 11289-11295.
- Loughney, K., Kreber, R. & Ganetzky, B. (1989). Molecular analysis of the *para* locus, a sodium channel gene in *Drosophila*. *Cell*, 58, 1143-1154.
- Lucas, P. T., Meadows, L. S., Nicholls, J. & Ragsdale, D. S. (2005). An epilepsy mutation in the beta1 subunit of the voltage-gated sodium channel results in reduced channel sensitivity to phenytoin. *Epilepsy Res*, 64, 77-84.
- Lukacsovich, T., Asztalos, Z., Awano, W., Baba, K., Kondo, S., Niwa, S. & Yamamoto, D. (2001). Dual-tagging gene trap of novel genes in *Drosophila melanogaster*. *Genetics*, 157, 727-742.
- Lundell, M. J. & Hirsh, J. (1994). Temporal and spatial development of serotonin and dopamine neurons in the *Drosophila* CNS. *Dev Biol*, 165, 385-396.

- Luo, L., Liao, Y. J., Jan, L. Y. & Jan, Y. N. (1994). Distinct morphogenetic functions of similar small GTPases: *Drosophila Drac1* is involved in axonal outgrowth and myoblast fusion. *Genes Dev*, 8, 1787-1802.
- Marshall, C. J. (1997). Cold-adapted enzymes. *Trends Biotechnol*, 15, 359-364.
- Martin, R. L., Pittendrigh, B., Liu, J., Reenan, R., French-Constant, R. & Hanck, D. A. (2000). Point mutations in domain III of a *Drosophila* neuronal Na channel confer resistance to allethrin. *Insect Biochem Mol Biol*, 30, 1051-1059.
- Martinez-Torres, D., Chandre, F., Williamson, M. S., Darriet, F., Berge, J. B., Devonshire, A. L., Guillet, P., Pasteur, N. & Pauron, D. (1998). Molecular characterization of pyrethroid knockdown resistance (kdr) in the major malaria vector *Anopheles gambiae* s.s. *Insect Mol Biol*, 7, 179-184.
- Mayoh, H. & Suzuki, D. T. (1973). Temperature-sensitive mutations in *Drosophila melanogaster*. XVI. The genetic properties of sex-linked cold-sensitive mutants. *Can. J. Genet. Cytol.*, 15, 237-254.
- McClatchey, A. I., McKenna-Yasek, D., Cros, D., Worthen, H. G., Kuncl, R. W., DeSilva, S. M., Cornblath, D. R., Gusella, J. F. & Brown, R. H., Jr. (1992a). Novel mutations in families with unusual and variable disorders of the skeletal muscle sodium channel. *Nat Genet*, 2, 148-152.
- McClatchey, A. I., Van den Bergh, P., Pericak-Vance, M. A., Raskind, W., Verellen, C., McKenna-Yasek, D., Rao, K., Haines, J. L., Bird, T. & Brown, R. H., Jr. (1992b). Temperature-sensitive mutations in the III-IV cytoplasmic loop region of the skeletal muscle sodium channel gene in paramyotonia congenita. *Cell*, 68, 769-774.
- McLellan, A., Phillips, H. A., Rittey, C., Kirkpatrick, M., Mulley, J. C., Goudie, D., Stephenson, J. B., Tolmie, J., Scheffer, I. E., Berkovic, S. F. & Zuberi, S. M. (2003). Phenotypic comparison of two Scottish families with mutations in different genes causing autosomal dominant nocturnal frontal lobe epilepsy. *Epilepsia*, 44, 613-617.

- McNamara, J. O. (1994). Cellular and molecular basis of epilepsy. *J Neurosci*, 14, 3413-3425.
- McPhee, J. C., Ragsdale, D. S., Scheuer, T. & Catterall, W. A. (1998). A critical role for the S4-S5 intracellular loop in domain IV of the sodium channel alpha-subunit in fast inactivation. *J Biol Chem*, 273, 1121-1129.
- Mee, C. J., Pym, E. C., Moffat, K. G. & Baines, R. A. (2004). Regulation of neuronal excitability through *pumilio*-dependent control of a sodium channel gene. *J Neurosci*, 24, 8695-8703.
- Melov, S., Coskun, P., Patel, M., Tuinstra, R., Cottrell, B., Jun, A. S., Zastawny, T. H., Dizdaroglu, M., Goodman, S. I., Huang, T. T., Mizioro, H., Epstein, C. J. & Wallace, D. C. (1999). Mitochondrial disease in *superoxide dismutase 2* mutant mice. *Proc Natl Acad Sci U S A*, 96, 846-851.
- Millar, N. S., Baylis, H. A., Reaper, C., Bunting, R., Mason, W. T. & Sattelle, D. B. (1995). Functional expression of a cloned *Drosophila* muscarinic acetylcholine receptor in a stable *Drosophila* cell line. *J Exp Biol*, 198, 1843-1850.
- Millar, N. S., Buckingham, S. D. & Sattelle, D. B. (1994). Stable expression of a functional homo-oligomeric *Drosophila* GABA receptor in a *Drosophila* cell line. *Proc Biol Sci*, 258, 307-314.
- Miller, J. A., Agnew, W. S. & Levinson, S. R. (1983). Principal glycopeptide of the tetrodotoxin/saxitoxin binding protein from *Electrophorus electricus*: isolation and partial chemical and physical characterization. *Biochemistry*, 22, 462-470.
- Misener, S. R., Chen, C. & Walker, V. K. (2001). Cold tolerance and proline metabolic gene expression in *Drosophila melanogaster*. *J Insect Physiol*, 47, 393-400.
- Mitrovic, N., George, A. L., Jr., Lerche, H., Wagner, S., Fahlke, C. & Lehmann-Horn, F. (1995). Different effects on gating of three myotonia-causing mutations in the inactivation gate of the human muscle sodium channel. *J Physiol*, 487 (Pt 1), 107-114.

- Muhlig Nielsen, M., Overgaard, J., Sorensen, J. G., Holmstrup, M., Justesen, J. & Loeschcke, V. (2005). Role of HSF activation for resistance to heat, cold and high-temperature knock-down. *J Insect Physiol.*
- Mutero, A., Bride, J. M., Pralavorio, M. & Fournier, D. (1994). *Drosophila melanogaster* acetylcholinesterase: identification and expression of two mutations responsible for cold- and heat-sensitive phenotypes. *Mol Gen Genet*, 243, 699-705.
- Neckameyer, W. S. & White, K. (1993). *Drosophila* tyrosine hydroxylase is encoded by the *pale* locus. *J Neurogenet*, 8, 189-199.
- Nilsson, C. L. & Davidsson, P. (2000). New separation tools for comprehensive studies of protein expression by mass spectrometry. *Mass Spectrom Rev*, 19, 390-397.
- Noebels, J. L. (1996). Targeting epilepsy genes. *Neuron*, 16, 241-244.
- O'Dell, K. M. (2003). The voyeurs' guide to *Drosophila melanogaster* courtship. *Behav Processes*, 64, 211-223.
- O'Kane, C. J. (2003). Modelling human diseases in *Drosophila* and *Caenorhabditis*. *Semin Cell Dev Biol*, 14, 3-10.
- Ohtsu, T., Kimura, M. T. & Katagiri, C. (1998). How *Drosophila* species acquire cold tolerance--qualitative changes of phospholipids. *Eur J Biochem*, 252, 608-611.
- Okazaki, Y. & Katayama, T. (2003). Effects of dietary carbohydrate and myo-inositol on metabolic changes in rats fed 1,1,1-trichloro-2,2-bis(p-chlorophenyl)ethane (DDT). *J. Nutr. Biochem*, 14, 81-89.
- Overgaard, J., Sorensen, J. G., Petersen, S. O., Loeschcke, V. & Holmstrup, M. (2005). Changes in membrane lipid composition following rapid cold hardening in *Drosophila melanogaster*. *J Insect Physiol.*
- Palladino, M. J., Hadley, T. J. & Ganetzky, B. (2002). Temperature-sensitive paralytic mutants are enriched for those causing neurodegeneration in *Drosophila*. *Genetics*, 161, 1197-1208.

- Patel, M. (2004). Mitochondrial dysfunction and oxidative stress: cause and consequence of epileptic seizures. *Free Radic Biol Med*, 37, 1951-1962.
- Pauron, D., Barhanin, J., Amichot, M., Pralavorio, M., Berge, J. B. & Lazdunski, M. (1989). Pyrethroid receptor in the insect sodium channel: alteration of its properties in pyrethroid-resistant flies. *Biochemistry*, 28, 1673-1677.
- Pavlidis, P., Ramaswami, M. & Tanouye, M. A. (1994). The *Drosophila easily shocked* gene: a mutation in a phospholipid synthetic pathway causes seizure, neuronal failure, and paralysis. *Cell*, 79, 23-33.
- Pavlidis, P. & Tanouye, M. A. (1995). Seizures and failures in the giant fiber pathway of *Drosophila* bang-sensitive paralytic mutants. *J Neurosci*, 15, 5810-5819.
- Pedra, J. H., Festucci-Buselli, R. A., Sun, W., Muir, W. M., Scharf, M. E. & Pittendrigh, B. R. (2005). Profiling of abundant proteins associated with dichlorodiphenyltrichloroethane resistance in *Drosophila melanogaster*. *Proteomics*, 5, 258-269.
- Pittendrigh, B., Reenan, R., French-Constant, R. H. & Ganetzky, B. (1997). Point mutations in the *Drosophila* sodium channel gene *para* associated with resistance to DDT and pyrethroid insecticides. *Mol Gen Genet*, 256, 602-610.
- Plummer, N. W. & Meisler, M. H. (1999). Evolution and diversity of mammalian sodium channel genes. *Genomics*, 57, 323-331.
- Prosser, H. M., Gill, C. H., Hirst, W. D., Grau, E., Robbins, M., Calver, A., Soffin, E. M., Farmer, C. E., Lanneau, C., Gray, J., Schenck, E., Warmerdam, B. S., Clapham, C., Reavill, C., Rogers, D. C., Stean, T., Upton, N., Humphreys, K., Randall, A., Geppert, M., Davies, C. H. & Pangalos, M. N. (2001). Epileptogenesis and enhanced prepulse inhibition in *GABA(B1)*-deficient mice. *Mol Cell Neurosci*, 17, 1059-1070.
- Ptacek, L. J., George, A. L., Jr., Barchi, R. L., Griggs, R. C., Riggs, J. E., Robertson, M. & Leppert, M. F. (1992). Mutations in an S4 segment of the adult skeletal muscle sodium channel cause paramyotonia congenita. *Neuron*, 8, 891-897.

- Ptacek, L. J., George, A. L., Jr., Griggs, R. C., Tawil, R., Kallen, R. G., Barchi, R. L., Robertson, M. & Leppert, M. F. (1991). Identification of a mutation in the gene causing hyperkalemic periodic paralysis. *Cell*, 67, 1021-1027.
- Qu, S. & Cavener, D. R. (1994). Isolation and characterization of the *Drosophila melanogaster* eIF-2 alpha gene encoding the alpha subunit of translation initiation factor eIF-2. *Gene*, 140, 239-242.
- Ramaswami, M. & Tanouye, M. A. (1989). Two sodium-channel genes in *Drosophila*: implications for channel diversity. *Proc Natl Acad Sci U S A*, 86, 2079-2082.
- Ranganayakulu, G., Schulz, R. A. & Olson, E. N. (1996). Wingless signaling induces *nautilus* expression in the ventral mesoderm of the *Drosophila* embryo. *Dev Biol*, 176, 143-148.
- Reiter, L. T., Potocki, L., Chien, S., Gribskov, M. & Bier, E. (2001). A systematic analysis of human disease-associated gene sequences in *Drosophila melanogaster*. *Genome Res*, 11, 1114-1125.
- Rhodes, T. H., Lossin, C., Vanoye, C. G., Wang, D. W. & George, A. L., Jr. (2004). Noninactivating voltage-gated sodium channels in severe myoclonic epilepsy of infancy. *Proc Natl Acad Sci U S A*, 101, 11147-11152.
- Ricker, K., Moxley, R. T., 3rd, Heine, R. & Lehmann-Horn, F. (1994). Myotonia fluctuans. A third type of muscle sodium channel disease. *Arch Neurol*, 51, 1095-1102.
- Robertson, J. L., Russell, R. M. & Savin, N. E. (1980). POLO: a user's guide to probit or logic analysis. *US Forestry Service Technical Report PSW*.
- Rohl, C. A., Boeckman, F. A., Baker, C., Scheuer, T., Catterall, W. A. & Klevit, R. E. (1999). Solution structure of the sodium channel inactivation gate. *Biochemistry*, 38, 855-861.

- Rojas, C. V., Wang, J. Z., Schwartz, L. S., Hoffman, E. P., Powell, B. R. & Brown, R. H., Jr. (1991). A Met-to-Val mutation in the skeletal muscle Na⁺ channel alpha-subunit in hyperkalaemic periodic paralysis. *Nature*, 354, 387-389.
- Rong, Y. S. & Golic, K. G. (2000). Gene targeting by homologous recombination in *Drosophila*. *Science*, 288, 2013-2018.
- Roseman, R. R., Johnson, E. A., Rodesch, C. K., Bjerke, M., Nagoshi, R. N. & Geyer, P. K. (1995). A P element containing *suppressor of hairy-wing* binding regions has novel properties for mutagenesis in *Drosophila melanogaster*. *Genetics*, 141, 1061-1074.
- Rudolph, J. A., Spier, S. J., Byrns, G., Rojas, C. V., Bernoco, D. & Hoffman, E. P. (1992). Periodic paralysis in quarter horses: a sodium channel mutation disseminated by selective breeding. *Nat Genet*, 2, 144-147.
- Sakmann, B. & Neher, E. (1984). Patch clamp techniques for studying ionic channels in excitable membranes. *Annu Rev Physiol*, 46, 455-472.
- Sardiello, M., Licciulli, F., Catalano, D., Attimonelli, M. & Caggese, C. (2003). MitoDrome: a database of *Drosophila melanogaster* nuclear genes encoding proteins targeted to the mitochondrion. *Nucleic Acids Res*, 31, 322-324.
- Schlitt, S. C. & Russell, P. J. (1974). *Neurospora crassa* cytoplasmic ribosomes: isolation and characterization of a cold-sensitive mutant defective in ribosome biosynthesis. *J Bacteriol*, 120, 666-671.
- Schneider, I. (1972). Cell lines derived from late embryonic stages of *Drosophila melanogaster*. *J Embryol Exp Morphol*, 27, 353-365.
- Scholz, H., Franz, M. & Heberlein, U. (2005). The *hangover* gene defines a stress pathway required for ethanol tolerance development. *Nature*, 436, 845-847.
- Schwartz, M. & Vissing, J. (2002). Paternal inheritance of mitochondrial DNA. *N Engl J Med*, 347, 576-580.

- Schwarz, T. L., Tempel, B. L., Papazian, D. M., Jan, Y. N. & Jan, L. Y. (1988). Multiple potassium-channel components are produced by alternative splicing at the *Shaker* locus in *Drosophila*. *Nature*, 331, 137-142.
- Shoffner, J. M., Lott, M. T., Lezza, A. M., Seibel, P., Ballinger, S. W. & Wallace, D. C. (1990). Myoclonic epilepsy and ragged-red fiber disease (MERRF) is associated with a mitochondrial DNA tRNA(Lys) mutation. *Cell*, 61, 931-937.
- Siddiqi, O. & Benzer, S. (1976). Neurophysiological defects in temperature-sensitive paralytic mutants of *Drosophila melanogaster*. *Proc Natl Acad Sci U S A*, 73, 3253-3257.
- Simon, D. K. & Johns, D. R. (1999). Mitochondrial disorders: clinical and genetic features. *Annu Rev Med*, 50, 111-127.
- Singh, K. K. (1998). *Mitochondrial DNA mutations in Aging, Disease, and Cancer*, New York, Springer.
- Singh, N., Zhu, W. & Hanes, S. D. (2005). *Sap18* is required for the maternal gene *bicoid* to direct anterior patterning in *Drosophila melanogaster*. *Dev Biol*, 278, 242-254.
- Smith, M. R. & Goldin, A. L. (1997). Interaction between the sodium channel inactivation linker and domain III S4-S5. *Biophys J*, 73, 1885-1895.
- Soderlund, D. M. & Bloomquist, J. R. (1989). Neurotoxic actions of pyrethroid insecticides. *Annu Rev Entomol*, 34, 77-96.
- Sokolowski, M. B. (2001). *Drosophila*: genetics meets behaviour. *Nat Rev Genet*, 2, 879-890.
- Song, J. & Tanouye, M. A. (2005). Seizure Suppression by *shakB2*, a Gap Junction Connexin Mutation in *Drosophila*. *J Neurophysiol*.
- Spampanato, J., Kearney, J. A., de Haan, G., McEwen, D. P., Escayg, A., Aradi, I., MacDonald, B. T., Levin, S. I., Soltesz, I., Benna, P., Montalenti, E., Isom, L. L., Goldin, A. L. & Meisler, M. H. (2004). A novel epilepsy mutation in the sodium

channel *SCN1A* identifies a cytoplasmic domain for beta subunit interaction. *J Neurosci*, 24, 10022-10034.

St Johnston, D. (2002). The art and design of genetic screens: *Drosophila melanogaster*. *Nat Rev Genet*, 3, 176-188.

Stern, M., Kreber, R. & Ganetzky, B. (1990). Dosage effects of a *Drosophila* sodium channel gene on behavior and axonal excitability. *Genetics*, 124, 133-143.

Stuhmer, W., Conti, F., Suzuki, H., Wang, X. D., Noda, M., Yahagi, N., Kubo, H. & Numa, S. (1989). Structural parts involved in activation and inactivation of the sodium channel. *Nature*, 339, 597-603.

Sugawara, T., Tsurubuchi, Y., Agarwala, K. L., Ito, M., Fukuma, G., Mazaki-Miyazaki, E., Nagafuji, H., Noda, M., Imoto, K., Wada, K., Mitsudome, A., Kaneko, S., Montal, M., Nagata, K., Hirose, S. & Yamakawa, K. (2001). A missense mutation of the Na⁺ channel alpha II subunit gene *Na(v)1.2* in a patient with febrile and afebrile seizures causes channel dysfunction. *Proc Natl Acad Sci U S A*, 98, 6384-6389.

Suzuki, D. T., Grigliatti, T. & Williamson, R. (1971). Temperature-sensitive mutations in *Drosophila melanogaster*, VII. A mutation (*para^{ts}*) causing reversible adult paralysis. *Proc Natl Acad Sci U S A*, 68, 890-893.

Swatton, J. E., Prabakaran, S., Karp, N. A., Lilley, K. S. & Bahn, S. (2004). Protein profiling of human postmortem brain using 2-dimensional fluorescence difference gel electrophoresis (2-D DIGE). *Mol Psychiatry*, 9, 128-143.

Sweeney, S. T., Broadie, K., Keane, J., Niemann, H. & O'Kane, C. J. (1995). Targeted expression of tetanus toxin light chain in *Drosophila* specifically eliminates synaptic transmission and causes behavioral defects. *Neuron*, 14, 341-351.

Søndergaard, L. (1975). A temperature-sensitive behavioural mutant of *Drosophila melanogaster*: *Out-cold*. *Hereditas*, 81, 199-210.

Søndergaard, L. (1976). Temperature-induced changes in succinate-cytochrome c reductase in behavioural mutants of *Drosophila*. *Hereditas*, 82, 51-55.

- Søndergaard, L. (1979a). Dominant cold paralytic mutations on the X chromosome of *Drosophila melanogaster*. *Hereditas*, 90, 93-101.
- Søndergaard, L. (1979b). Role of proteins and lipids in non-linear Arrhenius plots of *Drosophila* mitochondrial succinate-cytochrome c reductase studied by rebinding experiments. *Biochim Biophys Acta*, 557, 208-216.
- Søndergaard, L. (1980). Dominant cold paralytic mutations on the autosomes of *Drosophila melanogaster*. *Hereditas*, 92, 335-340.
- Søndergaard, L. (1986). The nuclear mutation *Ocdts-1* changes the 2-D electrophoretic pattern of *Drosophila* mitochondria. *Hereditas*, 104, 313-315.
- Søndergaard, L., Nielsen, N. C. & Smillie, R. M. (1975). The effect of the *Out-cold-ts* mutation on temperature induced changes in the Arrhenius activation energy of succinate-cytochrome c reductase activity in *Drosophila*. *FEBS Lett*, 51, 126-129.
- Taylor, R. W. & Turnbull, D. M. (2005). Mitochondrial DNA mutations in human disease. *Nat Rev Genet*, 6, 389-402.
- Thackeray, J. R. & Ganetzky, B. (1994). Developmentally Regulated Splicing Generates a Complex Array of *Drosophila para* Sodium Channel Isoforms. *J. Neuroscience*, 14, 2569-2578.
- Toivonen, J. M., O'Dell, K. M., Petit, N., Irvine, S. C., Knight, G. K., Lehtonen, M., Longmuir, M., Luoto, K., Touraille, S., Wang, Z., Alziari, S., Shah, Z. H. & Jacobs, H. T. (2001). *technical knockout*, a *Drosophila* model of mitochondrial deafness. *Genetics*, 159, 241-254.
- Twomey, C. & McCarthy, J. V. (2005). Pathways of apoptosis and importance in development. *J Cell Mol Med*, 9, 345-359.
- Unlu, M., Morgan, M. E. & Minden, J. S. (1997). Difference gel electrophoresis: a single gel method for detecting changes in protein extracts. *Electrophoresis*, 18, 2071-2077.

- Upton, N. & Stratton, S. (2003). Recent developments from genetic mouse models of seizures. *Curr Opin Pharmacol*, 3, 19-26.
- van der Blik, A. M. & Meyerowitz, E. M. (1991). Dynamin-like protein encoded by the *Drosophila shibire* gene associated with vesicular traffic. *Nature*, 351, 411-414.
- Vassilev, P. M., Scheuer, T. & Catterall, W. A. (1988). Identification of an intracellular peptide segment involved in sodium channel inactivation. *Science*, 241, 1658-1661.
- Venken, K. J. & Bellen, H. J. (2005). Emerging technologies for gene manipulation in *Drosophila melanogaster*. *Nat Rev Genet*, 6, 167-178.
- Verrotti, A., Trotta, D., Salladini, C., di Corcia, G. & Chiarelli, F. (2004). Photosensitivity and epilepsy. *J Child Neurol*, 19, 571-578.
- Vilin, Y. Y. & Ruben, P. C. (2001). Slow inactivation in voltage-gated sodium channels: molecular substrates and contributions to channelopathies. *Cell Biochem Biophys*, 35, 171-190.
- Vita, G. M., Olckers, A., Jedlicka, A. E., George, A. L., Heiman-Patterson, T., Rosenberg, H., Fletcher, J. E. & Levitt, R. C. (1995). Masseter muscle rigidity associated with glycine1306-to-alanine mutation in the adult muscle sodium channel alpha-subunit gene. *Anesthesiology*, 82, 1097-1103.
- Wagner, C. A., Friedrich, B., Setiawan, I., Lang, F. & Broer, S. (2000). The use of *Xenopus laevis* oocytes for the functional characterization of heterologously expressed membrane proteins. *Cell Physiol Biochem*, 10, 1-12.
- Wagner, S., Lerche, H., Mitrovic, N., Heine, R., George, A. L. & Lehmann-Horn, F. (1997). A novel sodium channel mutation causing a hyperkalemic paralytic and paramyotonic syndrome with variable clinical expressivity. *Neurology*, 49, 1018-1025.
- Waldron, C. & Roberts, C. F. (1974). Cold-sensitive mutants in *Aspergillus nidulans*. II. Mutations affecting ribosome production. *Mol Gen Genet*, 134, 115-132.

- Wallace, D. C. (1999). Mitochondrial diseases in man and mouse. *Science*, 283, 1482-1488.
- Wallace, R. H., Wang, D. W., Singh, R., Scheffer, I. E., George, A. L., Jr., Phillips, H. A., Saar, K., Reis, A., Johnson, E. W., Sutherland, G. R., Berkovic, S. F. & Mulley, J. C. (1998). Febrile seizures and generalized epilepsy associated with a mutation in the Na⁺-channel beta1 subunit gene *SCN1B*. *Nat Genet*, 19, 366-370.
- Wang, D. W., Yazawa, K., George, A. L., Jr. & Bennett, P. B. (1996). Characterization of human cardiac Na⁺ channel mutations in the congenital long QT syndrome. *Proc Natl Acad Sci U S A*, 93, 13200-13205.
- Wang, P., Saraswati, S., Guan, Z., Watkins, C. J., Wurtman, R. J. & Littleton, J. T. (2004). A *Drosophila* temperature-sensitive seizure mutant in phosphoglycerate kinase disrupts ATP generation and alters synaptic function. *J Neurosci*, 24, 4518-4529.
- Wang, S. Y. & Wang, G. K. (2003). Voltage-gated sodium channels as primary targets of diverse lipid-soluble neurotoxins. *Cell Signal*, 15, 151-159.
- Warmke, J. W., Reenan, R. A., Wang, P., Qian, S., Arena, J. P., Wang, J., Wunderler, D., Liu, K., Kaczorowski, G. J., Van der Ploeg, L. H., Ganetzky, B. & Cohen, C. J. (1997). Functional expression of *Drosophila para* sodium channels. Modulation by the membrane protein *TipE* and toxin pharmacology. *J Gen Physiol*, 110, 119-133.
- West, J. W., Patton, D. E., Scheuer, T., Wang, Y., Goldin, A. L. & Catterall, W. A. (1992). A cluster of hydrophobic amino acid residues required for fast Na⁽⁺⁾-channel inactivation. *Proc Natl Acad Sci U S A*, 89, 10910-10914.
- Williamson, M. S., Martinez-Torres, D., Hick, C. A. & Devonshire, A. L. (1996). Identification of mutations in the housefly *para*-type sodium channel gene associated with knockdown resistance (kdr) to pyrethroid insecticides. *Mol Gen Genet*, 252, 51-60.
- Wodarz, A., Hinz, U., Engelbert, M. & Knust, E. (1995). Expression of *crumbs* confers apical character on plasma membrane domains of ectodermal epithelia of *Drosophila*. *Cell*, 82, 67-76.

- Wright, T. R. (1973). The recovery, penetrance, and pleiotropy of X-linked, cold sensitive mutants in *Drosophila*. *Mol Gen Genet*, 122, 101-118.
- Wu, F. F., Gordon, E., Hoffman, E. P. & Cannon, S. C. (2005). A C-terminal skeletal muscle sodium channel mutation associated with myotonia disrupts fast inactivation. *J Physiol*, 565, 371-380.
- Yu, F. H. & Catterall, W. A. (2003). Overview of the voltage-gated sodium channel family. *Genome Biol*, 4, 207. Epub 2003 Feb 2024.
- Zhai, R. G., Hiesinger, P. R., Koh, T. W., Verstreken, P., Schulze, K. L., Cao, Y., Jafar-Nejad, H., Norga, K. K., Pan, H., Bayat, V., Greenbaum, M. P. & Bellen, H. J. (2003). Mapping *Drosophila* mutations with molecularly defined *P* element insertions. *Proc Natl Acad Sci U S A*, 100, 10860-10865.
- Zhang, H., Tan, J., Reynolds, E., Kuebler, D., Faulhaber, S. & Tanouye, M. (2002). The *Drosophila slamdance* gene: a mutation in an aminopeptidase can cause seizure, paralysis and neuronal failure. *Genetics*, 162, 1283-1299.
- Zlotkin, E. (1999). The insect voltage-gated sodium channel as target of insecticides. *Annu Rev Entomol*, 44, 429-455.